CalVal Saral/ Altika

Saral/ Altika validation and cross calibration activities (Annual report 2015)

Contract No 104685/00 - lot 1.2A

Reference : CLS.DOS/NT/15-064

Nomenclature : SALP-RP-MA-EA-22957-CLS

Issue : 1rev 1

Date : January 22, 2016

CLS - 11 Rue Hermès - Parc Technologique du Canal - 31520 Ramonville St-Agne - FRANCE
Telephone 33 5 61 39 47 00 / Fax 33 5 61 75 10 14

Chronology Issues:		
Issue:	Date:	Reason for change:
1rev0	Nov 23, 2015	Creation

People involved in this issue :				
	AUTHORS	**COMPANY**	**DATE**	**INITIALS**
Written by:	P. Prandi	CLS		
Checked by:		CLS		
Approved by:		CLS CLS		
Application authorised by:				

Index Sheet :	
Context:	
Keywords:	
Hyperlink:	

Distribution:		
Company	Means of distribution	Names
CLS/DOS	electronic copy	G.DIBARBOURE
		J.DORANDEU
CNES	electronic copy	thierry.guinle@cnes.fr emilie.bronner@cnes.fr nicolas.picot@cnes.fr amandine.guillot@cnes.fr jean-damien.desjonqueres@cnes.fr aqgp_rs@cnes.fr dominique.chermain@cnes.fr delphine.vergnoux@cnes.fr

List of tables and figures

List of Tables

List of Figures

List of items to be defined or to be confirmed

Applicable documents / reference documents

Contents

1. Introduction

This document presents the synthesis report concerning validation activities of Saral/AltiKa GDRs in 2015 under SALP contract (N° 104685/00 Lot 1.2A) supported by CNES at the CLS Space Oceanography Division. It covers several points: CAL/VAL Saral/AltiKa activities, Saral/AltiKa / Jason-2 cross-calibration, and particular studies and investigations. **The focus is on GDR products, but results using IGDR products are also shown.** The present report is based exclusively on GDR-T/Patch2 data. For details concerning the Patch2 reprocessing of Saral/AltiKa data can be found at chapter 11.2. or in [11].
The ISRO/CNES mission Saral/AltiKa was successfully launched on February, 25th 2013 and reached its operationnal orbit on March, 13th. However it was not exactly on the same ground track as Envisat (roughly 2 km difference at maximum latitude). After inclination maneuvers, Saral reached the same ground track as Envisat on October, 7th 2013.
Since the beginning of the mission, Saral/AltiKa data have been analyzed and monitored in order to assess the quality of Saral/AltiKa products. Cycle per cycle reports are available through the AVISO web page (http://www.aviso.altimetry.fr/en/data/calval/systematic-calval/validation-reports.html). Main performance metrics were also summarized in a paper published in the Marine Geodesy special issue on SARAL/AltiKa published in 2015.
This report presents the activities undertaken in the framework of the SALP contract to assess and monitor Saral/AltiKa data quality. We present a summary of the main performance metrics of the mission including:

- monitoring of missing and edited parameters,
- analysis of geophysical parameters and corrections,
- accuracy of SLA measurements.

We also present the results of cross-calibration analysis performed between SARAL/AltiKa and Jason-2. Even if both satellites are on different ground tracks, comparisons remains possible, and are necessary to ensure the continuity of ocean observations through high precision altimetry.
Routine validation of SARAL/AltiKa mission and cross-calibration with Jason-2 activities generate a large number of graphs, plots and figures. The purpose os this report is to give the reader a useful and reader-friendly summary of the most important results of the daily monitoring of the mission performed at CLS.
This report also presents to results of particular investigations undertaken this year on SARAL/AltiKa, either to better characterise the mission or as a response to mission events.

2. Processing status

2.1. Processing

Only about 4 months after launch of the Saral/AltiKa mission, Ogdr and Igdr data were available to all users beginning of July 2013. They were first released with some flaws (unit problem for liquid cloud water,...) or some corrections voluntarily disabled (atmospheric attenuation at default value) or with disclaimers (ice_flag, altimeter wind not to use, ...). Some of these issues were addressed by the Patch1 (see table 1 for when this patch was applied on the different products and 11.1. for its content). Beginning of September 2013 the GDR products were released with consistent Patch1 standards since the beginning of the mission. A description of the different Saral/AltiKa products and their disclaimers is available in the Saral/AltiKa Products handbook ([4]).
Patch2, containing several improvements for Saral/AltiKa data, has been launched on February 2014. It has been applied for Ogdr data from cycle 10 pass 0407, then for Igdr data from cycle 10 pass 0566. Finally, Patch2 has been applied for Gdr data from cycle 8 onwards and cycles 1 to 7 were reprocessed. The GDR-E orbit standard has been applied on SARAL from June 30th on Igdr and from cycle 25 (July 3rd) on Gdr. The detailed content of Patch2 can be found in chapter 11.2..
The current SARAL/AltiKa products are GDR-T Patch2, and are used as the standard products for the results presented in this report.
A Patch3, which will provide an improvement of several standards is foreseen, but there is no delivery date available for this new version yet.

Data version	Ogdr	Igdr	Gdr
Version T without Patch	till cycle 4 segment 0609	till cycle 4 pass 394	-
Version T with Patch1 (chapter 11.1.) (L1 library=V3.1p1p2, L2 library=V4.2p1p6p9 Processing Pilot=V3-4-1p2p5p6p7p8p9)	from cycle 4 segment 0611 onwards (2013-07-18 13h44m04)	from cycle 4 pass 0395 onwards (2013-07-10 23h56m18)	from cycle 1 pass 0001 onwards
Version T with Patch2 (chapter 11.2.)	from cycle 10 segment 0407 onwards (2014-02-06 10h46m58)	from cycle 10 pass 0566 onwards (2014-02-11 23h17m37)	from cycle 8 onwards (cycles 1 to 7 have been reprocessed)

.../...

Data version	Ogdr	Igdr	Gdr
(L1 library=V4.2p1, L2 library=V5.2p1, Processing Pilot=V4.1)			

Table 1: *Product versions*

2.2. CAL/VAL status

In order to improve the visibility, the following tables will be presented in yellow or blue color. Color will switch for each cycle. The red color indicates an important event (safe-hold mode).

2.2.1. Acquisition/tracking modes

The following table shows the acquisition/tracking modes since the beginning of Saral/AltiKa mission.

cycle	pass	start time	stop time	altimeter mode
1	0001-0200	2013-03-14	2013-03-21	DIODE acquisition / median tracking
1	0201-0400	2013-03-21	2013-03-28	DIODE acquisition / EDP tracking
1	0401-0600	2013-03-28	2013-04-04	DIODE acquisition / median tracking
1	0601-0800	2013-04-04	2013-04-11	DIODE / DEM tracking
1	0801-1002	2013-04-11	2013-04-18	DIODE acquisition / EDP tracking
2	0001-1002	2013-04-18	2013-05-23	DIODE acquisition / median tracking
3	0001-0400	2013-05-23	2013-06-06	DIODE acquisition / median tracking
3	0401-0800	2013-06-06	2013-06-20	DIODE acquisition / EDP tracking
3	0801-1002	2013-06-20	2013-06-27	DIODE acquisition / median tracking
				.../...

cycle	pass	start time	stop time	altimeter mode
4 to 9	0001-1002	2013-06-27	2014-01-23	DIODE acquisition / median tracking
10	0001-0127	2014-01-23	2014-01-27	DIODE acquisition / median tracking
10	0128-0135	2014-01-27	2014-01-27	autonomous DIODE / median tracking
10	0136-1002	2014-01-27	2014-02-27	DIODE acquisition / median tracking
11 to 16	0001-1002	2014-02-27	2014-09-25	DIODE acquisition / median tracking
17	0001-0324	2014-09-25	2014-10-06	DIODE acquisition / median tracking
17	0414-0457	2014-10-09	2014-10-11	autonomous DIODE / median tracking
17	0457-1002	2014-10-11	2014-10-30	DIODE acquisition / median tracking
18	0001-1002	2014-10-30	2014-12-04	DIODE acquisition / median tracking
19	0001-1002	2014-12-04	2015-01-08	DIODE acquisition / median tracking
20	0001-1002	2015-01-08	2015-02-12	DIODE acquisition / median tracking
21	0001-1002	2015-02-12	2015-03-19	DIODE acquisition / median tracking
22	0001-1002	2015-03-19	2015-04-23	DIODE acquisition / median tracking
23	0001-1002	2015-04-23	2015-05-28	DIODE acquisition / median tracking
24	0001-1002	2015-05-28	2015-07-02	DIODE acquisition / median tracking
25	0001-1002	2015-07-02	2015-08-06	DIODE acquisition / median tracking
26	0001-1002	2015-08-06	2015-09-10	DIODE acquisition / median tracking
				.../...

cycle	pass	start time	stop time	altimeter mode
27	0001-1002	2015-09-10	2015-10-15	DIODE acquisition / median tracking
28	0001-1002	2015-10-15	2015-11-19	DIODE acquisition / median tracking

Table 2: *A*cquisition and tracking modes

2.2.2. List of events

The following table shows the major events of Saral/AltiKa mission.

cycle	pass	start time	stop time	event
1		2013-03-14	2013-03-17	X-band stations acquisition problems (a few missing data)
1	0172-0175	2013-03-20 05:10:03	08:30	calibration I2+Q2 and I&Q for expertise
1	0266	2013-03-23 12:13:52	12:13:55	semi major axis maneuver
1	0372, 0374	2013-03-27		CAL2 long calibrations at 04:51 (28min missing data) and 06:40 (11min missing data)
1	0801	2013-04-11 04:42:00	04:59:45	altimeter gain calibration I2+Q2 (mostly over land)
1	0868	2013-04-13 12:53:52	12:53:54	station keeping maneuver
1	0898	2013-04-14 13:42:00	13:59:45	altimeter gain calibration I&Q (mostly over land)
1	0984	2013-04-17 13:47:00	14:04:45	altimeter gain calibration I2+Q2 (mostly over land)
2	0034, 0035	2013-04-19 9:37	10:25	cross calibration test over S-band station Biak (Indonesia)
2	0057	2013-04-20 04:53	05:12	altimeter gain calibration I&Q (over land)
2	0127	2013-04-22 15:26	15:54	cross calibration maneuver
				.../...

cycle	pass	start time	stop time	event
2	0206	2013-04-25 9:53		pitch maneuver (0.045°) to correct the PF/RF alignment (alignment between the platform and the radiofrequency axis)
2	0355	2013-04-30 14:35	15:03	cross calibration maneuver
2	0782	2013-05-15 12:48:23	12:48:26	station keeping maneuver
3	0438	2013-06-07 12:25:11	12:25:13	station keeping maneuver
3	0887-0890	2013-06-23 05:06:55	06:56:57	no O/I/GDR product due to PLTM lost
3	0926	2013-06-24 13:31:11	13:31:13	station keeping maneuver
4	0498	2013-07-14 14:42:44	14:42:47	station keeping maneuver
4	0556	2013-07-16 15:01:01	15:19:00	altimeter gain calibration I&Q (mostly over land)
4	0586	2013-07-17 16:13:01	16:30:45	altimeter gain calibration I2+Q2 (mostly over land)
4	0911	2013-07-29 00:54:25	00:58:26	inclination maneuver (1 burn on Y and Z axis)
4	0984	2013-07-31 14:08:03	14:08:11	station keeping maneuver
5	0182	2013-08-07 13:48:06	13:48:09	station keeping maneuver
5	0726	2013-08-26 13:51:02	13:51:05	station keeping maneuver
5	0958	2013-09-03 16:02:01	16:20:00	altimeter gain calibration I&Q (mostly over land)
6	0038	2013-09-06 12:44:01	13:01:45	altimeter gain calibration I2+Q2 (over land)
6	0812	2013-10-03 13:55:39	13:57:17	1st inclination maneuver to reach the Envisat ground track (1 burn on Z axis)
6	0926	2013-10-07 13:29:45	13:31:25	2nd inclination maneuver to reach the Envisat ground track

.../...

cycle	pass	start time	stop time	event
6	0984	2013-10-09 14:07:52	14:07:57	station keeping maneuver
7	0526	2013-10-28 14:11:24	14:11:26	station keeping maneuver
7	0586	2013-10-30 16:11	16:28:45	altimeter gain calibration I2+Q2
7	0812	2013-11-07 13:57:01	13:57:03	station keeping maneuver
8	0326	2013-11-25 14:31:29	14:31:32	station keeping maneuver
8	0812	2013-12-12 13:56:58	13:57:01	station keeping maneuver
9	0240	2013-12-27 14:25:41	14:25:44	station keeping maneuver
10	0128	2014-01-27 16:15	16:32:45	altimeter gain calibration I2+Q2 (mostly over land)
10	0152	2014-01-28 12:38:43	12:38:45	station keeping maneuver
11	0126	2014-03-03 14:50:53	14:50:56	station keeping maneuver
11	0782	2014-03-26 12:47:17	12:47:20	station keeping maneuver
12	0438	2014-04-18 12:24:16	12:24:19	station keeping maneuver
12	0728	2014-04-28 15:12:55	15:30:45	expertise calibration CAL1
13	0326-0327	2014-05-19 14:31:18	14:31:21	station keeping maneuver with two consecutive mis-pointing events between 14:38 and 14:43 and between 15:03 and 15:12
14	0782	2014-07-09 12:47:10	12:47:12	station keeping maneuver
15	0356	2014-07-29 15:22:00	15:39:45	altimeter gain calibration I2+Q2 (mostly over land)
15	0782	2014-08-13 12:47:06	12:47:08	station keeping maneuver
				.../...

cycle	pass	start time	stop time	event
16	0539	2014-09-09		No TM from 01:02:30 to 01:06:16 and from 01:09:25 to 01:14:08 due to the update of MNT onboard parameters
16	0640	2014-09-12 13:44:34	13:44:36	station keeping maneuver
16	0406 0474 0690	2014-09-04 09:44:24 2014-09-06 18:38:32 2014-09-14 07:36:44	09:47:15 18:41:55 07:38:50	several platform mispointing events caused by a rise in reaction wheel friction due to movement of lubricant. Only the 3 largest events are shown.
17	0324	2014-10-06 12:40:00	12:40:02	station keeping maneuver
17	0324-0414	2014-10-06 13:03:22	2014-10-09 16:27:46	safe hold mode
17	0438	2014-10-10 12:14:14	12:14:34	station keeping maneuver
17	0610	2014-10-16 12:26:26	12:26:35	station keeping maneuver
17	0958	2014-10-28 16:02:00	16:19:45	altimeter gain calibration I2&Q2
18	0152	2014-11-04 12:26:39	12:26:41	station keeping maneuver
18	0640	2014-11-21 13:39:10	13:39:12	station keeping maneuver
19	0182	2014-12-10 13:47:02	13:47:04	station keeping maneuver
19	0640	2014-12-26 13:44:42	13:44:45	station keeping maneuver
20		2015-01-12 11:30		software patch applied by ISRO in order to avoid zero-crossings of RW speed
20		2015-01-17	2015-01-18	platform pointing disturbance (fluctuations in RW friction)
				.../...

cycle	pass	start time	stop time	event
20	0412	2015-01-22 14:31:03	14:31:06	station keeping maneuver
20	0586	2015-01-28 16:11		CNG calibration
21	0268	2015-02-21 13:47:56	13:47:58	station keeping maneuver
22	0354	2015-03-31 13:50:16	13:50:18	station keeping maneuver. Delta_Vy twice more than expected.
22	0610	2015-04-09 12:28:10	12:28:14	station keeping maneuver to stop the westward drift.
22	0986	2015-04-22 15:30		CNG calibration
23	0954	2015-05-26 12:51:07	12:51:12	station keeping maneuver. Delta_V applied twice less than expected. thruster firing has taken place between 10:00 to 10:04 UT to control a reaction wheel error guidance has been performed with thrusters (instead of RW)
24	0554	2015-06-16 13:23	13:39	station keeping maneuver (to calibrate satellite rotation with thrusters). The main objective is not to recover the nominal ground track but to calibrate this new way of performing satellite rotation
24		2015-06-30		introduction of a leap second =¿ UTC = TAI-36s The sequence of dates of the UTC second markers is: 2015 June 30, 23h 59m 59s 2015 June 30, 23h 59m 60s 2015 July 1, 0h 0m 0s
24		2015-06-30		First MOE with GDR-E orbit standard
25				Orbit standard = GDR-E
25	0182	2015-07-08 13:40:55	13:40:58	station keeping maneuver (only with thrusters). Thruster activity is expected from 13:31:50 UT to 13:50 UT
25	0758	2015-07-28 16:22		Altika quarterly expertise CNG calibration
26	0152	2015-08-11 12:32:56	12:32:59	station keeping maneuver (to stop western drift and stay in the +/-1km ground track window) only with thrusters
				.../...

cycle	pass	start time	stop time	event
26	0524	2015-08-24 12:24:12	12:24:14	station keeping maneuver, performed only with thrusters.
26		2015-09-05	2015-09-06	mispointing events attributed to sudden changes in friction torque of reaction wheel (RW-4).
27		2015-09-15		Update of CoG historic file: the initial value of Zcog value has been updated by POD team and propagated to IDS teams through CoG historic file ; new value -0.6105 (instead of -0.6583)
28	0182	2015-10-21 13:41:40	13:41:43	station keeping maneuver
28	0195	2015-10-22		mising data due to issues on X-band stations network and the amount of TM_gaps
28	0614	2015-11-05 15:39		CNG Calibration
28	0812	2015-11-12 13:40:32	13:59:33	station keeping maneuver (3 bursts)

Table 3: *Events (red lines indicates safe hold mode event)*

2.3. Models and Standards History

During 2013 only GDR products in version T were available for cycles 1 to 7. These products were homogeneous and used all the Patch1 (see content of Patch 1 in chapter 11.1.).
At the beginning of 2014, improvements to Saral/AltiKa data have been applied with the Patch 2. This Patch 2 was applied from cycle 8 onwards and cycles 1 to 7 were reporcessed to provide a homogeneous GDR dataset. The content of Patch 2 in given in appendix 11.2., and the comparisons between Patch 1 and Patch 2 data can be found in [11]). The standards used in the GDR products version "T" Patch2 are listed in table 4.
From cycle 25 onwards (2015-07-02) GDR cycles were produced using the GDR-E orbit standard, but no reprocessing of previous cycles was performed.

Model	Product version "T" Patch2
Orbit	Based on Doris onboard navigator solution for OGDRS. DORIS tracking data for IGDRs DORIS+SLR tracking data for GDRs. Using POE-D, and POE-E from cycle 25
Altimeter Retracking	"Ocean MLE4" retracking: MLE4 fit from 2nd order Brown analytical model: MLE4 simultaneously retrieves 4 parameters from the altimeter waveforms: • Epoch (tracker range offset) → altimeter range • Composite Sigma → SWH • Amplitude → Sigma0 • Square of mispointing angle "Ice 1" retracking: Geometrical analysis of the altimeter waveforms, which retrieves the following parameters: • Epoch (tracker range offset) → altimeter range • Amplitude → Sigma0
	.../...

Model	Product version "T" Patch2
	"Ice 2" retracking: The aim of the ice2 retracking algorithm is to make the measured waveform coincide with a return power model, according to Least Square estimators. Retrieval of the following parameters: • Epoch → altimeter range • Width of the leading edge → SWH/ • Amplitude → Sigma0 • Slope of the logarithm of the waveform at the trailing edge → Mispointing angle/surface slope • the thermal noise level (to be removed from the waveform samples) "Sea Ice" retracking: In this algorithm, waveform parameterization based on peak threshold retracking is applied to the Ka-band waveform. From this parameterization, a tracking offset and backscatter estimate are determined. Tests are made on the extent of the tracking offset, and extreme values are flagged as retracking failures. The sea-ice waveform amplitude is determined by finding the maximum value of the waveform samples and the tracking offset is determined by finding the point on the waveform (by interpolation) where the waveform amplitude exceeds a threshold determined from the above sea-ice amplitude. A tracking offset is determined. The Centre Of Gravity offset correction must be included in the range measurement as the correction is not available separately in the L2 product. • Amplitude → Sigma0 • Tracking offset → altimeter range • Centre Of Gravity offset correction → correction to altimeter range measurement N.B.: the Ice2 retracking algorithm have been tuned to Ka-band since Patch2, but ont the Ice1 not Sea Ice algorithms
Altimeter Instrument Corrections	consistent with MLE4 retracking
Saral/AltiKa Radiometer Parameters	Using on-board calibration
	.../...

Model	Product version "T" Patch2
Dry Troposphere Range Correction	From ECMWF atmospheric pressures and model for S1 and S2 atmospheric tides
Wet Troposphere Range Correction from Model	From ECMWF model
Ionosphere correction	Based on Global Ionosphere TEC Maps from JPL
Sea State Bias Model	Hybrid SSB model from [12]
Mean Sea Surface	MSS_CNES-CLS11
Mean Dynamic Topography	MDT_CNES-CLS09
Geoid	EGM96
Bathymetry Model	DTM2000.1
Inverse Barometer Correction	Computed from ECMWF atmospheric pressures after removing S1 and S2 atmospheric tides
Non-tidal High-frequency De-aliasing Correction	Mog2D high resolution ocean model on (I)GDRs. None for OGDRs. Ocean model forced by ECMWF atmospheric pressures after removing S1 and S2 atmospheric tides.
Tide Solution 1	GOT4.8
Tide Solution 2	FES2012 + S1 and M4 ocean tides. S1 and M4 load tides ignored
Equilibrium long-period ocean tide model.	From Cartwright and Taylor tidal potential.
Non-equilibrium long-period ocean tide model.	Mm, Mf, Mtm, and Msqm from FES2004
Solid Earth Tide Model	From Cartwright and Taylor tidal potential.
Pole Tide Model	Equilibrium model
Wind Speed from Model	ECMWF model
Altimeter Wind Speed	wind speed model from [9]
Trailing edge variation Flag	Derived from Matching Pursuit algorithm (from J. Tournadre, IFREMER)
	.../...

Model	Product version "T" Patch2
Ice flag	Initialized in climatological areas based on wind speed values and updated by comparing the model wet tropospheric correction and the dual-frequency wet tropospheric correction retrieved from radiometer brightness temperatures

Table 4: Models and standards adopted for the Saral/AltiKa version "T" products (using Patch 2). Adapted from [4]

3. Data coverage and edited measurements

3.1. Missing measurements

3.1.1. Over land and ocean

Determination of missing measurements relative to the theoretically expected orbit ground pattern is an essential tool to detect missing telemetry or satellite events for instance. The number of missing measurements is routinely monitored by Cal/Val tools. Saral/AltiKa's performance regarding the number of missing measurements is compared to Jason-2, through the comparison of the percentage of missing measurements estimated in a consistent manner for the two missions.

AltiKa can use several on board tracking modes: Median, EDP (Earliest Detectable Part) and Diode/DEM (see chapter 2.2.1.). Median mode is similar to the one used by Envisat and for most cycles of Jason-2. EDP tracker should improve the tracker behavior above continental ice surfaces and hydrological zones. Finally, Diode/DEM mode is a technique using information coming from Diode and a digital elevation model available on board. It was already tested on Jason-2. For more information about the different on board tracker algorithms see [6]. The information about the acquisition / tracking mode used is available in the GDR (fields alt_state_flag_acq_mode_40hz and alt_state_flag_tracking_mode_40hz).
From cycle 4 onwards, Saral/AltiKa used the **DIODE acquisition / median tracking mode**, except for two short periods of autonomous DIODE acquisition at cycles 10 and 17.

Considering all surface types, Saral/AltiKa has more data available than Jason-2 (which also uses most of the time the median tracker), independently from the tracker mode used for Saral. Figure 1 shows the percentage of available measurements for Saral/AltiKa and Jason-2 (all surfaces) computed with respect to a theoretical possible number of measurements. As long as a record exists for a given date, the measurement is accounted as present (though it may be that there is no useful science data). Differences appear on land surfaces as shown in figure 2. The missing data are highly correlated with the mountains location. Note that the routine calibrations for Saral/AltiKa are done over desert regions, such as Sahara, over Australia, in the south of Africa and over Asia (Mongolia), the percentage of available data is therefore low in these regions. Otherwise Saral has more available data over land surface than Jason-2. This is probably due to the reduced footprint of Saral compared to Jason-2.

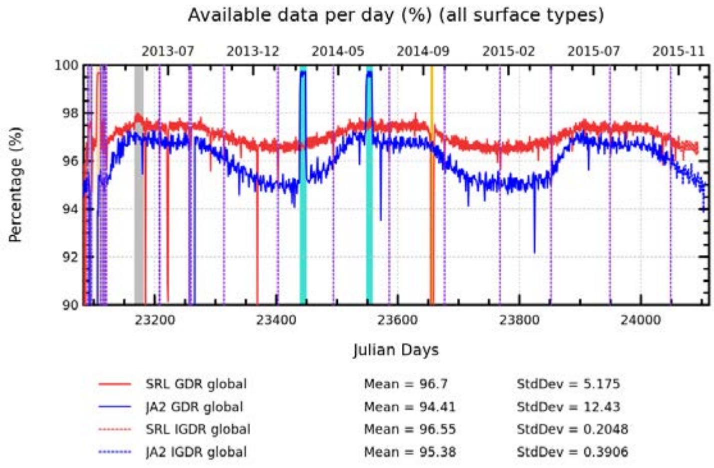

Figure 1: *Percentage of available measurements over all types of surfaces for SRL and JA2. Gray bands indicate when Saral/AltiKa uses EDP tracking, wheat color band indicates when Saral/AltiKa used Diode/DEM tracking, turquoise color band indicates when Jason-2 used Diode/DEM tracking, gold color band indicates when Saral/AltiKa is on safe-hold mode. Vertical dotted lines in lilac indicate days with special calibrations.*

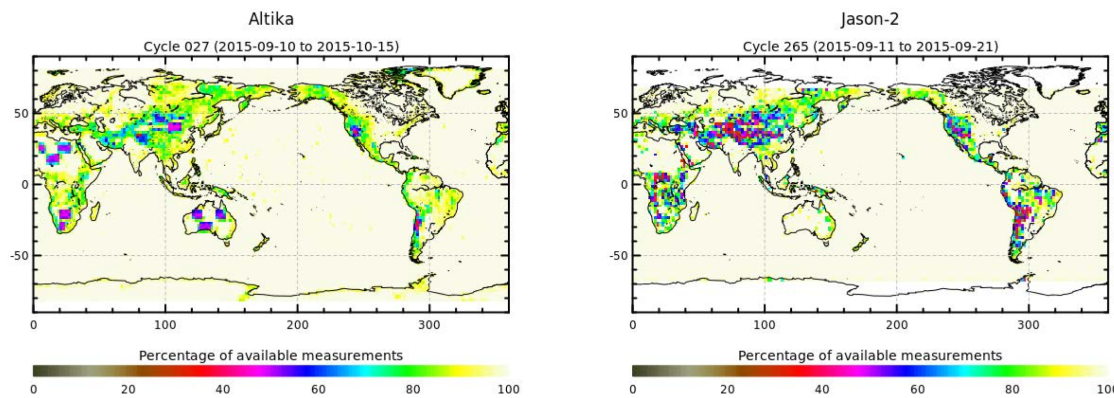

Figure 2: *Map of percentage of available measurements over land for Saral/AltiKa on cycle 27 and for Jason-2 on cycle 265 (right).*

3.1.2. Over ocean

When considering ocean surface, the same analysis method leads generally to slightly less available data for Saral/AltiKa compared to Jason-2 data coverage, as plotted on the left of figure 3, which represents the percentage of available measurements limited to ocean surfaces. Over the shown period, the mean value is about 97.1% for Jason-2, and 99.2% for Saral/AltiKa, but please consider that Jason-2 encoutered two safe-hold mode periods and Saral/AltiKa one safe-hold mode period, which explains the globally lower value for Jason-2. Saral/AltiKa had other periods with reduced data availability. All these events are described on table 3.

On the right of figure 3, the percentage of available measurements is plotted without taking into account the days where instrumental events or other big anomalies occurred. The mean value of available measurements increases to 99.98% for Jason-2 and 99.88% for Saral/AltiKa. These 0.1% of fewer data over ocean for Saral/AltiKa compared to Jason-2 are likely due to the impact of rain due to the Ka-band frequency. This exceeds largely the specifications for Saral/AltiKa, which were (see [14]) 95% of all possible over-ocean data during a 3-year period with no systematic gaps plus the specific Ka-band limitation (5% of measurements may be not achieved due to rain rates > 1.5 mm/h according to geographic areas).

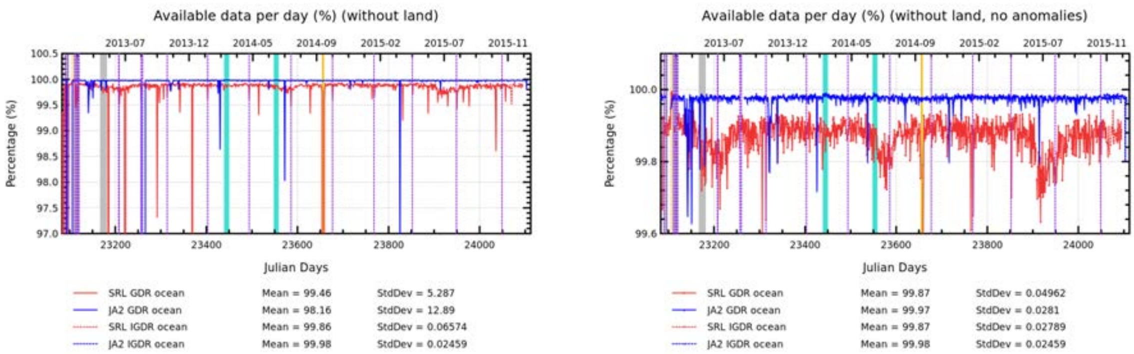

Figure 3: *Cycle per cycle percentage of available measurements over ocean (left) and without anomalies (right) for Saral/AltiKa and Jason-2. Gray bands indicate when Saral/AltiKa uses EDP tracking, wheat color band indicates when Saral/AltiKa used Diode/DEM tracking, turquoise color band indicates when Jason-2 used Diode/DEM tracking, gold color band indicates when Saral/AltiKa is on safe-hold mode. Lilac vertical lines, indicate days with special calibrations, which can be over ocean.*

3.2. Edited measurements

3.2.1. Editing criteria definition

Editing criteria are used to select valid measurements over ocean. The editing process is divided into 4 parts. First, only measurements over ocean and lakes are kept (see section 3.2.2.). Second, some flags are used as described in section 3.2.3.. Note that the rain flag is not usable yet in the GDR products (always set to zero). But most measurements corrupted by rain are well detected by other altimeter parameter criteria. Then, threshold criteria are applied on altimeter, radiometer and geophysical parameters and are described in the table 5. Moreover, a spline criterion is applied to remove the remaining spurious data. For each criterion, the day per day percentage of edited measurements has been monitored. This allows detection of anomalies in the number of removed data, which could come from instrumental, geophysical or algorithmic changes. Cycle per cycle statistics of edited data are also routinely monitored, but not shown here, as only a few cycles are available.
Note that the altimeter wind speed is usable since the GDR-T Patch2 has been applied.

Parameter	Min thresholds	Max thresholds	mean edited
Sea surface height	$-130\,m$	$100\,m$	0.47%
Sea level anomaly	$-2\,m$	$2\,m$	0.79%
Number measurements of range	20	*Not applicable*	1.10%
Standard deviation of range	0	$0.2\,m$	1.50%
Squared off-nadir angle	$-0.2\,deg^2$	$0.0625\,deg^2$	0.39%
Dry troposphere correction	$-2.5\,m$	$-1.9\,m$	0.00%
Inverted barometer correction	$-2\,m$	$2\,m$	0.00%
Radiometer wet troposphere correction	$-0.5m$	$0\,m$	0.06%
Significant wave height	$0\,m$	$11\,m$	0.41%
Sea State Bias	$-0.5\,m$	$0.0025\,m$	0.29%
Number measurements of Ka-band Sigma0	20	*Not applicable*	1.03%
Standard deviation of Ka-band Sigma0	0	$1\,dB$	0.94%
Ka-band Sigma0	$3\,dB$	$30\,dB$	0.35%
Ocean tide	$-5\,m$	$5\,m$	0.18%
Equilibrium tide	$-0.5\,m$	$0.5\,m$	0.17%
			.../...

Parameter	Min thresholds	Max thresholds	mean edited
Earth tide	$-1\,m$	$1\,m$	0.00%
Pole tide	$-0.15\,m$	$0.15\,m$	0.00%
Altimeter wind speed	$0\,m.s^{-1}$	$30\,m.s^{-1}$	0.29%
All together	-	-	2.60%

Table 5: *Editing thresholds, statistics obtained for cycles 1 to 28*

3.2.2. Selection of measurements over ocean and lakes

In order to remove data over land, a land-water mask is used (surface_type field in the GDR products). Only measurements over ocean or lakes are kept. This allows to keep data near the coasts and to detect potential anomalies in these areas. Furthermore, there is no impact on global performance estimations since the most significant results are derived from analyzes in deep ocean areas. Figure 4 shows the day per day percentage of measurements eliminated by this selection. The curve is quite stable even after the safe-hold mode. But it reveals the impact of the different altimeter tracking modes: when the DIODE/DEM (digital elevation model) tracking mode is used (wheat colored stripe), slightly more data are edited by land flag. This is an expected result: less data are missing in DIODE/DEM mode over land, as a consequence there is a higher percentage of edited data.

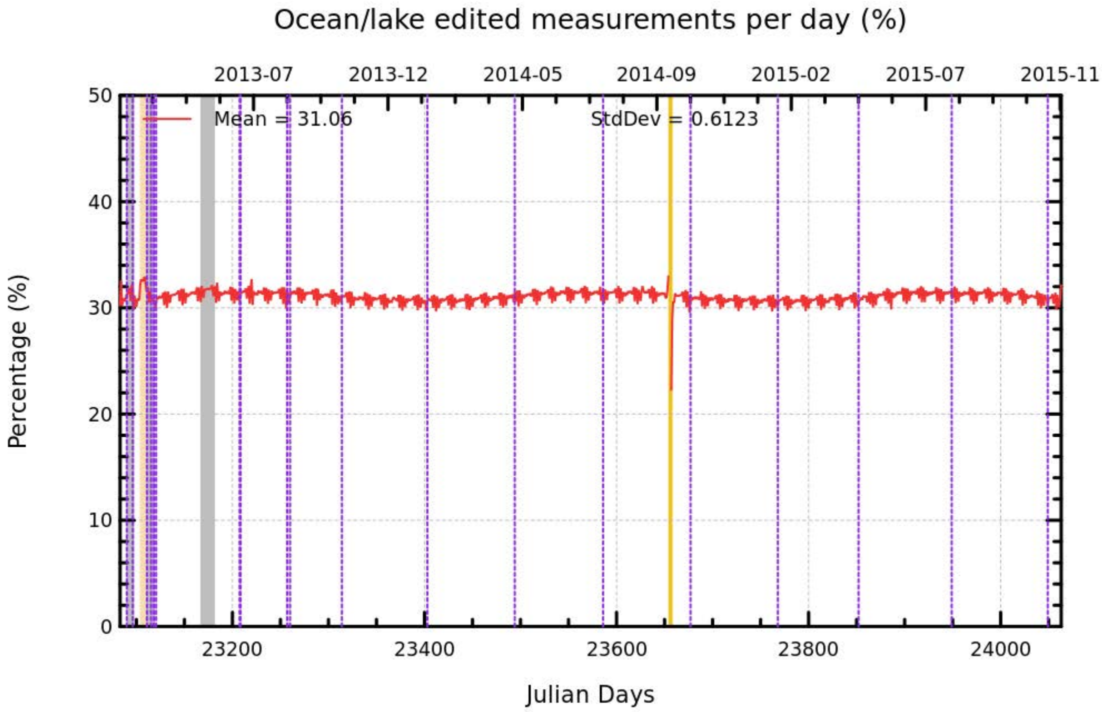

Figure 4: *Day per day percentage of eliminated measurements during selection of ocean/lake measurements. Gray bands indicate when Saral/AltiKa uses EDP tracking, wheat color band indicates when Saral/AltiKa used Diode/DEM tracking, elsewhere Median tracking is used. Gold color band indicates when Saral/AltiKa is on safe-hold mode. Vertical dotted lines in lilac indicate days with special calibrations.*

3.2.3. Flagging quality criteria: Ice flag

The ice flag (ice_flag in the GDR products) is used to remove the sea ice data. Left of figure 5 shows the day per day percentage of measurements edited by this criterion. Over the shown period, no anomalous trend is detected but the nominal seasonal cycle is visible. Considering the black curve, which indicates the percentage of edited Saral/AltiKa data without geographical selections, the minima (∼16% of edited data) appears yearly in February and September. These are also the periods where the antarctic or arctic sea ice extension are minimum. The maxima (∼20% of edited data) of the curve are around May/June and October/November. These are the periods, where arctic or antarctic sea ice extension have approximately mid-values. When limited to |latitude| <66°, Saral/AltiKa and Jason-2 percentage of data edited by sea ice have a similar annual cycle, which is correlated to the antarctic sea ice extension. Indeed, the maximum number of points over ice is reached during the southern winter (ie. August - October). When limiting measurements between 66° north and south, thawing of sea ice, which takes place especially in northern hemisphere over 66°N, can not be detected. The percentage of measurements edited by ice flag is plotted in the right of figure 5 for all the period since the beginning of mission. White color indicates when the flag is set to 0 (no ice).

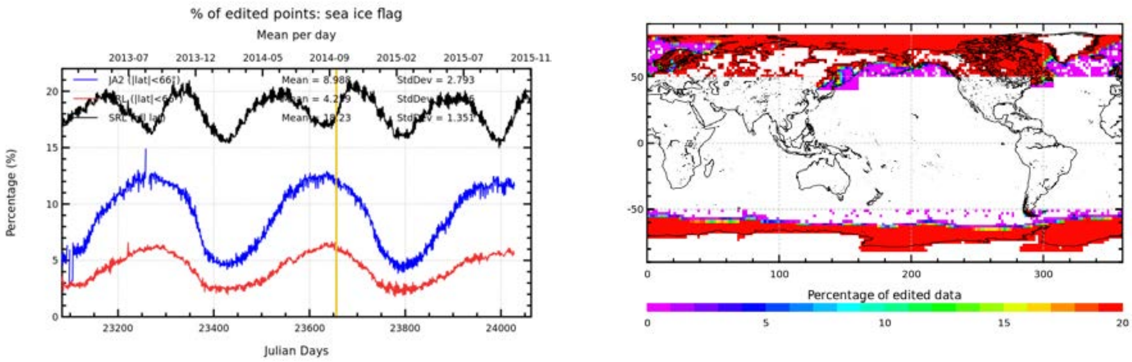

Figure 5: *Percentage of edited measurements by ice flag criterion. Left: Daily statistics for GDR Saral/AltiKa (all latitudes: black, limited to 66° latitude: red) and Jason-2 (blue). Gold color band indicates when Saral/AltiKa is on safe-hold mode. Right: Map since beginning of mission (cycles 1 to 28).*

3.2.4. Threshold criteria: Global

The quality of instrumental and geophysical parameters is checked with respect to thresholds, after having selected only ocean/lakes measurements and removing sea ice with the ice flag. Note that no measurement is edited by the following corrections : dry troposphere correction, inverted barometer correction (including DAC), equilibrium tide, earth and pole tide. Indeed these parameters are only verified in order to detect data at default values, which might happen during a processing anomaly.

The percentage of edited measurements using each criterion is monitored on a day per day basis (figure 6). The mean percentage of edited measurements is about 2.6% (2.4% when |latitude| is limited to 66°). This is about 1% below the Jason-2 figure. Some weak variation is visible.

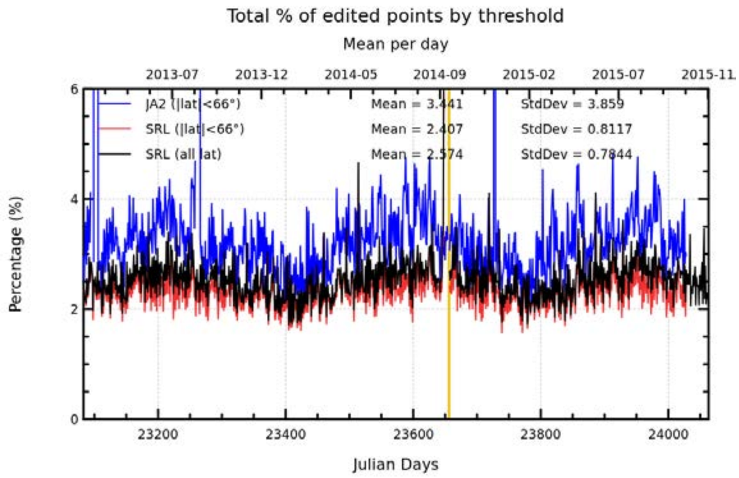

Figure 6: *Daily statistics of percentage of edited measurements by threshold criteria for GDR Saral/AltiKa (all latitudes: black, limited to 66° latitude: red) and Jason-2 (blue). Gold color band indicates when Saral/AltiKa is on safe-hold mode.*

3.2.5. Threshold criteria: 40-Hz measurements number

The percentage of edited measurements because of a too low number of 40-Hz measurements is represented on the left side of figure 7. No trend nor any anomaly has been detected. The statistics, when limiting the latitude to less than 66° are slightly reduced. The percentage of edited data is similar for SARAL/AltiKa and Jason-2.

The map of measurements edited by 40-Hz measurements number criterion is plotted on right side of figure 7 and shows correlation with heavy rain and wet areas (in general regions with disturbed sea state), as well as regions close to sea ice. Indeed waveforms are distorted by rain cells or sigma bloom events, which makes them often meaningless for SSH calculation. As a consequence, edited measurements due to several altimetric criteria are often correlated with wet areas (rain cells/sigma bloom events).

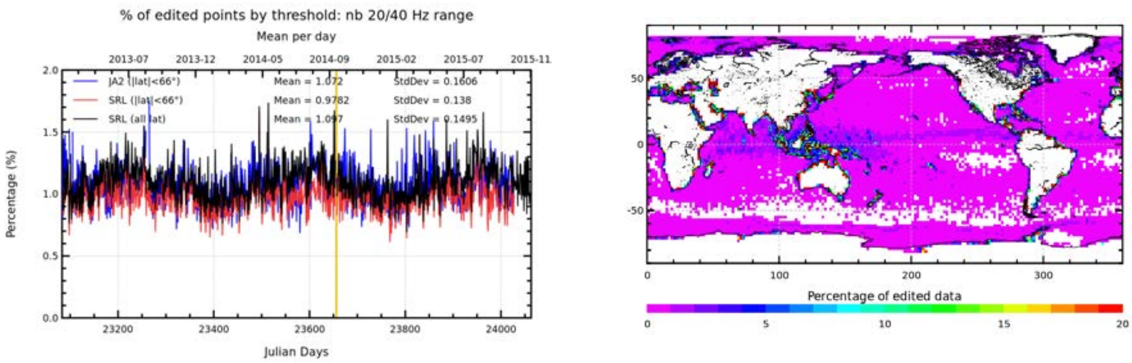

Figure 7: *Percentage of edited measurements by 40-Hz measurements number criterion (20-Hz for Jason-2). Left: Daily statistics for SARAL/AltiKa (all latitudes: black, limited to 66° latitude: red) and Jason-2 (blue). Gold color band indicates when SARAL/AltiKa is on safe-hold mode. Right: Map since beginning of mission (cycles 1 to 28).*

3.2.6. Threshold criteria: 40-Hz measurements standard deviation

The percentage of edited measurements due to 40-Hz measurements standard deviation criterion (∼1.5%) is shown in figure 8 (left). Several days show an increase in the numbre of data edited by this criterion. These are mostly due to safe-hold mode or to maneuver burns (see also table 3), indicated by green vertical lines. In this case, the data a few minutes before and after the maneuver are edited (in general several parameters are out of thresholds) as a consequence of the lower platform pointing accuracy. Since cycle 24, platform pointing during maneuvers is achieved by the thrusters instead of the reaction wheels. The impact of this change on the number of edited GDR data is small. The right side of figure 8 shows a map of measurements edited by the 40-Hz measurements standard deviation criterion. As in section 3.2.5., edited measurements are correlated with wet areas.

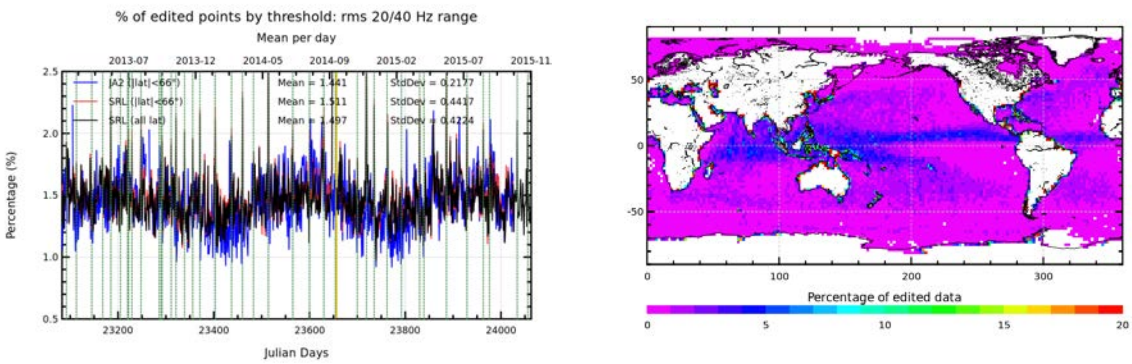

Figure 8: *Percentage of edited measurements by 40-Hz measurements standard deviation criterion (20-Hz for Jason-2). Left: Daily statistics for Saral/AltiKa (all latitudes: black, limited to 66° latitude: red) and Jason-2 (blue). Green vertical lines indicate days with maneuvers on Saral/AltiKa and gold band indicates the safe-hold mode on Saral/AltiKa. Right: Map since beginning of mission (cycles 1 to 28).*

3.2.7. Threshold criteria: Significant wave height

The percentage of edited measurements due to significant wave height criterion is represented in figure 9. It is about 0.42%. As for standard deviation of 40-Hz data, several days show an increased numbre if data edited by this criterion. Again, this is mostly due to safe-hold mode and maneuver burns (see also table 3), indicated by green vertical lines. In this case, the data a few minutes before and after the maneuver are edited. Note that for Jason-2, roughly 0.66% of data are edited by SWH out of thresholds. This is mainly due to Jason-2 having almost twice as much SWH data at default values than Saral/AltiKa. Figure 9 (right part) shows that measurements edited by SWH criterion are especially found in wet regions where heavy rains and sigma bloom events can occur, as well as in high sea state regions.

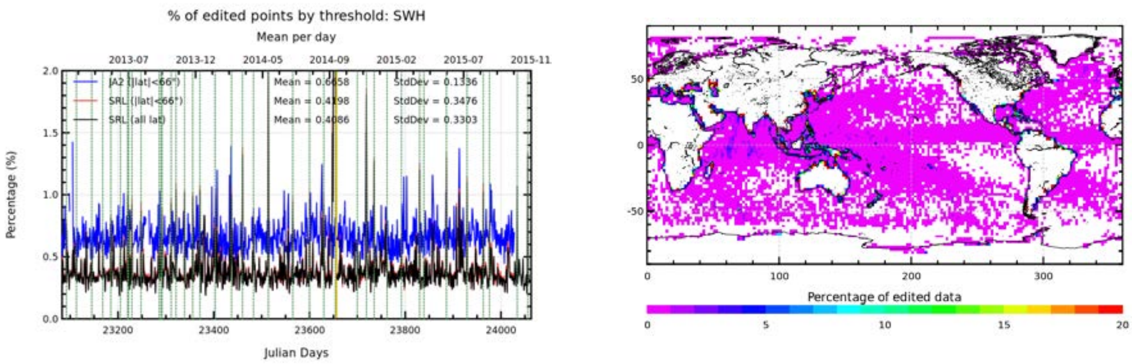

Figure 9: *Percentage of edited measurements by SWH criterion. Left: Daily statistics for GDR Saral/AltiKa and Jason-2 (blue). Green vertical lines indicate days with maneuvers on Saral/AltiKa and gold band indicates the safe-hold mode on Saral/AltiKa. Right: Map since beginning of mission (cycles 1 to 28).*

3.2.8. Backscatter coefficient

The percentage of edited measurements due to backscatter coefficient criterion is represented in figure 10. It is about 0.35% (whether considering all latitudes or limiting to 66°), compared to 0.61% for Jason-2. It is also impacted by the safe-hold mode and most of the maneuvers (see vertical green lines). As for SWH, Jason-2 has almost twice as much backscattering values at default values than SARAL/AltiKa. The right part of figure 10 shows that measurements edited by backscatter coefficient criterion are especially found in wet regions where measurements are impacted by rain or sigma bloom events.

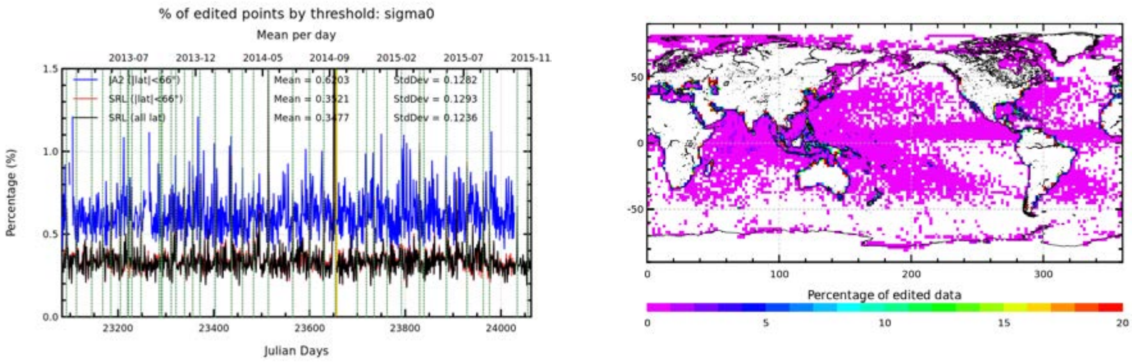

Figure 10: *Percentage of edited measurements by Sigma0 criterion. Left: Daily statistics for Saral/AltiKa (all latitudes: black, limited to 66° latitude: red) and Jason-2 (blue). Green vertical lines indicate days with maneuvers on Saral/AltiKa and gold band indicates the safe-hold mode on Saral/AltiKa. Right: Map since beginning of mission (cycles 1 to 28).*

3.2.9. Backscatter coefficient: 40 Hz standard deviation

The percentage of edited measurements due to 40 Hz backscatter coefficient standard deviation criterion is represented in figure 11. It is about 0.94%, compared to 1.99% for Jason-2. It is also impacted by the safe-hold mode and some of the maneuvers (see vertical green lines). The right part of figure 10 shows that measurements edited by 40 Hz backscatter coefficient standard deviation criterion are mostly found in wet regions.

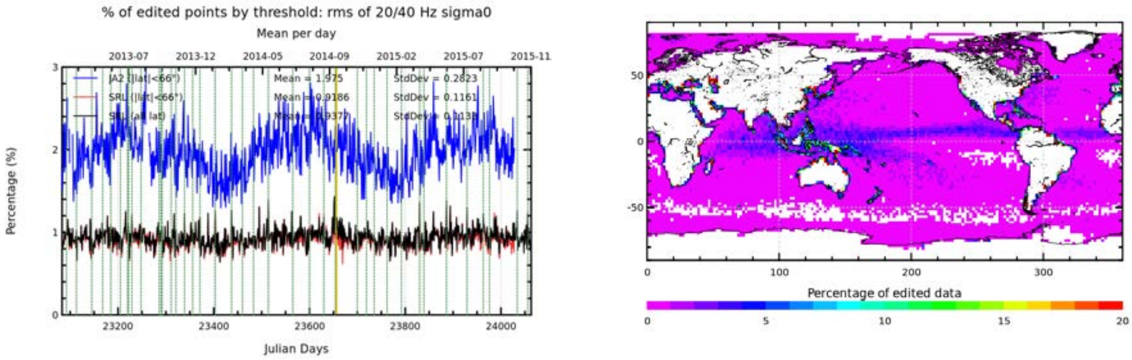

Figure 11: *Percentage of edited measurements by 40 Hz Sigma0 standard deviation criterion. Left: Daily statistics for Saral/AltiKa (all latitudes: black, limited to 66° latitude: red) and Jason-2 (blue). Green vertical lines indicate days with maneuvers on Saral/AltiKa and gold band indicates the safe-hold mode on Saral/AltiKa. Right: Map since beginning of mission (cycles 1 to 28).*

3.2.10. Radiometer wet troposphere correction

The percentage of edited measurements due to radiometer wet troposphere correction criterion is represented in figure 12. It is about 0.06%. Jason-2 edits generally slightly less data (except after safe-hold modes, when the radiometer is switched on some time after the altimeter). The edited data for Saral/AltiKa are generally due to wet troposphere wetter than the −0.5 m threshold.

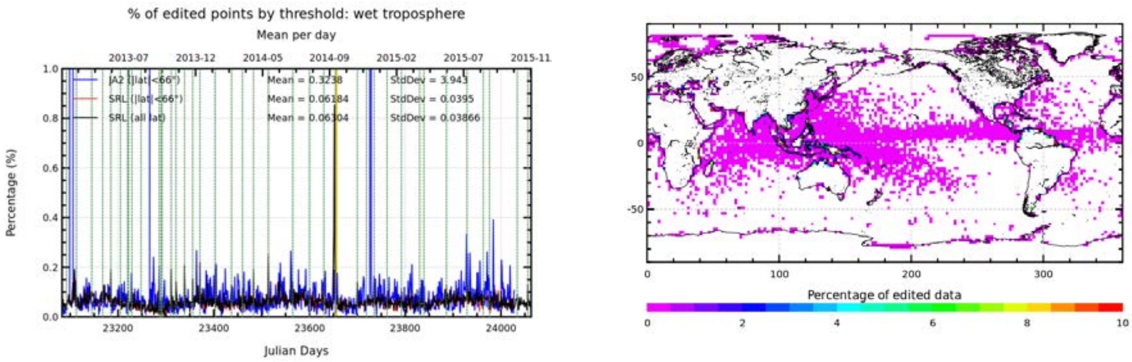

Figure 12: *Percentage of edited measurements by radiometer wet troposphere criterion. Left: Daily statistics for Saral/AltiKa (all latitudes: black, limited to 66° latitude: red) and Jason-2 (blue). Green vertical lines indicate days with maneuvers on Saral/AltiKa and gold band indicates the safe-hold mode on Saral/AltiKa. Right: Map since beginning of mission (cycles 1 to 28).*

3.2.11. Square off-nadir angle

The percentage of edited measurements due to square off-nadir angle criterion is represented in figure 13. It is about 0.42% (when considering all latitudes, and 0.34% when considering only data with latitudes up to 66°). As for other parameters, maneuvers have an impact on the number of edited data. The daily mean increases a few weeks before the safe-hold mode and stays high after the safe-hold mode. These high values are caused by a rise in reaction wheel friction due to movement of lubricant (see section 7.1. for more details) causing platform pointing errors. The map 13 shows that edited measurements are mostly found in wet regions or places, where the maneuvers take place (Indian Ocean).

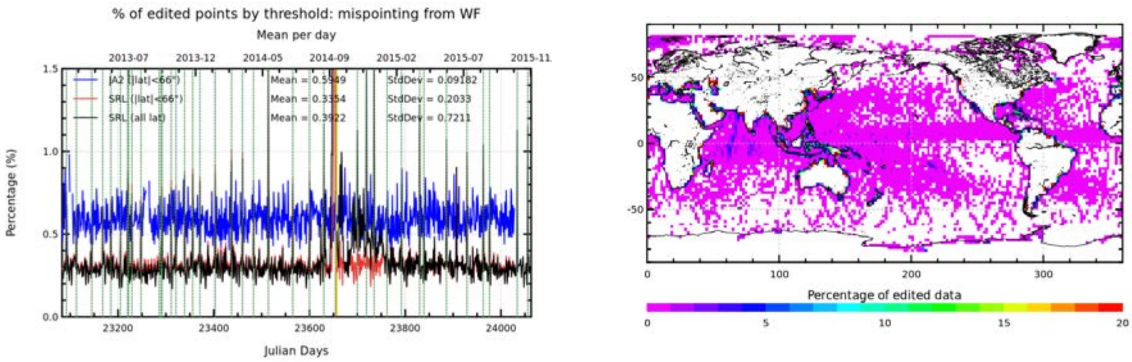

Figure 13: *Percentage of edited measurements by square off-nadir angle criterion. Left: Daily statistics for Saral/AltiKa (all latitudes: black, limited to 66° latitude: red) and Jason-2 (blue). Green vertical lines indicate days with maneuvers on Saral/AltiKa and gold band indicates the safe-hold mode on Saral/AltiKa. Right: Map since beginning of mission (cycles 1 to 28).*

3.2.12. Sea state bias correction

The percentage of edited measurements due to sea state bias correction criterion is represented in figure 14. The percentage of edited measurements is about 0.29% and increases when maneuver take place. The percentage of edited Jason-2 on the same criterion is about twice as high, mainly due to more data at default value as a consequence of SWH and *sigma*0 values at default.
The map 14 shows that edited measurements are mostly found in wet regions and the Artic.

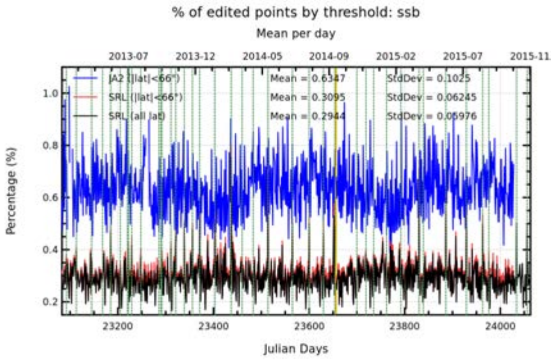

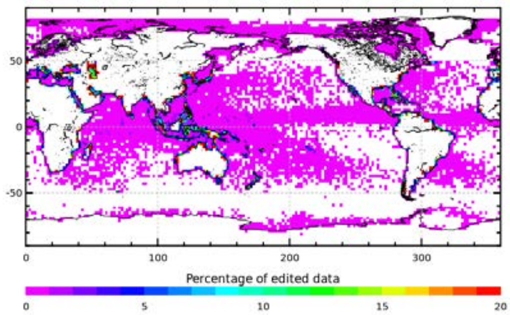

Figure 14: *Percentage of edited measurements by sea state bias criterion. Left: Daily statistics for Saral/AltiKa (all latitudes: black, limited to 66° latitude: red) and Jason-2 (blue). Green vertical lines indicate days with maneuvers on Saral/AltiKa and gold band indicates the safe-hold mode on Saral/AltiKa. Right: Map since beginning of mission (cycles 1 to 28).*

3.2.13. Altimeter wind speed

The percentage of edited measurements due to altimeter wind speed criterion is represented in figure 15. It is about 0.29%. The measurements are mostly edited when sigma0 shows very high values (higher than 25 dB) or default values, which occur during sigma bloom and also over sea ice. Indeed, the wind speed algorithm (which uses backscattering coefficient and significant wave height) can not retrieve values for sigma0 higher than 25 dB. For such backscattering values, wind speeds would in any case be very low.
Wind speed is also edited during maneuvers, or when it has negative values, which can occur in GDR products. Therefore, the percentage of edited altimeter wind speed is similar to the percentage of edited sea state bias.

The map 15 showing percentage of measurements edited by altimeter wind speed criterion is correlated with maps 14 and 9.

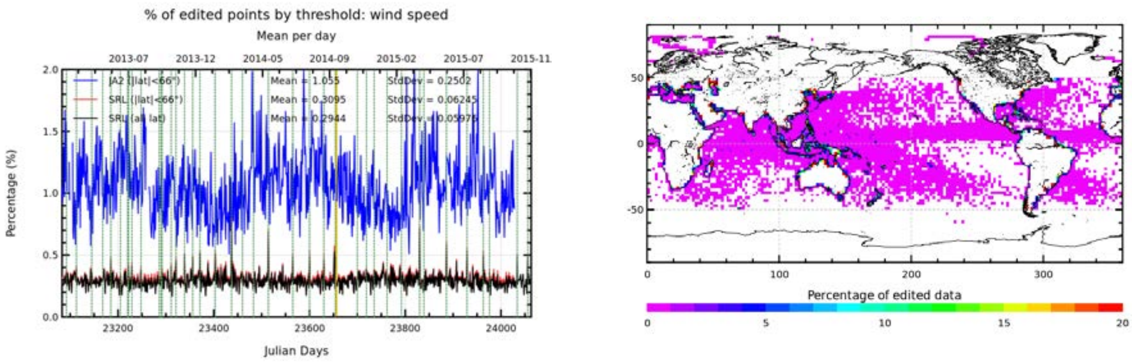

Figure 15: *Percentage of edited measurements by altimeter wind speed criterion. Left: Cycle per cycle monitoring. Green vertical lines indicate days with maneuvers on Saral/AltiKa and gold band indicates the safe-hold mode on Saral/AltiKa. Right: Map since beginning of mission (cycles 1to 28).*

3.2.14. Ocean tide correction

The percentage of edited measurements due to ocean tide correction criterion is represented in figure 16. It is about 0.18% which is greater than the percentage edited by Jason-2 (0.009%). Since the launching of the GDR-T Patch2 version, the geocentric ocean tide (GOT4.8) has no data over land, including enclosed water bodies such as Caspian Sea. Furthermore this impacts some data near coasts. This is due to the equilibrium long-period tide height (included in the global ocean tide) which, for Patch2, is computed with FES2012 algorithm, which tests previously if the grid of the FES2012 tide atlas is defined or not. Consequently, the equilibrium tide is set to default values over land (and therefore also the geocentric ocean tide).
That explains the presence of edited data (map 16) near coasts and in Caspian Sea.

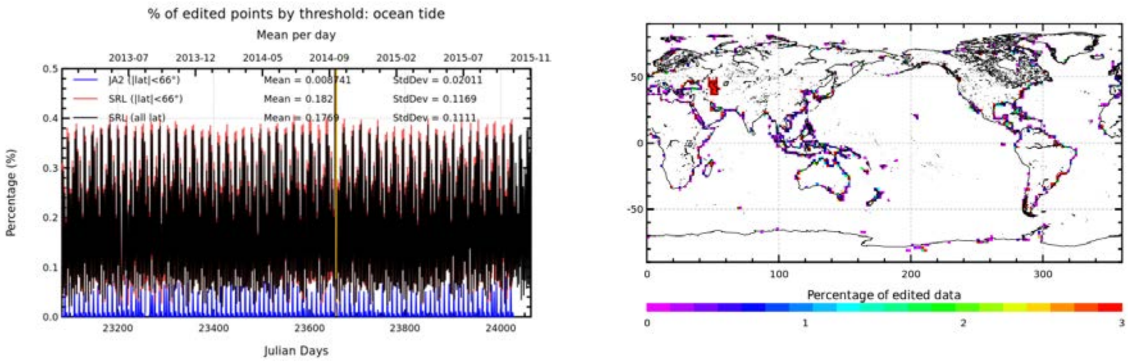

Figure 16: *Percentage of edited measurements by ocean tide criterion. Left: Daily statistics for Saral/AltiKa (all latitudes: black, limited to 66° latitude: red) and Jason-2 (blue). Gold band indicates the safe-hold mode on Saral/AltiKa. Right: Map since beginning of mission (cycles 1 to 28).*

3.2.15. Sea surface height

The percentage of edited measurements due to sea surface height (orbit - Ka-band range) criterion is represented in figure 17. It is about 0.47% (considering all latitudes and 0.49% considering only data with latitudes up to 66°). The measurements edited by sea surface height criterion are mostly found near coasts in equatorial and mid-latitude regions, as well as for regions with low significant wave heights (see map 17). The majority of the edited measurements has defaulted range values, due to default values of the sea state bias and the ocean tide correction.

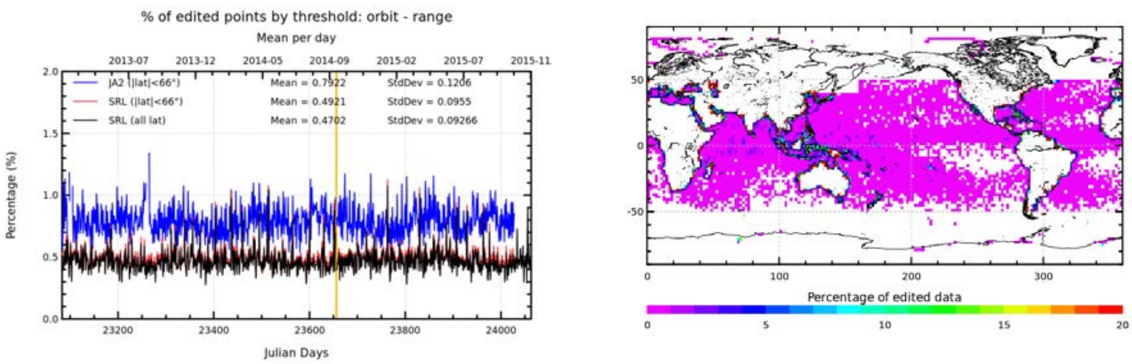

Figure 17: *Percentage of edited measurements by sea surface height criterion. Left: Daily statistics for Saral/AltiKa (all latitudes: black, limited to 66° latitude: red) and Jason-2 (blue). Gold band indicates the safe-hold mode on Saral/AltiKa. Right: Map since beginning of mission (cycles 1 to 28).*

3.2.16. Sea level anomaly

The percentage of edited measurements due to sea level anomaly criterion is represented in figure 18. It is about 0.80% (considering all latitudes and 0.76% considering only data with latitudes up to 66°). During maneuvers, the percentage of edited data is generally slightly increased as well as before safe-hold mode.
Whereas the map in figure 18 allows us to plot the measurements edited due to sea level anomaly out of thresholds (after applying all other threshold criteria). There are only very few measurements, mostly located near Antarctic, when data were neither edited by surface type flag nor by ice flag.

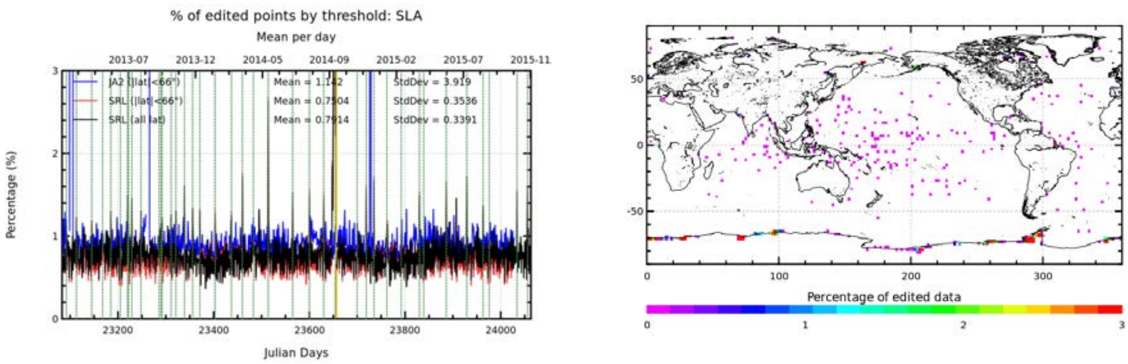

Figure 18: *Percentage of edited measurements by sea level anomaly criterion. Left: Daily statistics for Saral/AltiKa (all latitudes: black, limited to 66° latitude: red) and Jason-2 (blue). Green vertical lines indicate days with maneuvers on Saral/AltiKa and gold band indicates the safe-hold mode on Saral/AltiKa. Right: Map since beginning of mission (cycles 1 to 28).*

4. Monitoring of altimeter and radiometer parameters

4.1. Methodology

Both mean and standard deviation of the main parameters of **valid** Saral/AltiKa (GDR-T Patch2) data have been monitored since the beginning of the mission. Therefore ordinary daily statistics have been computed, but also box statistics with weighting based on latitude. Indeed, as the measurement distribution is not homogeneous with latitude, this can skew the statistics to values of the data in data-rich latitudes. Moreover, a comparison with Jason-2 parameters has been performed to monitor the stability of both missions. As both satellites are on different ground tracks no point-to-point comparisons (as it was possible during flight formation phase between Jason-1 and Jason-2) are feasible. Comparisons are done by superposing daily or cycle per cycle statistics or histograms. Furthermore, parameters are averaged on a grid-structure for both satellites, which are then subtracted one from the other. Another mean of comparison are dispersion diagrams between Saral/AltiKa and Jason-2 data at 3h-crossover points.

Note that for daily monitoring, there are some gaps end of March/ early April and in September 2013 for Jason-2 and in October 2014 (from October 6 to 9) for Saral/AltiKa. These gaps due to safe-hold modes on both missions.
Most of the monitoring is this sections are based GDR data in plain lines and are continued with IGDR data in dotted lines.

4.2. 40 Hz Measurements

The monitoring of the number and standard deviation of 40 Hz elementary range measurements used to derive 1 Hz data is presented here. These two parameters are computed during the altimeter ground processing. For both SARAL/AltiKa and Jason-2, before performing a regression to derive the 1 Hz range from 40 Hz or 20 Hz data, a MQE (mean quadratic error) criterion is used to select valid 40/20 Hz measurements. This first selection step consists in verifying that the 40/20 Hz waveforms can be approximated by a Brown echo model (Brown, 1977 [3]) (Thibaut et al. 2002 [15]). Then, through an iterative regression process, elementary ranges too far from the regression line are discarded until convergence is reached. Thus, monitoring the number of 40/20 Hz range measurements and the standard deviation computed among them is likely to reveal changes at instrumental level.

4.2.1. 40 Hz measurements number

Number of elementary 40 Hz range measurements is close to 38.5 (black curve on figure 19). Before the correction of the PF/RF alignment (alignment between the platform and the radiofrequency axis) on 25th of April 2013 this value was slightly higher (around 38.6). Jason-2 has an average close to 19.6 as number of elementary 20 Hz range measurements (which is when multiplied by 2, resulting in higher value than Saral/AltiKa). It also shows smaller temporal variability. Note that before Patch1 version, the MQE threshold was not applied during the 40 Hz to 1 Hz compression (IGDR data till cycle 4, pass 394), the daily mean of the number of the elementary 40 Hz range measurements was 39.0. So on average 0.5 40 Hz elementary range measurements are removed during the 40 Hz to 1 Hz compression by the MQE criteria. These removed data might be due to perturbations in the footprint (rain, sigma bloom). For both missions, the number of elementary range measurements is correlated with the significant wave height (and, for SARAL/AltiKa, with sea ice extent). Figure 20 shows less elementary range measurements around Indonesia, the Mediterranean Sea and close to coasts, which are all regions of low significant wave heights (see also map of SWH 30) and therefore regions where sigma bloom may occur and also rain areas. High latitudes also show a lower number of range elementary measurements, due to the presence of sea-ice.

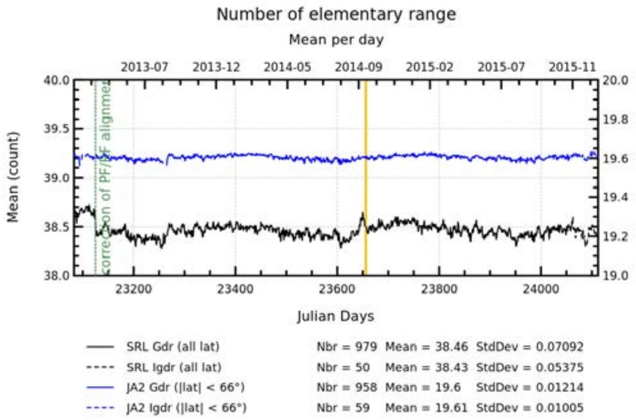

Figure 19: *Daily monitoring of mean of number of elementary Saral/AltiKa 40 Hz (left ordinate) and Jason-2 20 Hz (right ordinate) range measurements. The gold band indicates the safe hold mode on Saral/AltiKa.*

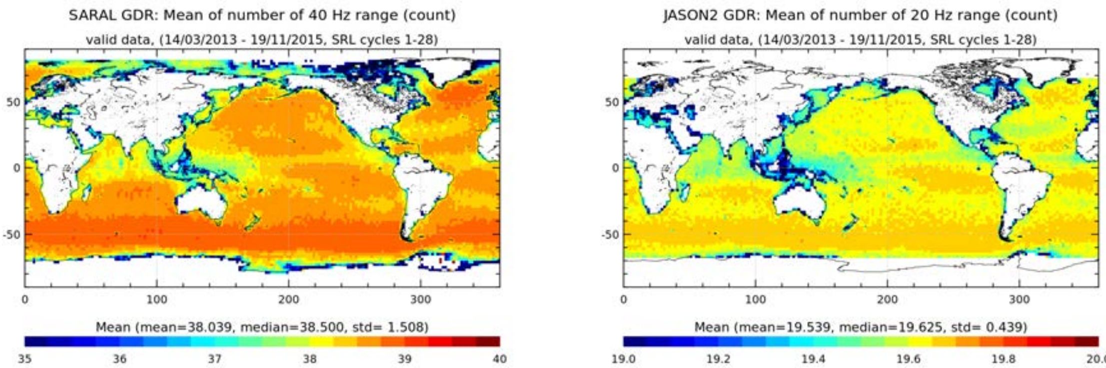

Figure 20: *Average map of number of Saral/AltiKa elementary 40 Hz range measurements (left) and Jason-2 elementary 20 Hz range measurement (right) over cycles 1 to 28.*

4.2.2. 40 Hz measurements standard deviation

Saral/AltiKa standard deviation of the 40 Hz measurements is 5.7 cm, whereas it is 8.0 cm for Jason-2 (right side of figure 21). Using latitude weighted box statistics (left side of figure 21), these values decrease to respectively 5.6 and 7.7 cm. These values are very close to the ones found when computing the power spectrum. The value of Saral/AltiKa is lower than the one of Jason-2 due to the altimeter band-width, which is 480 MHz for Saral/AltiKa instead of 320 MHz for Jason-2 (see [13]). As for the number of elementary range measurements, the standard deviation of the elementary range measurements are correlated to the significant wave height (see maps on figures 22 and 30).

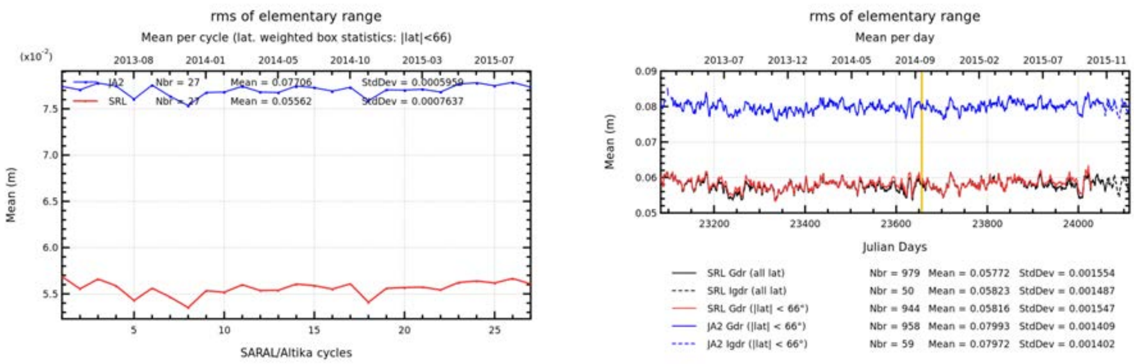

Figure 21: *Cyclic monitoring of rms of elementary 40/20 Hz range measurements for Saral/AltiKa and Jason-2 (left), computing latitude weighted box statistics. Daily mean of rms of elementary Saral/AltiKa 40 Hz and Jason-2 20 Hz range measurements (right). GDR data are plotted with plain lines, IGDR with dotted lines. The gold band indicates the safe hold mode on Saral/AltiKa.*

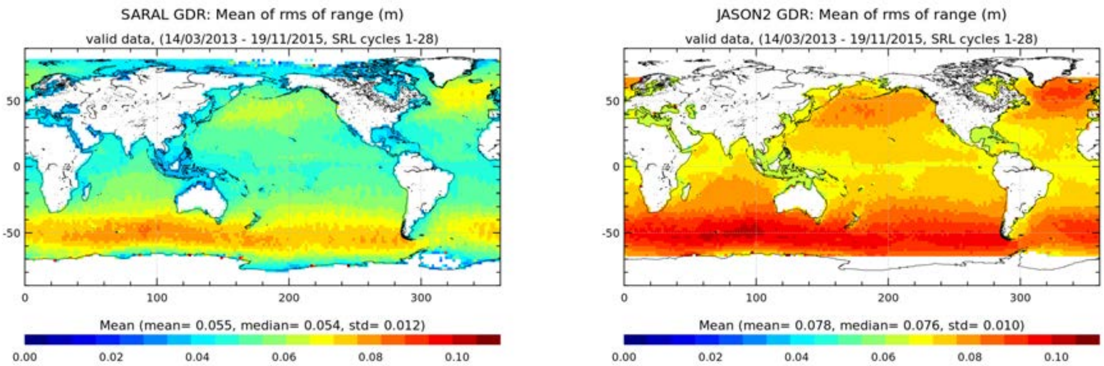

Figure 22: *Average map of rms of Saral/AltiKa elementary 40 Hz range measurements (left) and Jason-2 elementary 20 Hz range measurement (right) over cycles 1 to 28.*

4.3. Off-Nadir Angle from waveforms

The off-nadir angle is estimated from the waveform shape during the altimeter processing. The off-nadir angle, averaged on a daily basis, has been plotted for Saral/AltiKa and Jason-2 on the left side of figure 23, whereas the right side shows the daily standard deviation of the off-nadir angle from waveforms. In the beginning of the Saral/AltiKa mission the off-nadir angle from waveforms was slightly positive (around 0.003 degrees2), a X-cross calibration maneuver with $+0.3^{\circ}/-0.3^{\circ}$ in pitch and than $+0.3^{\circ}/-0.3^{\circ}$ in roll was done on 22th of April 2013 (see N. Stenou [13]). This allowed to determine that a correction of -0.045 degree in pitch direction was necessary. It was performed on April 25$^{\text{th}}$, 2013. A last X-cross calibration on April 30$^{\text{th}}$, 2013 showed that the correction was successful. Off-nadir angle from waveforms stayed from this day on close to zero and very stable spatially and temporally. Nevertheless, a few variations appeared during summer 2014 caused by a rise in reaction wheel friction due to movement of lubricant. This event ended with the loss of a wheel and an important increase of the daily mean of the off-nadir angle leading to a safe-hold mode between 6th and 9th of October 2014. After the safe-hold mode, the daily mean of the mispointing is not as stable as it used to be at the beginning of the mission, as illustrated by the slight rise of the daily standard deviation. These mispointing events are associated with zero-crossings of the RW speed. A patch was applied toa void these zero-crossings, resulting on a better pointing accuracy. However some mispointing events still randomly occur due to RW friction. The investigations performed this year on SARAL/AltiKa mispointing are further detailed in section 7.1.. Though Jason-2 off-nadir angle from waveforms is also close to zero (though mostly slightly negative), it shows more variations. Standard deviation of the off-nadir angle from waveforms is also higher for Jason-2 than for Saral/AltiKa (right of figure 23). This is also visible on the histograms (figure 25). The shape of Saral/AltiKa off-nadir angle from waveforms histogram is much narrower than for Jason-2.

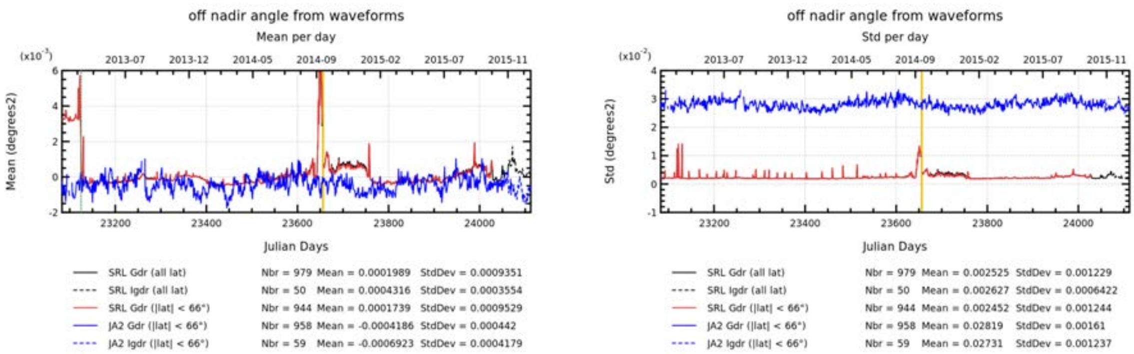

Figure 23: *Daily monitoring of mean (left) and standard deviation (right) of Saral/AltiKa and Jason-2 off-nadir angle from waveforms. GDR data are in plain lines, IGDR data in dotted lines. The vertical green line indicates the day where the PF/RF alignment (alignment between the platform and the radio-frequency axis) was corrected. The gold band indicates the safe hold mode on Saral/AltiKa.*

The off-nadir angle from waveforms represents either real mispointing or is due to backscattering properties of the surface, which can modify the slope of the trailing edge of the waveforms. Jason-2 shows more variation for the off-nadir angle from waveforms due to its larger antenna aperture. Jason-2 has an antenna beamwidth of 1.29°, whereas Saral/AltiKa has only 0.6°. In addition Jason-2 is in a higher orbit. The Jason-2 footprint is therefore larger (radius of 9.6 km) than the Saral/AltiKa footprint (5.7 km). Therefore the probability of perturbations within the footprint - which modify the backscattering properties of the surface - is higher for Jason-2 than for Saral/AltiKa.

The map of Saral/AltiKa off-nadir angle from waveforms (left of figure 24) is not homogeneous. The Indian ocean is impacted by platform mispointing due to maneuvers. High mispointing values are observed at high latitudes close to sea ice. Mispointing is slightly positive around Indonesia and equator and close to coasts. On the other hand, the region around 50˚S has slightly negative values. The map of Jason-2 (right of figure 24) is generally slightly negative, except for regions around Indonesia, and close to coasts (especially in the northern hemisphere), the amplitudes of the off-nadir angle from waveforms are greater for Jason-2 than for Saral/AltiKa. Because of platform mispointing events, Saral/AltiKa map of mispointing is now less correlated to the map of backscattering coefficient (figure 27).

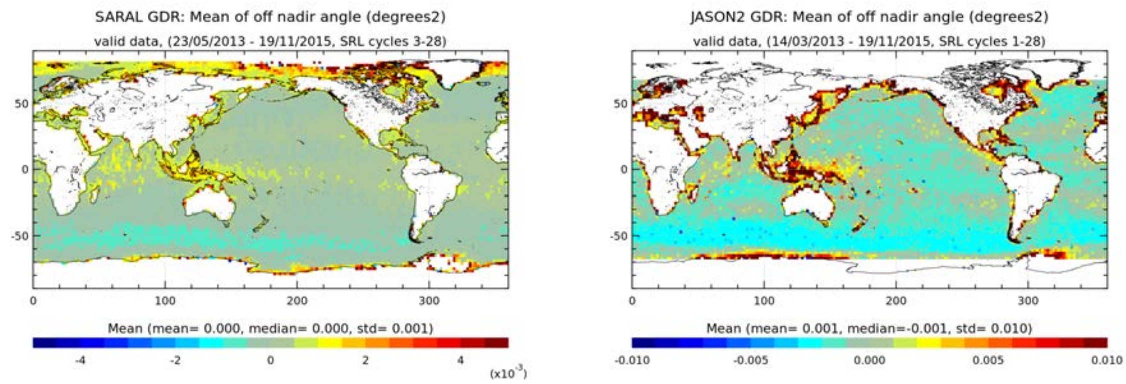

Figure 24: *Average map of off-nadir angle from waveforms for Saral/AltiKa (left) and Jason-2 (right) after the correction of the PF/RF alignment over cycles 3 to 28.*

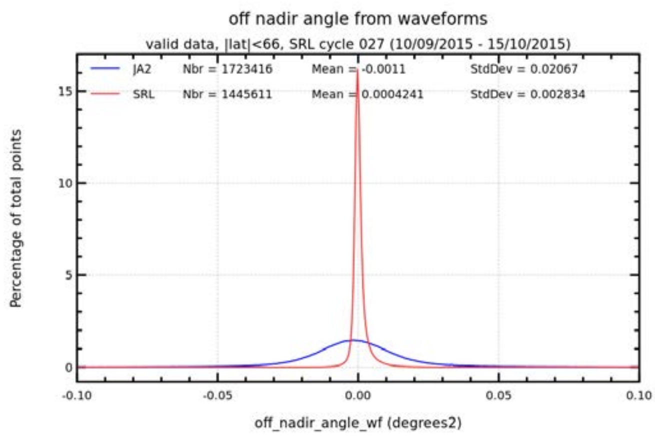

Figure 25: *Histogram (of along-track data) of off-nadir angle from waveforms for Saral/AltiKa and Jason-2 (computed for Saral/AltiKa cycle 14).*

4.4. Backscatter coefficient

Saral/AltiKa is the first altimeter mission using the Ka-band frequency. It has therefore a different behavior than altimeters using Ku-band frequency. Several studies were done to prepare the Saral/AltiKa mission. They found that the Ka-band backscattering coefficient will be about 3.5 dB smaller than the Ku-band backscattering coefficient (see [13]). Concerning the real Saral/AltiKa data, the difference to Ku-band backscattering coefficient is smaller: 2.5 dB in average (see bottom of figure 26). The daily evolution of Saral/AltiKa backscattering coefficient shows the same signals as the one of Jason-2 (top left of figure 26) and the dispersion diagram of backscattering coefficients at 3h crossover points (28) shows also a good correlation.

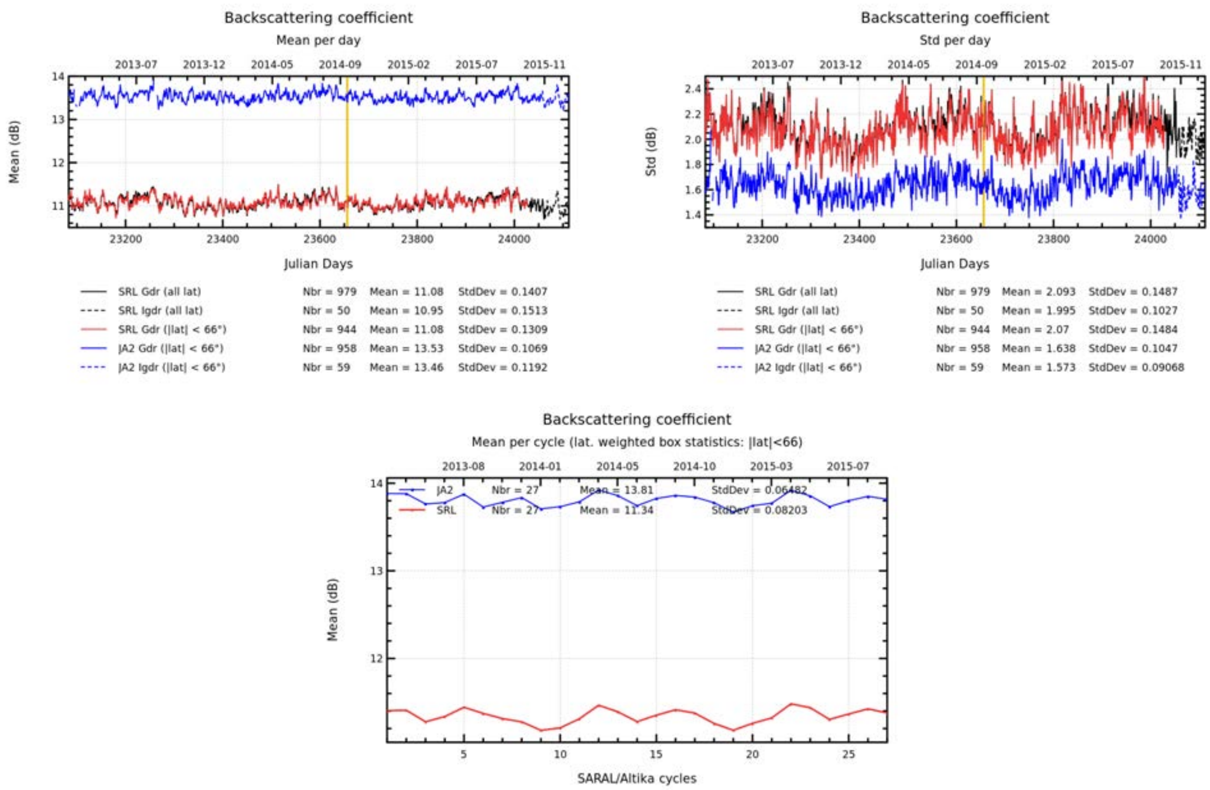

Figure 26: *Daily monitoring of mean and standard deviation of Saral/AltiKa and Jason-2 backscattering coefficient (top) and cycle per cycle monitoring of latitude weighted box mean for both missions on the bottom. The gold band indicates the safe hold mode on Saral/AltiKa.*

Nevertheless there is quite a dispersion, and indeed the daily standard deviation of backscattering coefficient is higher for Saral/AltiKa than for Jason-2 (top right of figure 26). Though the maps (centered around the mean value for better comparison between Saral and Jason-2) of backscattering coefficient show the same structures for both missions (see top of figure 27), the amplitudes of these structures are stronger for Saral/AltiKa than for Jason-2. Also the difference between Ka- and Ku-band backscattering coefficient is not a simple bias, as shown on the difference map (bottom of figure 27).
Furthermore the shape of the histograms is quite different for the Ka- and Ku-band frequencies. The backscattering coefficient is one of the parameters which is quite different for the two frequencies.

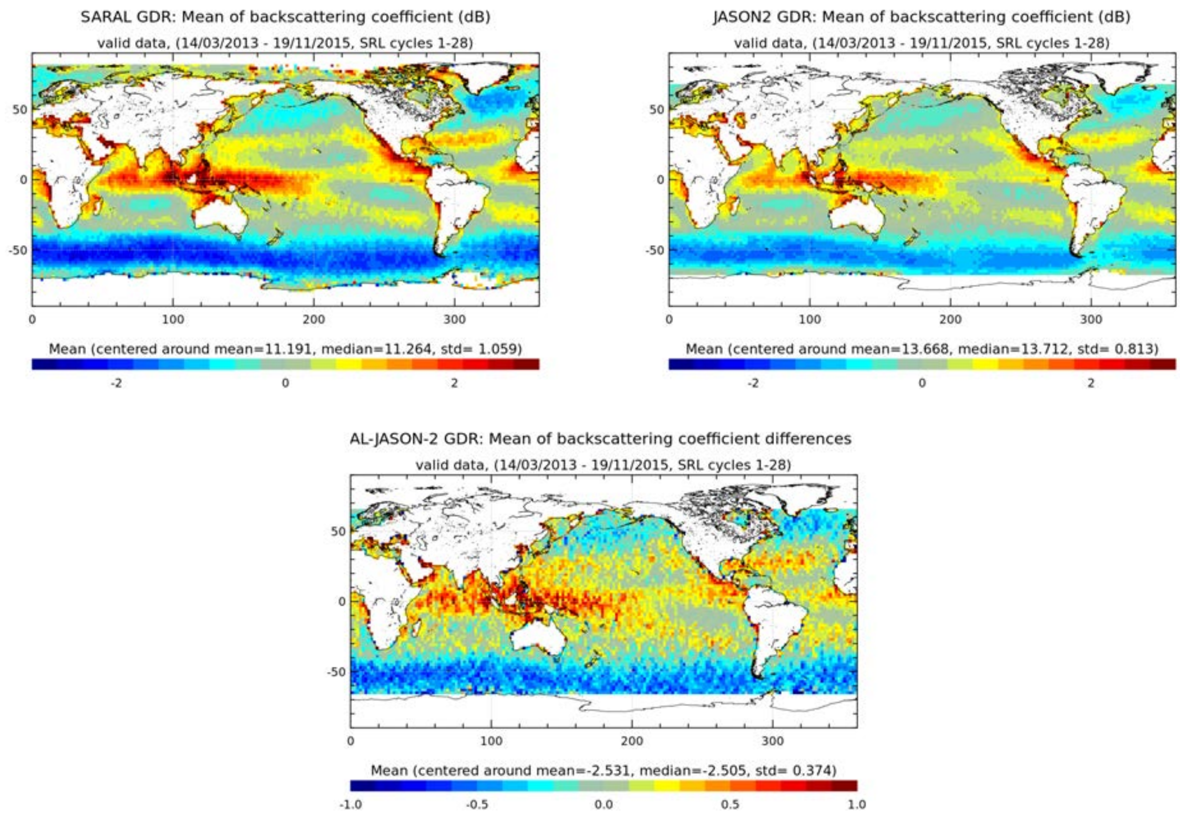

Figure 27: *Average map of backscattering coefficient for Saral/AltiKa (left) and Jason-2 (right) cycles 1 to 28. Difference map of gridded Saral and Jason-2 backscattering coefficient for cycles 1 to 28.*

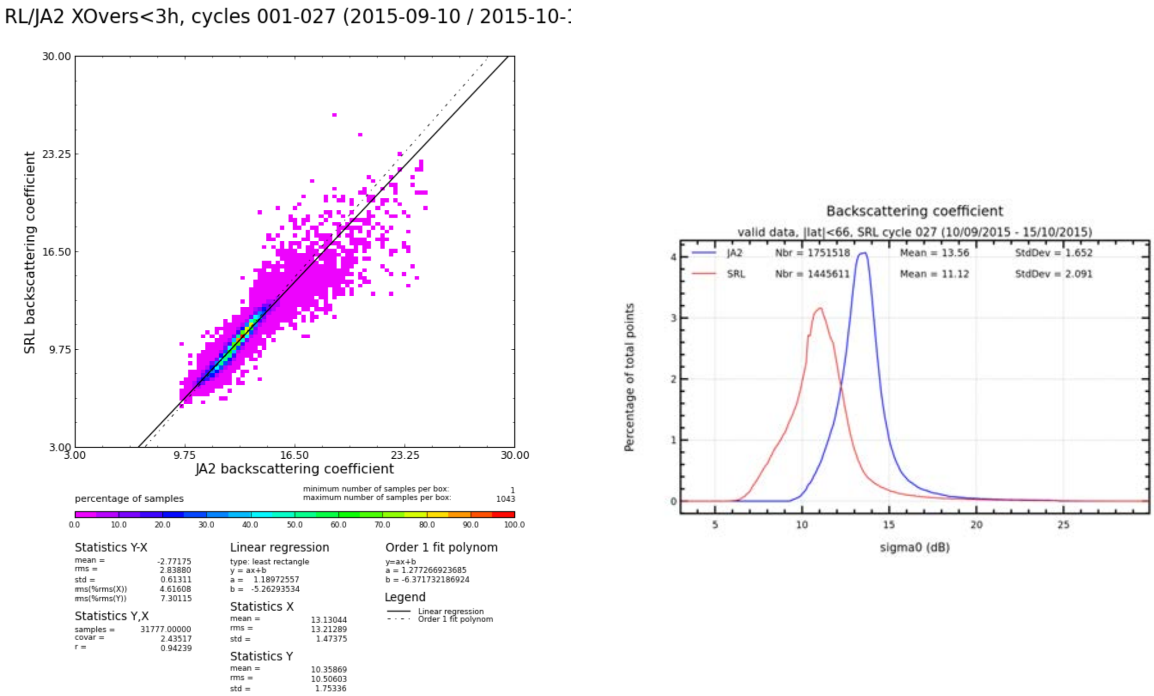

Figure 28: *Dispersion diagram of backscattering coefficient between Saral/AltiKa and Jason-2 at 3h crossover points (computed for cycles 1 to 28) on the left and histogram (of along-track data) computed for Saral/AltiKa cycle 14 on the right.*

4.5. Significant wave height

The significant wave height (SWH) is one of the parameters derived from the waveforms. Daily monitoring of mean and standard deviation of SWH vary temporally, but are very similar for SARAL/AltiKa and Jason-2 (see top of figure 29). The mean is very close for both missions when limited to 66° latitude. When taking into account all latitudes, SWH is slightly reduced for Saral/AltiKa as small SWH occur in very high northern latitudes when the sea ice recedes (see also left map of figure 30). The maps of SWH show the same structures: low SWH around Indonesia, in the Mediterranean Sea and the Gulf of Mexico and high SWH around 50°S (as well as in North Atlantic). The difference map between the two satellites (bottom of figure 30) is centered around a difference of 3 to 4 cm, with slightly higher values for Saral/AltiKa. Stronger differences occur in high latitudes (in regions, where SWH is higher than 2-3 m). These differences are probably due to time differences in the sampling. When considering dispersion diagram of SARAL/AltiKa and Jason-2 SWH at 3h crossovers (left of figure 31), a strong correlation coefficient of over 0.98 is obtained.

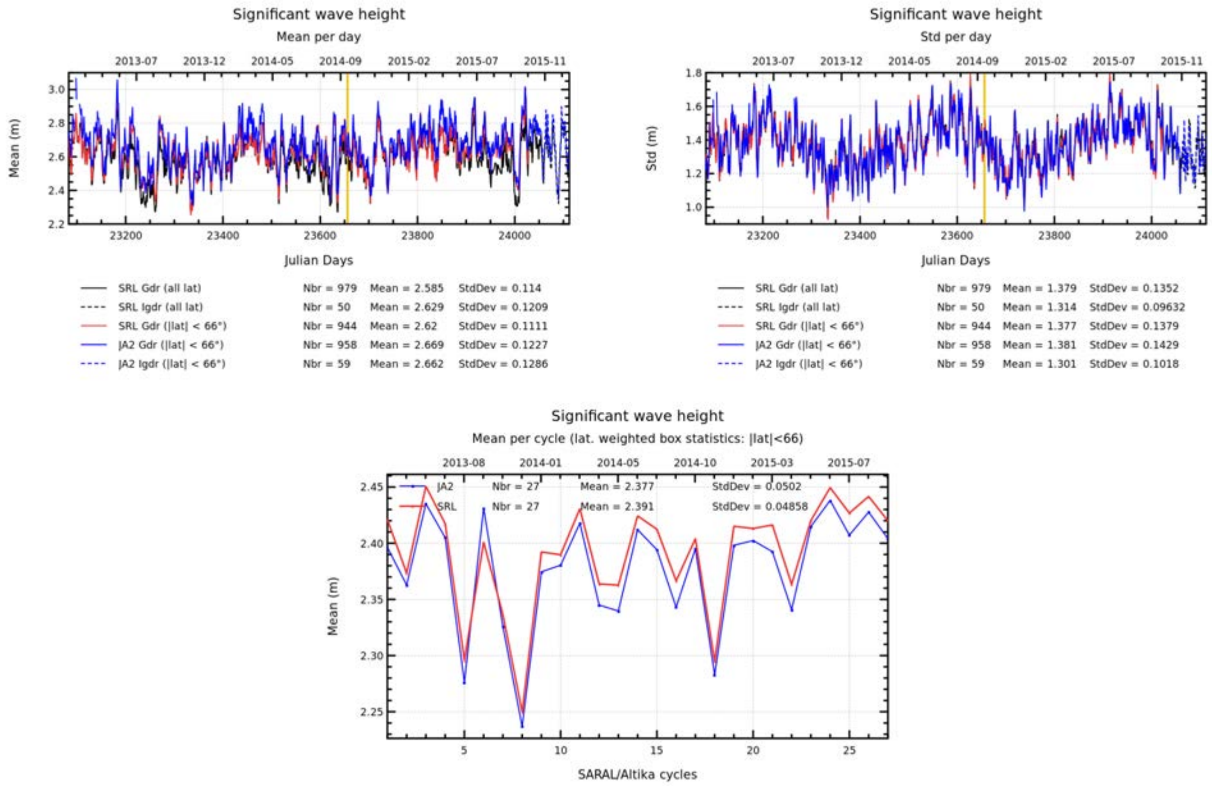

Figure 29: *Daily monitoring of mean and standard deviation significant wave height for Saral/AltiKa and Jason-2 (top) and cycle per cycle monitoring of latitude weighted box mean for both missions on the bottom. The gold band indicates the safe hold mode on Saral/AltiKa.*

The dispersion diagram shows a mean value for Jason-2 SWH at 3h SRL/JA2 crossover points of 3.06 m and 3.12 m for Saral/AltiKa. This is considerably higher than the mean values of daily along-track SWH (around 2.60 m). This is related to the geographical positions of the 3h crossover points: there are more crossover points in latitudes around 50°, than in low latitudes. And around

50˚S the SWH has high values (see also top of figure 30), which skews the mean of SWH computed at 3h crossovers to higher values. Nevertheless, this diagnostic shows that for the same positions (SRL/JA2 3h crossovers) with a time difference less than 3h, Saral/AltiKa SWH is slightly higher than Jason-2. This is also the case when computing latitude weighted box statistics (in order to compensate for uneven data distribution), as shown on bottom of figure 29, where Jason-2 SWH is generally slightly lower than Saral/AltiKa SWH. When considering along-track statistics (top of figure 29), this order is inverted (Jason-2 SWH higher than Saral/AltiKa SWH), as Jason-2 has more data in high latitudes, especially in southern hemisphere, where there is less land. In these regions the SWH is high and skews the mean to higher values.

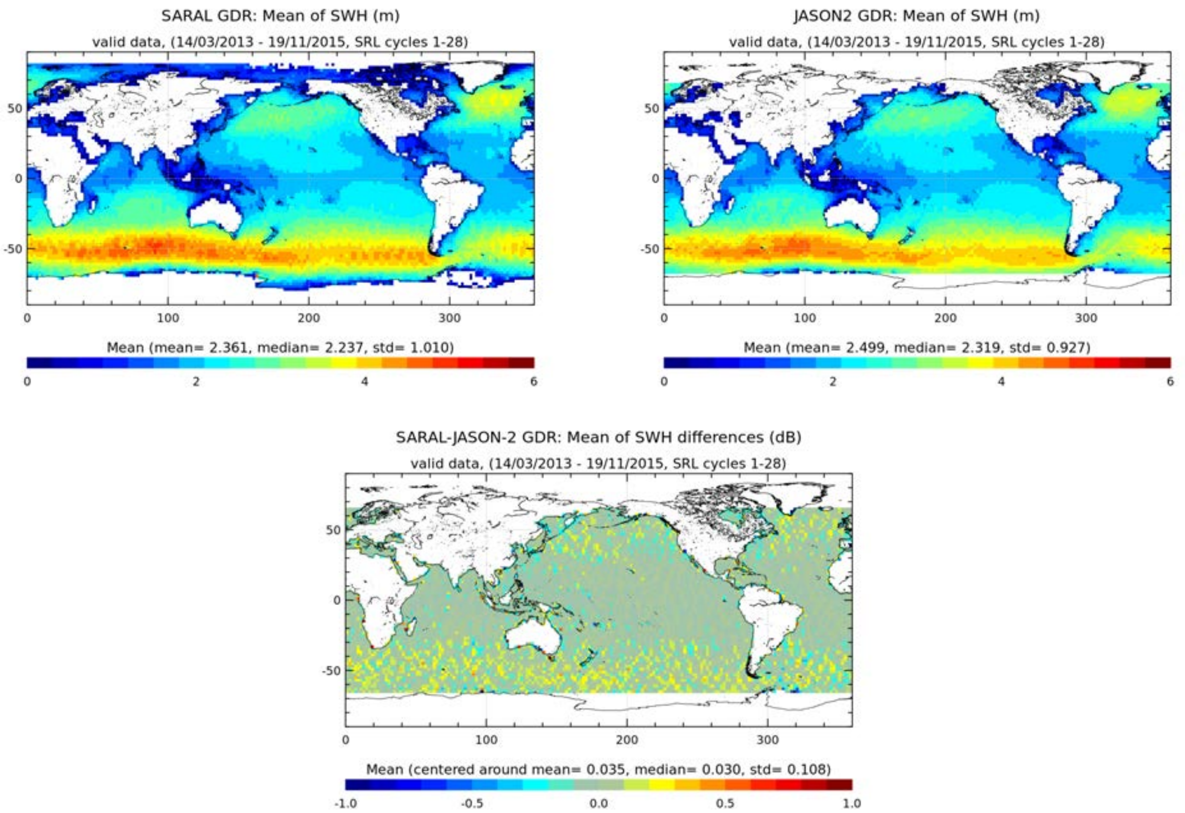

Figure 30: *Average map of significant wave height for Saral/AltiKa (left) and Jason-2 (right) cycles 1 to 28. Difference map of gridded Saral and Jason-2 significant wave height for cycles 1 to 28.*

The shapes of the histograms are very similar (see right side of figure 31) for Jason-2 and Saral/AltiKa, except for small SWH. The minimum SWH value of Saral/AltiKa SWH is 12.6 cm (related to the look-up table), it is 0 for Jason-2. Nevertheless, small SWH of current Jason-2 or Jason-1 data are not precise (errors of about 15 cm), as the look-up table correction for small SWH is not correct, whereas the Saral/AltiKa look-up tables were updated for Patch2. Furthermore, the histogram for Saral/AltiKa shows a small bump for SWH around 50cm. Note that in the wave forecasting systems of Meteo-France, altimeter significant wave height from Jason-2 and Saral/AltiKa are only assimilated for values higher than 50 cm. According to L. Aouf, the Saral/AltiKa SWH data have a positive impact on the wave analysis and forecast of the Meteo-France wave analysis model ([2]).

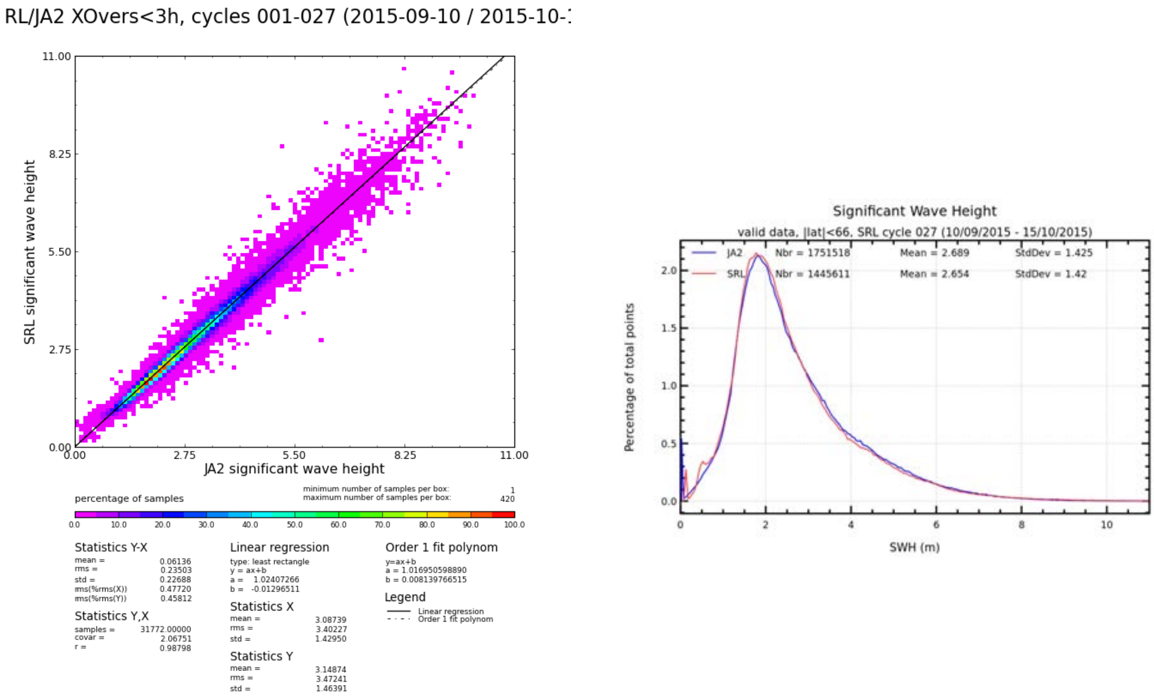

Figure 31: *Dispersion diagram of significant wave height between Saral/AltiKa and Jason-2 at 3h crossover points (computed for cycles 1 to 28) on the left and histogram (of along-track data) computed for Saral/AltiKa cycle 14 on the right.*

4.6. Ionosphere correction

As the Saral/AltiKa altimeter uses a frequency of 35.75 GHz (Ka-band), the ionospheric effects are very small (divided by roughly seven compared to Ku-band frequency). Therefore a mono-frequency altimeter was chosen for the Saral/AltiKa mission, so it is not possible to compute a dual-frequency ionospheric correction such as for Jason-2. Instead, the Saral/AltiKa GDR products contain only the GIM ionosphere correction.
The large differences between Ka-band and Ku-band ionosphere corrections are shown on the latitude weighted box statistics (bottom of figure 32), where Saral/AltiKa GIM ionosphere correction has small values (around 7 mm) and it varies little in time, whereas Jason-2 filtered dual-frequency ionosphere correction has values of around 7 cm, which vary temporally. Also the standard deviation of along-track data is higher for Jason-2 than for Saral/AltiKa (right of figure 32).

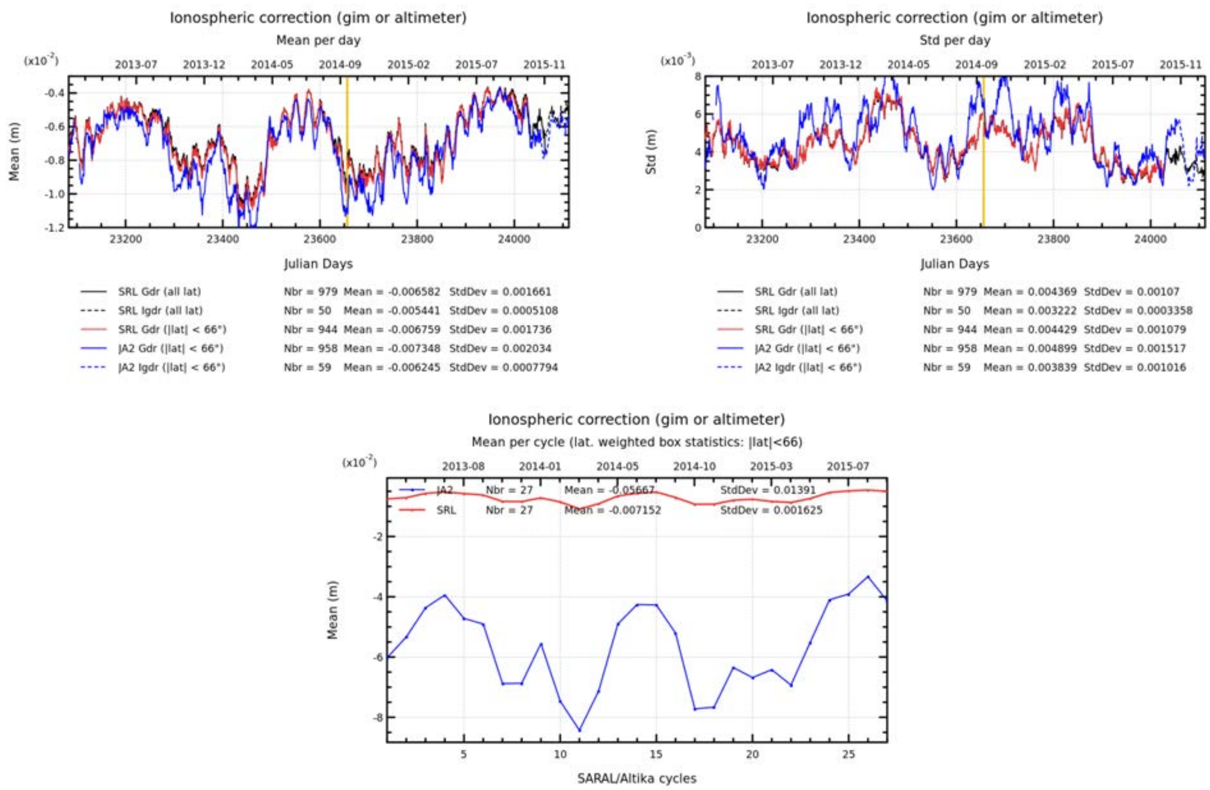

Figure 32: *Daily monitoring of mean and standard deviation ionosphere correction for Saral/AltiKa (GIM) and Jason-2 (filtered dual-frequency ionosphere correction with scale factor 0.14418 for mean computation) on top and cycle per cycle monitoring of latitude weighted box mean for both missions (without the scale factor for Jason-2) on the bottom. The gold band indicates the safe hold mode on Saral/AltiKa.*

Top left of figure 32 shows the daily mean of ionosphere correction for Saral/AltiKa (GIM ionosphere using all latitudes (black line) or limiting to 66° latitude) and for Jason-2 (filtered dual-frequency ionosphere correction), where a scale factor of 0.14418 is applied in order to set it on the same level as Ka-band frequency ($13.575^2/35.75^2$). Generally the two curves show a similar evolution, but locally differences of around 2 mm may occur (with generally Jason-2 having stronger values).

This may be due to the fact that Saral/AltiKa uses a model ionosphere correction, whereas Jason-2 has a dual-frequency ionosphere correction. It may also be due to the fact that Saral/AltiKa is a sun-synchronous satellite with 6:00 local time for ascending node and 18:00 local time for descending node. As ionosphere correction varies with local time, it is very small for ascending (morning) passes and has absolute values up to 2 cm in the equatorial region for descending (evening) passes. Jason-2 on the other hand is not sun-synchronous and revisits only every 12 cycles the same local hours.

Highest ionosphere correction (absolute values) can be found in the same regions (equatorial region) for Saral/AltiKa and Jason-2 (see maps of figure 33), but the amplitude is of course very different (due to the different frequencies). This can also be seen on the histogram (right of figure 34), where the shape of Saral/AltiKa histogram is very narrow with a strong mode close to zero. The shape of Jason-2 histogram is much more spread out and flatter.

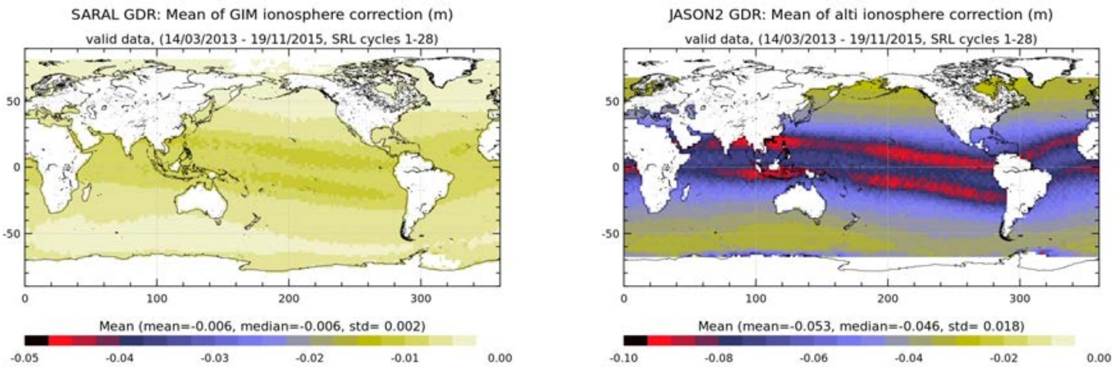

Figure 33: *Average map of ionosphere correction for Saral/AltiKa (GIM, left) and Jason-2 (filtered dual-frequency ionosphere correction, right) cycles 1 to 28. Note that color scales are different for Saral and Jason-2*

The dispersion diagram of ionosphere corrections (the Jason-2 one is rescaled to Ka-band frequency) at 3h multi-mission crossovers shows correlation, but not very good (with a correlation coefficient of only 0.80).

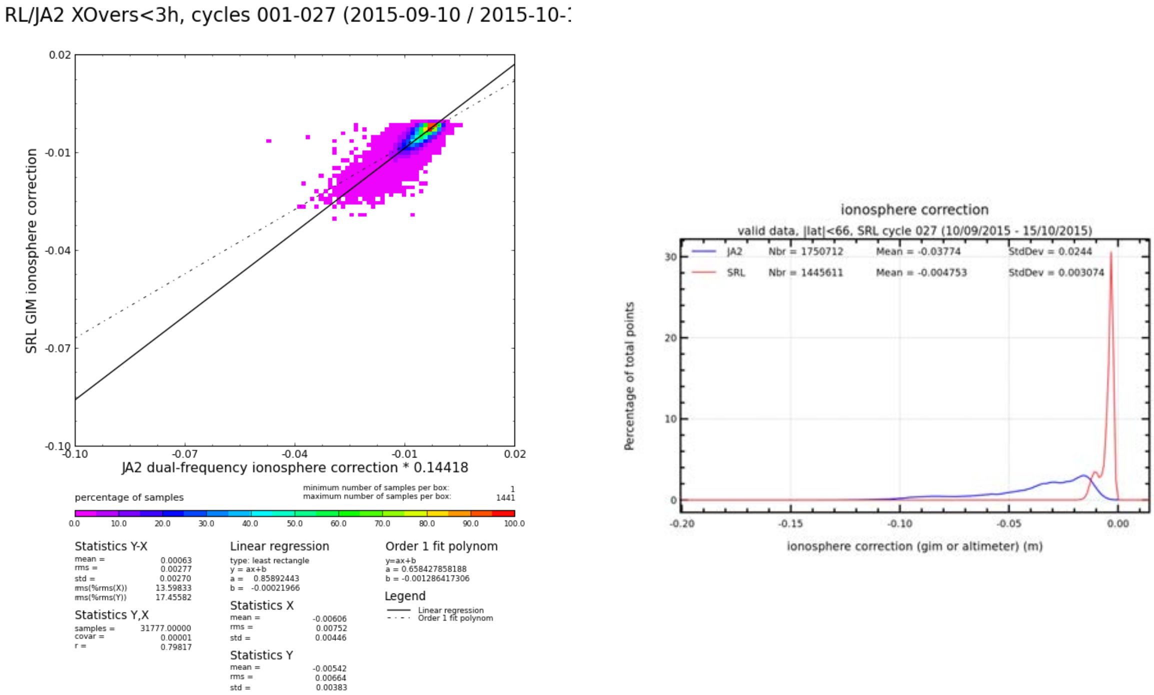

Figure 34: *Dispersion diagram of ionosphere correction between Saral/AltiKa (GIM) and Jason-2 (filtered dual-frequency with scale factor of 0.14418 for Jason-2) at 3h crossover points (computed for cycles 1 to 28) on the left and histogram of along-track data (without scale factor for Jason-2) computed for Saral/AltiKa cycle 14 on the right.*

4.7. Radiometer wet troposphere correction

4.7.1. Overview

In order to have access to radiometer wet troposphere correction, liquid water content, water vapor content and atmospheric attenuation, Saral/AltiKa uses a dual-frequency radiometer (23.8 GHz +/- 200 MHz & 37 GHz +/- 500 MHz), whereas Jason-2 has a three-frequency radiometer (18.7, 23.8 and 34.0 GHz). Figure 35 shows the daily mean and standard deviation of radiometer wet troposphere correction for Saral/AltiKa and Jason-2. Since Patch2, the standard deviation is smaller for Saral/AltiKa than for Jason-2. Concerning the mean of radiometer wet troposphere correction, Jason-2 has dryer values than Saral/AltiKa. This is on the one hand related to different radiometer wet troposphere correction retrieval algorithms, but on the other hand, this can also be related to different local times of the satellites (sun-synchronous 6h/18h for Saral/AltiKa). During several months the radiometer wet troposphere correction of Saral/AltiKa went dryer, this is related to the saturation of the hot calibration counts, which was corrected on 22 October 2013 (explaining the jump of around 5 mm amplitude visible on the monitoring). The safe-hold mode of Saral/AltiKa didn't generate any significant impact on the daily mean.

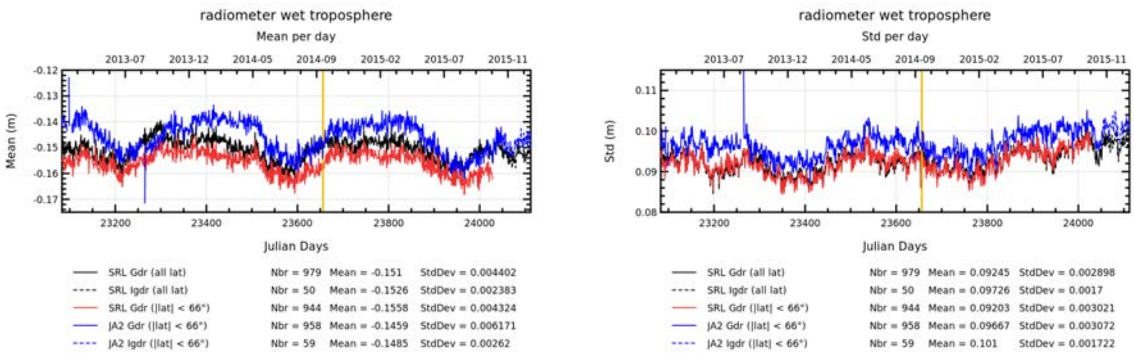

Figure 35: *Daily monitoring of mean and standard deviation of radiometer wet troposphere correction for Jason-2 (blue) and Saral/AltiKa (black all latitudes, red latitudes limited to ± 66°). The gold band indicates the safe hold mode on Saral/AltiKa.*

4.7.2. Comparison with the ECMWF model

The ECWMF wet troposphere correction has been used to check the Saral/AltiKa and Jason-2 radiometer corrections. Daily differences are calculated and plotted in figure 36. The drift in the radiometer wet troposphere correction of Saral/AltiKa due to the saturation of the hot calibration count is clearly visible on the left part of figure 36. Outside of this drift the difference between radiometer and ECMWF wet troposphere correction for Saral/AltiKa and Jason-2 is around 5 mm. The two ECMWF model updates (June and November 2013) occurred during the observed period, which might have an impact on the model wet troposphere correction, did not show any impact on the data.
The standard deviation of radiometer minus model wet troposphere correction is higher for Saral/AltiKa (around 1.6 cm) compared to Jason-2 (around 1.2 cm), shown on left of figure 36 and also on the histogram on figure 38.

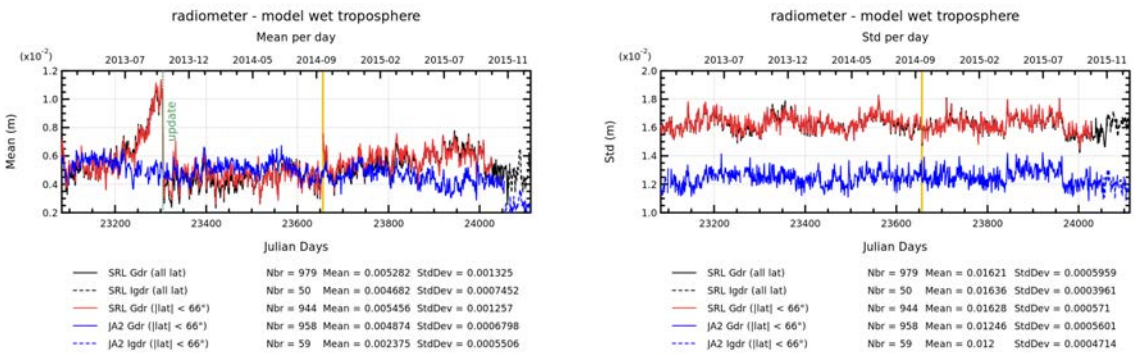

Figure 36: *Daily monitoring of mean and standard deviation of radiometer minus model wet troposphere correction for Saral/AltiKa and Jason-2. The gold band indicates the safe hold mode on Saral/AltiKa.*

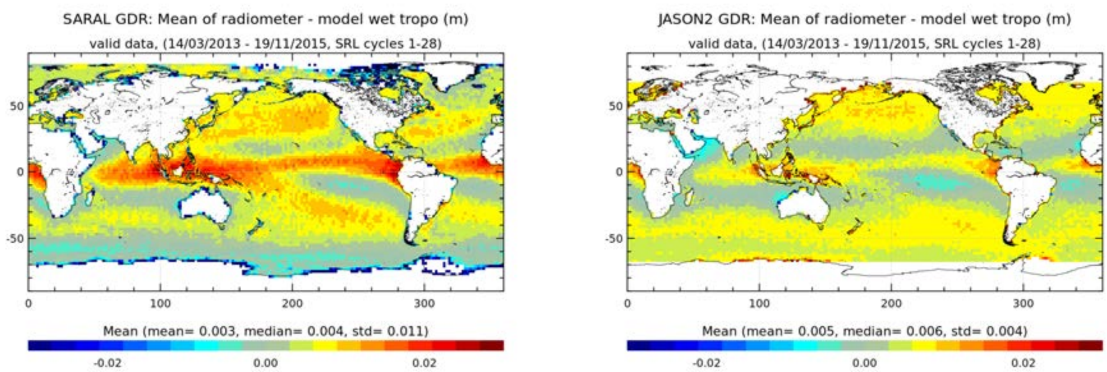

Figure 37: *Average map of radiometer minus ECMWF model wet troposphere correction for Saral/AltiKa (left) and Jason-2 (right) cycles 1 to 28.*

The maps of radiometer minus ECMWF model wet troposphere correction (figure 37) are centered around the mean value (5 mm for Jason-2, 2 mm for Saral/AltiKa). The mean of the Saral/AltiKa map is impacted on the one side by the saturation of the hot calibration counts (which tends to overestimate the difference) and on the other side by some boxes near the frontier between sea-ice and free water (which tends to underestimate the mean). These boxes with strong negative values are an indication that probably not all sea ice cases are edited. In the frame of Cal/Val activities for the DUACS system, a new ice flagging procedure was tested, and will be implemented in routine Cal/Val analysis. Geographical structures of the radiometer minus model wet troposphere corrections are similar for the two satellites in high latitudes (around $\pm$ 50°), but quite different for low latitudes.

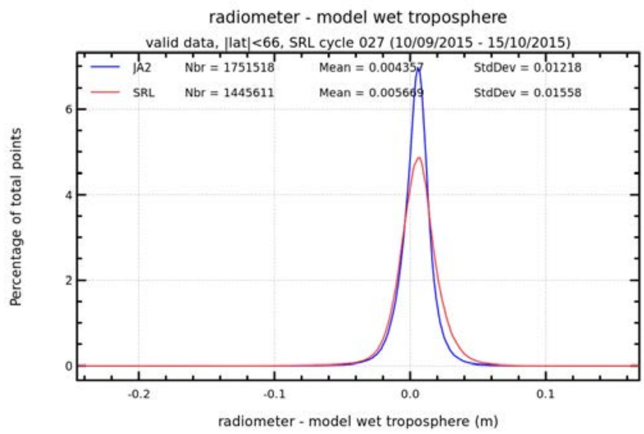

Figure 38: *Histogram (of along-track data) of radiometer minus ECMWF model wet troposphere correction between Saral/AltiKa and Jason-2 computed for Saral/AltiKa cycle 14.*

4.8. Altimeter wind speed

The altimeter wind speed present in Patch1 was not usable, since the look-up table from Jason-1 was used, but with the Ka-band backscattering coefficient is very different from the Ku-band one. For Patch2 version, the altimeter wind speed algorithm developed by [9] for Ka-band altimetry is used. Figure 39 shows the daily monitoring of the mean and standard deviation of altimeter wind speed for Saral/AltiKa and Jason-2. The Patch2 altimeter wind speed has values similar to the Jason-2 altimeter wind speed.
It should be noted that in the current products, the SARAL/AltiKa wind speed is impacted by the saturation of the radiometer hot calibration counts through the estimation of atmospheric attenuation which is then applied on the backscatter coefficient. The maps of altimeter wind speed for both missions are similar (see 40).
The figure 41 shows a good correlation of wind speed data between the two missions (over 0.95), yet the relationship between Jason-2 and SARAL/AltiKa remains non truly linear.

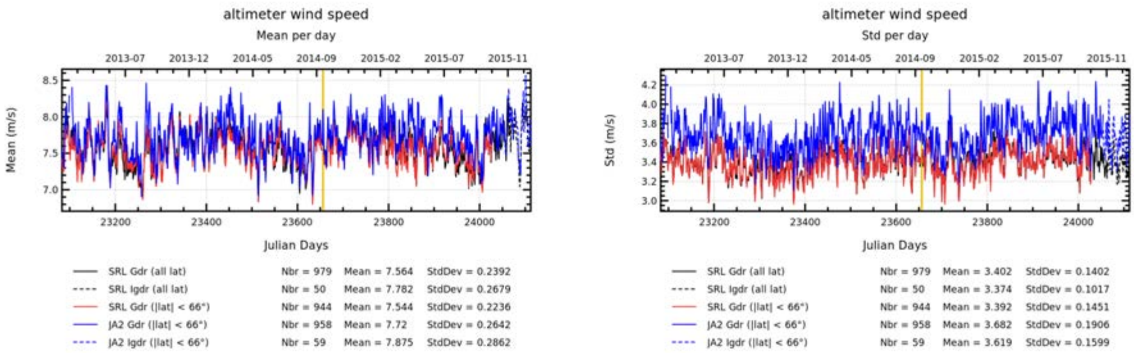

Figure 39: *Daily monitoring of mean and standard deviation of altimeter wind speed for Saral/AltiKa and Jason-2. The gold band indicates the safe hold mode on Saral/AltiKa.*

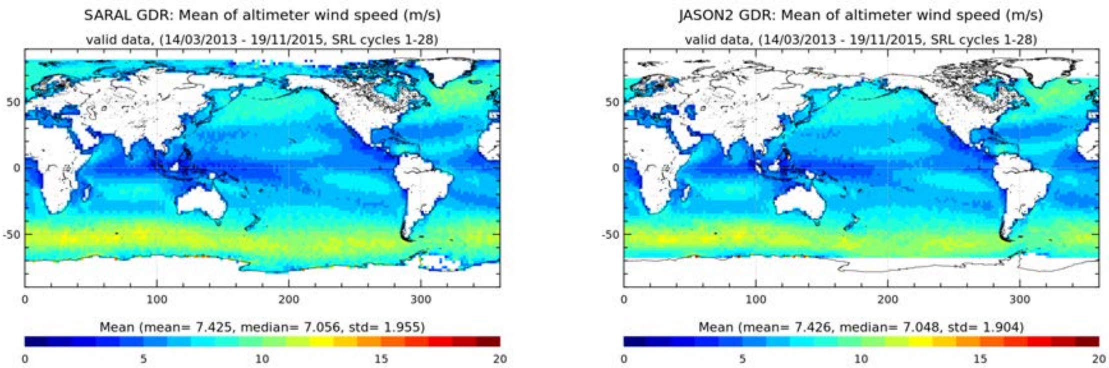

Figure 40: *Average map of altimeter wind speed for Saral/AltiKa (left) and Jason-2 (right) cycles 1 to 28.*

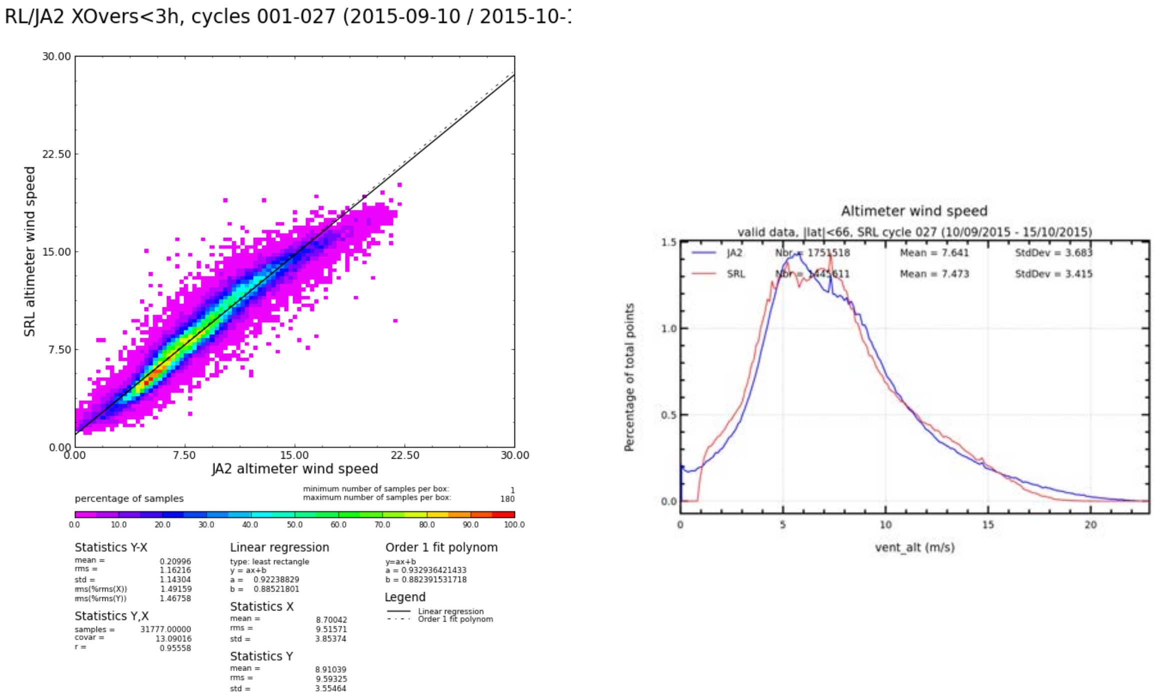

Figure 41: *Dispersion diagram of altimeter wind speed between Saral/AltiKa and Jason-2 at 3h crossover points (computed for cycles 1 to 28) on the left and histogram of along-track data (without scale factor for Jason-2) computed for Saral/AltiKa cycle 14 on the right.*

4.9. Sea state bias

In Patch1 version, the sea state bias was as a first approximation set equal to -3.5% of SWH.
For Patch2 a hybrid SSB solution developed by R. Scharroo was used (this SSB was computed using the same method as in [12]). The Patch2 SSB solution is in absolute values around 1.8cm stronger (which increases the Patch2 SLA) than the Patch1 solution. This is related to the method of SSB computation (hybrid method).
The daily monitoring of the along-track sea state bias for Saral/AltiKa and Jason-2 show similar temporal evolution, but Saral/AltiKa SSB has higher absolute values (around 2.5 cm higher) than Jason-2 (see left side of figure 42). This is also the case when considering latitude weighted box statistics (bottom of figure 42). But this is not a homogeneous bias, it varies geographically, as shown on bottom of figure 43. Furthermore the daily standard deviation is also slightly larger for Saral/AltiKa compared to Jason-2 (see right side of figure 42).

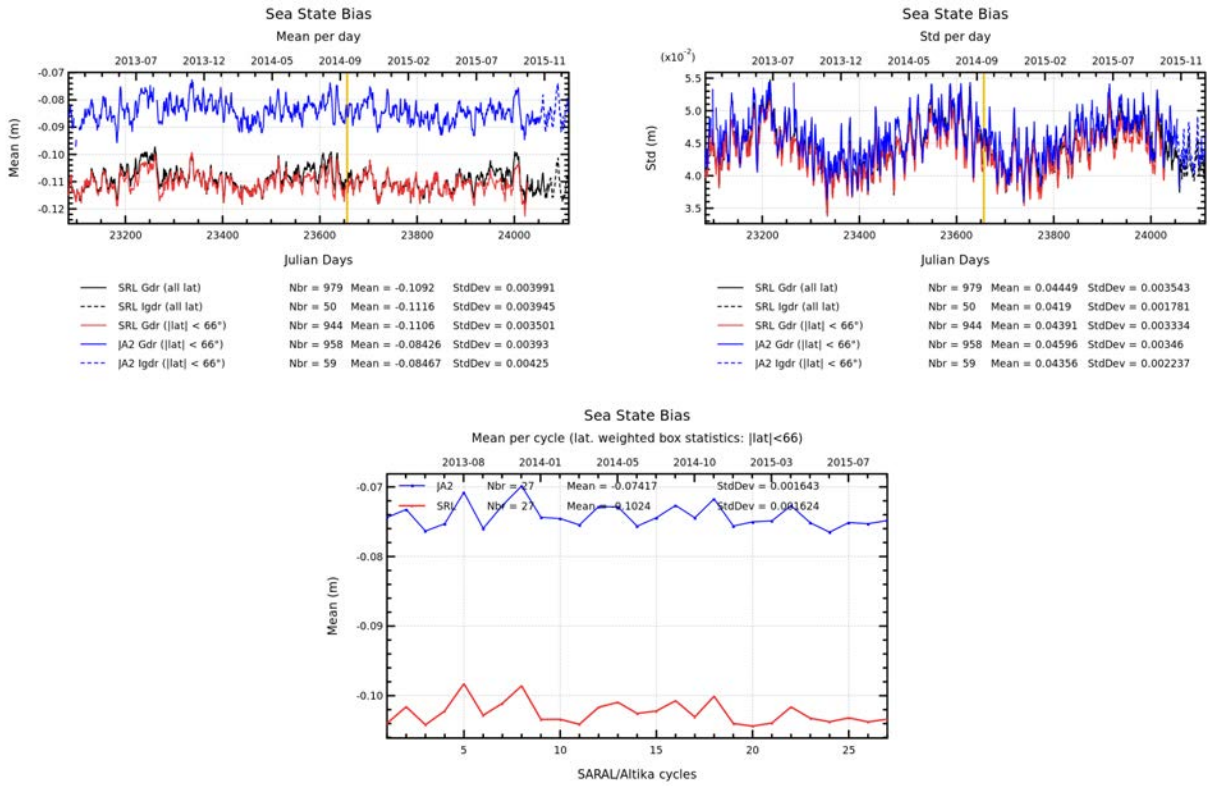

Figure 42: *Daily monitoring of mean and standard deviation of (along-track) sea state bias of Saral/AltiKa and Jason-2 on the top and cycle per cycle monitoring of latitude weighted box mean for both missions on the bottom. The gold band indicates the safe hold mode on Saral/AltiKa.*

Indeed the map of Saral/AltiKa sea state bias shows higher values in the region of 50°S (where SWH is strong) than the map of Jason-2 (top of figure 43). The dispersion diagram of Saral/AltiKa and Jason-2 sea state bias at 3h multi-mission crossovers confirms that the Saral/AltiKa SSB is overestimated for high SSB (equals high SWH). The different nature of the SSB models used for Saral/AltiKa and Jason-2 (dedicated model) is also visible on the right side of figure 44, showing very different shapes of histograms.

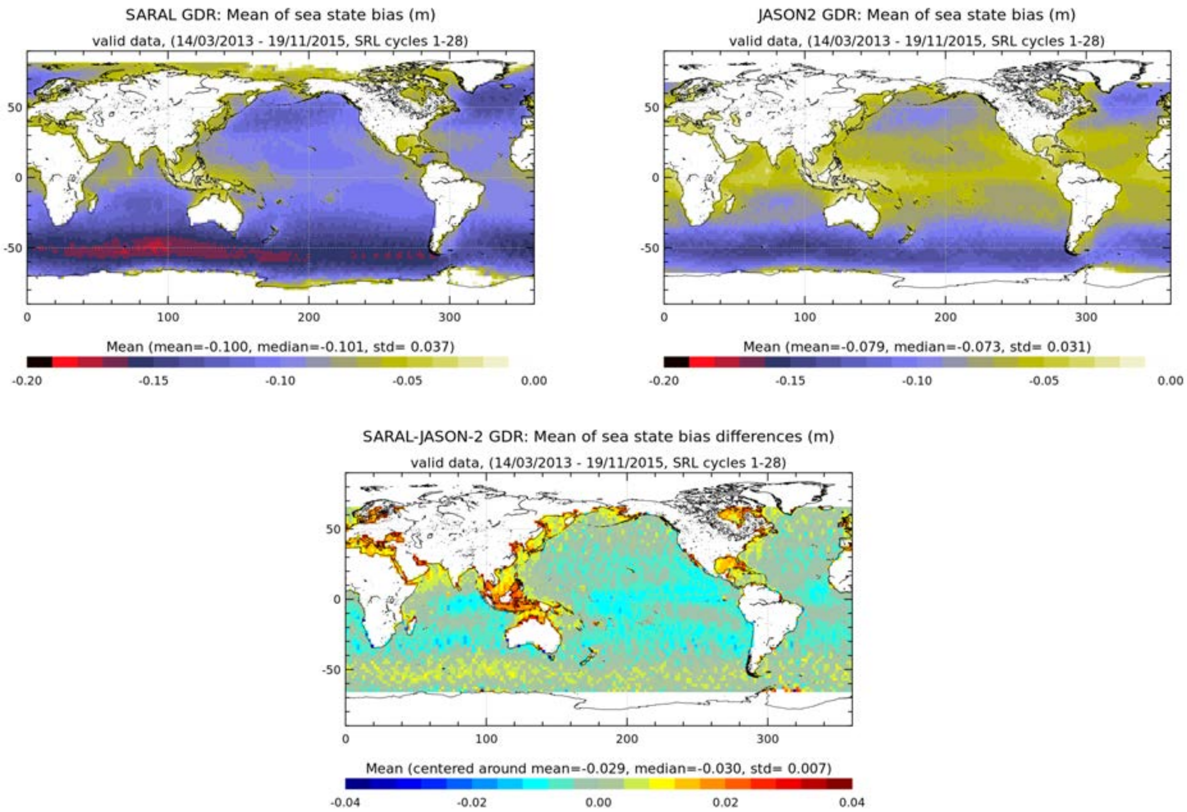

Figure 43: *Average map of sea state bias for Saral/AltiKa (left) and Jason-2 (right) cycles 1 to 28. Difference map of gridded Saral and Jason-2 sea state bias for cycles 1 to 28.*

This difference in sea state bias between the two missions has also an impact on the geographically correlated biases between the two missions, as shown in chapter 5.3., concerning maps of sea surface height differences at multi-mission crossover points.

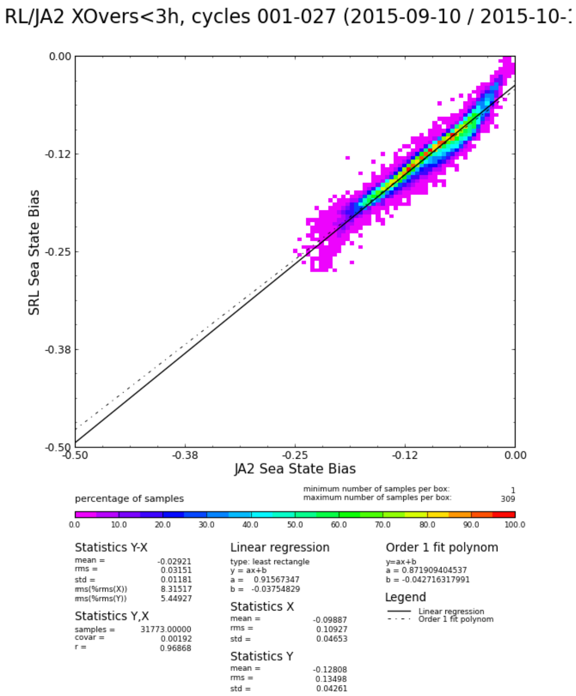

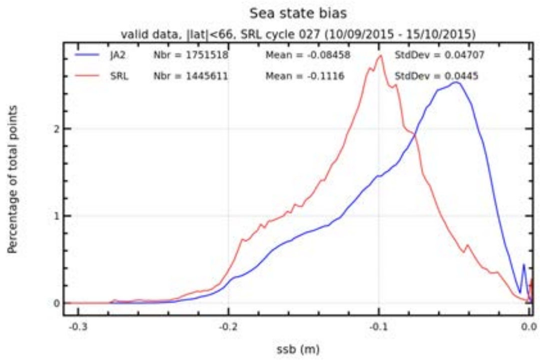

Figure 44: *Dispersion diagram of sea state bias between Saral/AltiKa and Jason-2 at 3h crossover points (computed for cycles 1 to 28) on the left and histogram (of along-track data) computed for Saral/AltiKa cycle 14 on the right.*

5. SSH crossover analysis

5.1. Overview

SSH crossover differences are the main tool to analyze the whole altimetry system performances. They allow us to analyze the SSH consistency between ascending and descending passes. In order to reduce the impact of oceanic variability, we select crossovers with a maximum time difference of 10 days. This gives a measure of the performance on mesoscale time/space scales. Mean and standard deviation of SSH crossover differences are computed from the valid data set to estimate maps and cycle per cycle monitoring over the altimeter period. In order to monitor the performances over stable surfaces, additional editing is applied to remove shallow waters (bathymetry above -1000m), areas of high ocean variability (variability above 20 cm rms) and high latitudes ($|lat| > 50\,\mathrm{deg}$). Under these conditions, SSH performances are always estimated with equivalent conditions.
The main SSH calculation for SARAL/AltiKa and Jason-2 are defined below.

$$SSH = Orbit - Altimeter\ Range - \sum_{i=1}^{n} Correction_i$$

and the corrections are:

$$\begin{aligned}
\sum_{i=1}^{n} Correction_i &= Dry\ troposphere\ correction \\
&+ Dynamical\ atmospheric\ correction \\
&+ Radiometer\ wet\ troposphere\ correction \\
&+ Ionospheric\ correction \\
&+ Sea\ state\ bias\ correction \\
&+ Ocean\ tide\ correction\ (including\ loading\ tide) \\
&+ Earth\ tide\ height \\
&+ Pole\ tide\ height
\end{aligned}$$

Hereafter a reminder of the standards used (from GDR products: GDR-T Patch2 for Saral/AltiKa and GDR-D for Jason-2):

Parameter	Saral/AltiKa	Jason-2
Orbit	CNES POE-D until cycle 24, POE-E afterwards	CNES POE-D (Doris/Laser/GPS)
Dynamic atmospheric correction (Inverse barometer correction + Non-tidal High-frequency Dealiasing Correction)	Computed from ECMWF atmospheric pressures after removing S1 and S2 atmospheric tides (for inverse barometer) + Mog2D High Resolution ocean model	
		.../...

Parameter	Saral/AltiKa	Jason-2
Radiometer wet troposphere correction	MWR using P2 (dual-frequency radiometer)	AMR (tri-frequency radiometer)
Ionospheric correction	Based on Global Ionosphere TEC Maps from JPL	dual-frequency altimeter ionosphere correction
Sea State Bias	Hybrid method of SSB computation developped by R. Scharroo	MLE4 version derived from 1 year of MLE4 Jason-2 altimeter data with version 'd' geophysical models
Global ocean tide (load tide included)	GOT 4.8 ocean tide	
Earth tide	From Cartwright and Taylor tidal potential	
Pole tide	Wahr [1985]	
Mean Sea Surface	CNES_CLS_2011	

Table 6: *S*tandards used for Saral and Jason-2

When not otherwise stated, the standards from table 6 are used.

5.2. Mean of SSH crossover differences

In this section, the analysis are done over the first 28 cycles of SARAL/AltiKa using GDR-T Patch2 products. For comparison, results from Jason-2 GDR data are shown over the same period. The map of SSH mean ascending/descending differences at crossovers should ideally be close to zero. Geographically correlated patterns on such maps indicate systematic differences between ascending and descending passes. This can indicate either problems in the orbit computation or in geophysical corrections. Figure 45 (left) shows the map of mean SSH differences at crossovers for SARAL/AltiKa. This map shows several geographically correlated patterns, with a longitude dependency (almost vertical stripes). Two negative patches are visible, one centered on South America, the other on southern Asia while two positive patches appear close to New Zealand and if the Gulf of Alaska. The amplitude of these differences is about $\tilde{2}$ cm. Slightly larger differences, but with smaller geographical extension, are observed in the Arctic and Southern Oceans.
Compared to a similar analysis performed on Jason-2 data (figure 45, right), SARAL/AltiKa differences exhibit a larger amplitude: Jason-2 map shows differences genrally lower than $\tilde{1}$ cm.
Part of the observed differences might come from orbit errors, part might come from systematic errors in the geophysical corrections. Figure 46, left, illustrates the impact of changing a geophysical correction on the maps of SSH differences at crossovers. The map on the left panel is estimated using FES2012 tide model instead of GOT4.8 model: the two negative patches are reduced, but a positive patch appears in the Pacific Ocean. Larger errors at high latitudes are not reduced by this tide model change. The right panel of figure 46 shows a similar analysis where the radiometer wet tropospheric correction is replaced by the model one. Switching to the model as little impact on

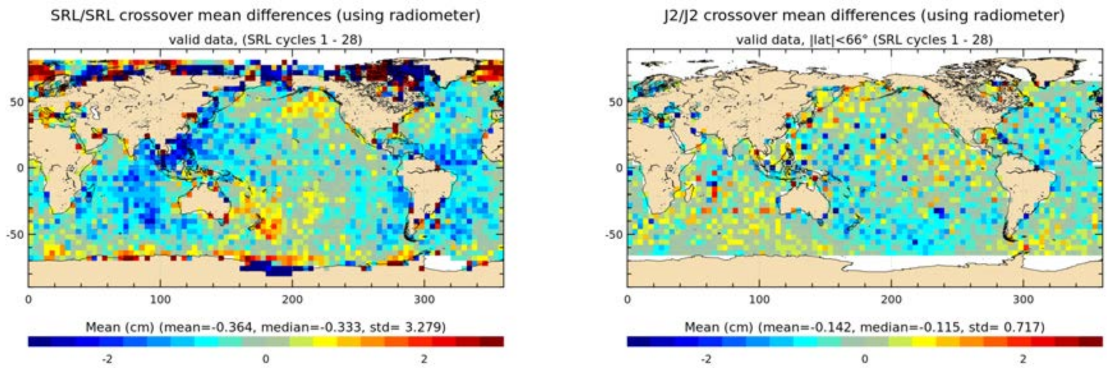

Figure 45: *Map of mean of SSH crossovers differences for Saral/AltiKa (left) and Jason-2 for Saral cycles 1 to 28. Color scales are between ± 3 cm.*

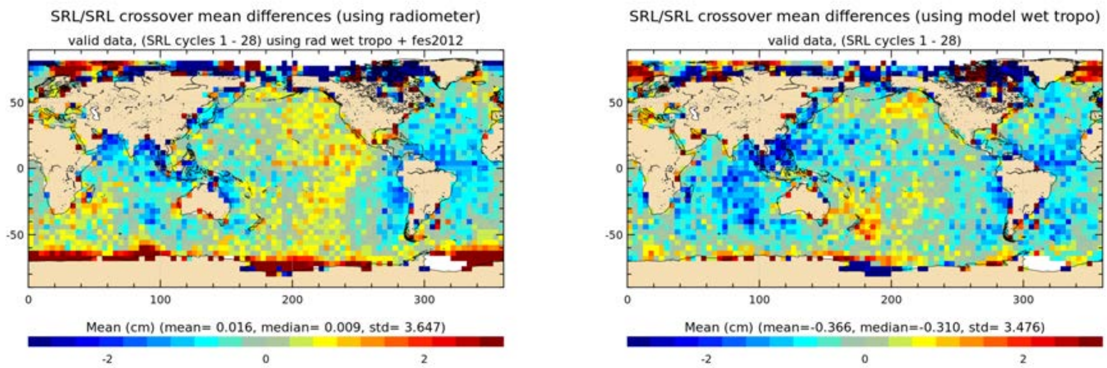

Figure 46: *Map of mean of SSH crossovers differences for Saral/AltiKa for Saral cycles 1 to 28. Color scales are between ± 3 cm. Using FES 2012 ocean tide instead of GOT 4.8 (left) and using model wet troposphere (right).*

the map of the mean differences at crossovers on SARAL/AltiKa.
In addition to mapping the differences, we estimate, at each cycle the global mean of SSH differences at crossovers and monitor this quantity over time to detect any issue on the mission. Over the first 28 cycles of the SARAL/AltiKa mission, the evolution of the cycle-average mean SSH difference at crossovers is plotted on figure 47 for SARAL/AltiKa and Jason-2. The left and right panels correspond to to types of selection for crossovers (no selection at all and selection on bathymetry, latitude and oceaninc variability), while plain and dotted lines correspon to two ways of averaging the SSH differences at crossovers (a simple ensemble mean and a latitude weighted based on the crossovers theoretical density). The weighted averaging method was described in last year's yearly report [16]. For SARAL/AltiKa, the mean difference is slightly negative $\approx -2/-3$ mm depending on the averaging method and the crossovers selection, Jason-2 being closer to zero at ≈ -1 mm. The mean value is very stable over time for both missions, with a slightly larger cycle to cycle varibility on Jason-2 than on SARAL/AltiKa.

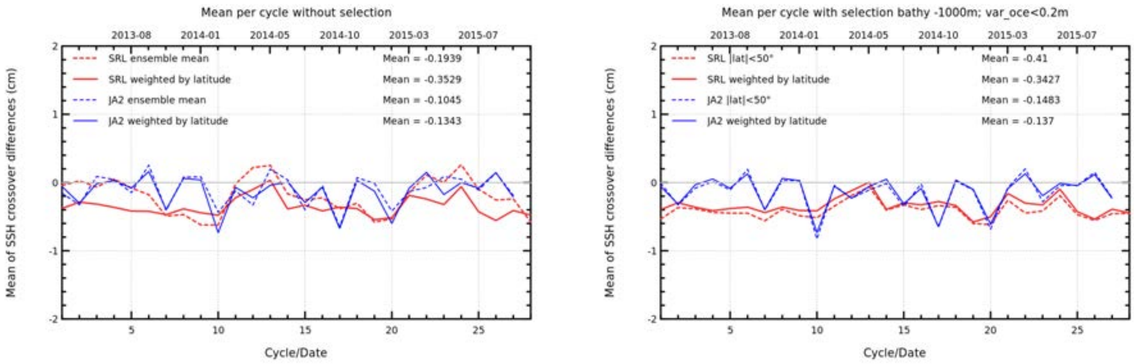

Figure 47: *Cycle per cycle monitoring of ascending/descending SSH differences at mono-mission crossovers for Saral/AltiKa and Jason-2 for Saral cycles 1 to 28.*

5.3. Mean of SSH crossover differences between Saral and other missions

Dual-mission crossover performances are computed between SARAL/AltiKa and Jason-2 in order to detect geographically correlated biases between missions as well as to check SARAL/AltiKa stability with respect to Jason-2. The temporal evolution of this difference is monitored in order to detect if there are drifts or jumps indicating a problem in one of the missions. The temporal evolution of the mean of SARAL/AltiKa/Jason-2 SSH differences at crossovers, based on Jason-2 cycles is shown on figure 48. On both panels a selection for latitudes lower than 50°, deep ocean and low oceanic varibility areas is used. The left panel uses an ensemble mean estimation while the right panel is based on a latitude weighted average. The green line uses the radiometer wet tropospheric correction while the black line is based on the modeled correction. In all cases the temporal evolution of SSH differences at crossovers between SARAL/AltiKa and Jason-2 is very similar. However two periods show larger differences: from Jason-2 cycles 190 to 195 and after cycle 230 approximately. For the first period, the difference is attributed to the radiometer saturation of hot calibration counts on SARAL/AltiKa, which xas corrected (see the blak vertical line). Over the end of the period, the difference between the radiometer and model derived curves is explained by a drift on the Jason-2 radiometer. More information on this drift is provided in section 7.4. The mean bias between the missions is estimated to -4.5 cm (Jason-2 being higher than SARAL/AltiKa) and is stable over the time period with a standard deviation of ≈ 0.2 cm. Over the available period, no significant SSH drift between the two missions is detectable.
Rather than looking at the temporal evolution, mapping the SSH differences between SARAL/AltiKa and Jason-2 over the first 27 cycles of SARAL/AltiKa provides information about geographically correlated biases between the two missions. Such maps are shown on figure 49, where both maps are centered before plotting. Large scale differences are visible between the two missions with amplitudes up to ± 3 cm. Using the radiometer on both missions (left of figure 49) shows a negative patch in the western tropical Pacific Ocean centered on Indonesia and a large positive patch in the Southern Ocean, which extends towards the north in Atlantic Ocean. As for mono-mission crossover differences, part of the observed pattern might come from orbit related issues and/or from geophysical corrections. Using the model wet tropospheric correction on both missions (right of figure 49) greatly reduces the Southern Ocean patch and to a lesser extent the negative Indonesian patch (though to a lesser extent), as well as a positive patch at the southern tip of Greenland. However the positive patch in the southern Atlantic Ocean remains. Improvements are expected from an improved radiometer retrieval algorithm, as well as a new SSB model for SARAL/AltiKa

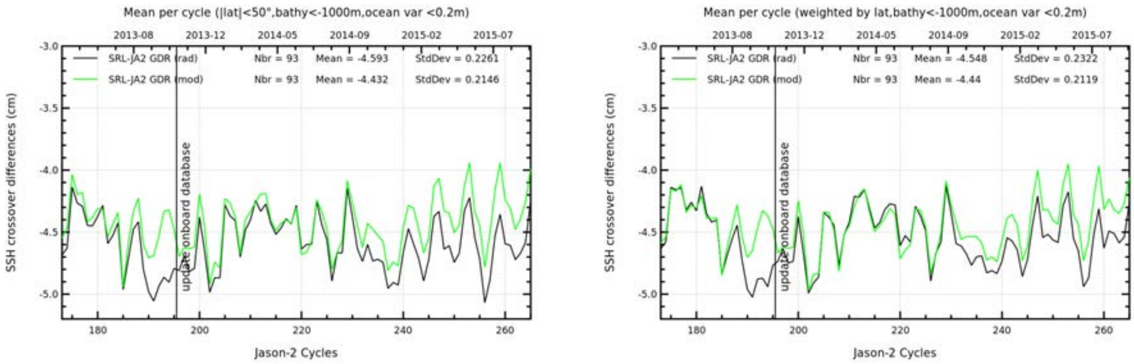

Figure 48: *Monitoring of mean of Saral - Jason-2 differences at crossovers using radiometer wet troposphere correction (black line) or ECMWF model wet troposphere correction (green line) for GDR data with different selections. Statistics are computed on base of Jason-2 cycles.*

as part of Patch 3.

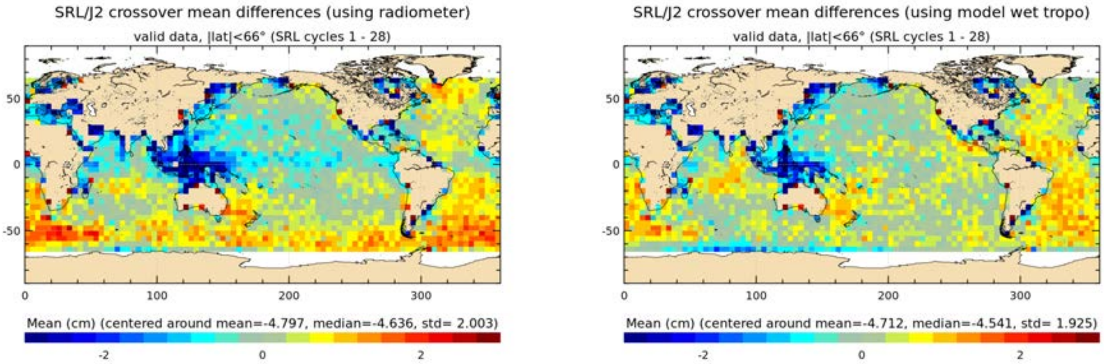

Figure 49: *Map of mean of SSH crossovers differences between Saral/AltiKa and Jason-2 using either radiometer wet troposphere correction (left) or ECMWF model wet troposphere correction (right) for both missions. The maps are centered around the mean.*

5.4. Standard deviation of SSH crossover differences

The standard deviation of SSH differences at crossovers is a key performance metric for satellite altimetry missions. In this section the standard deviation of SSH differences at crossovers is investigated for SARAL/AltiKa and compared to Jason-2.
The cycle per cycle standard deviation of SSH differences at crossovers is plotted on the left of figure 50 for different selections and averaging methods:

- black: no selection is applied, and the ensemble standard deviation is estimated without any weigthing. In this case the standard deviation mounts to 6.8 cm and its temporal evolution is impacted by an annual signal due to the sea ice extension variations. The curve also shows an increase at cycle 17 which is impacted by the safe hold mode event.
- purple: as above no selection is applied on the crossovers, but the standard deviation is estimated after weighting the crossovers following the method described in [16]. This process slighlty reduced de standard deviation (6.2 cm) due to downweighting of crossovers at high latitudes and reduces the amplitude of the annual signal. Statistics for cycle 17 remain impacted by the safe hold mode event.
- red: shallow waters have been removed (bathymetry $<$ -1000m) as well as latitudes greater than 50° and high ocean variability areas. This selection allows to validate the hypothesis of a steady ocean over 10 days which is underlying to crossovers analyis and therefere allows monitoring the SARAL/AltiKa system performance. In this case, the standard deviation of SSH differences drops to 5.3 cm and no annual cycle is observed. The statistic is also less impacted by the safe hold mode event.
- green: uses the same selection as above, combined to a latitude weighting of the crossovers before estimating the standard deviation (this method was described in last year's report). Using this method leads to a small increase of the standard deviation of SSH differences at crossovers (at 5.5 cm)

The right part of figure 50 displays the geographical distribution of the standard deviation of SSH differences at crossovers. This map shows the expected patterns with high standard deviation observed in high ocean varibility areas and in the Arctic Ocean (where some geosphysical corrections such as tides, are less accurate).

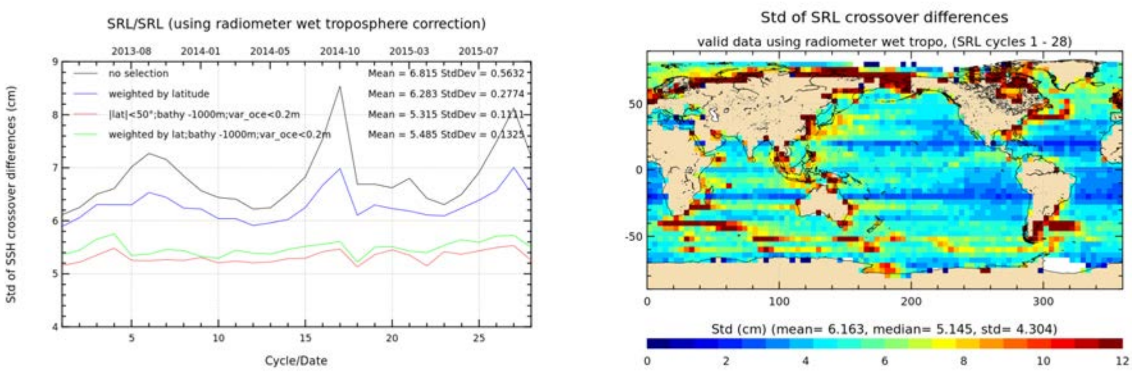

Figure 50: *Cycle by cycle standard deviation of SSH crossover differences for Saral/AltiKa using several selections (left), map of standard deviation at crossover points (right), the radiometer wet troposphere correction is used.*

As part of the routine Cal/Val activities, the performance of SARAL/AltiKa is compared to Jason-2 through the use of the standard deviation of SSH differences at crossovers. Figures 51 and 52 display comparisons between SARAL/AltiKa and Jason-2 performance at crossovers for different selections and weighing methods. In each case the performance using the radiometer and the model are displayed.
Figure 51 displays the ensemble standard deviation with no weighting applied. When using the radiometer, SARAL/AltiKa and Jason-2 performances are very close, especially when selecting only the deep ocean and removing high ocean variability areas. When using the model wet tropospheric correction, SARAL/AltiKa has a slightly lower standard deviation of SSH differences at crossovers than Jason-2. This indicates that using the radiometer correction rather than the modeled one brings a greater improvement on Jason-2 than on SARAL/AltiKa, but the future version of the product will have a new improved radiometer retrieval algorithm.

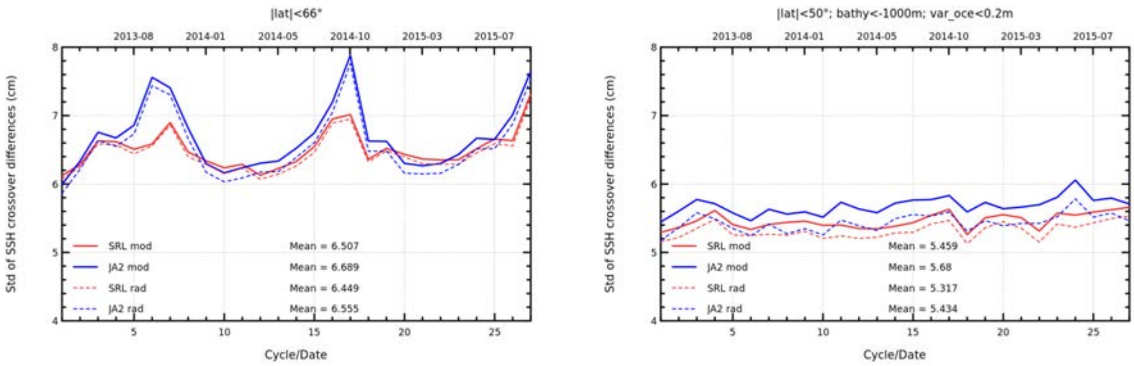

Figure 51: *monitoring of the standard deviaiton of SSH differences at crossovers for SARAL/AltiKa and Jason-2 for Saral cycles 1 to 27 using radiometer (dotted lines) or model (plain lines) wet troposphere correction*

To account for the uneven distribution of crossover points, we also estimate weighted statistics (figure 52) where the weights applied are a function of latitude based on the crossovers density. This allows to better compare the two missions that do not share the same ground track. Similar results are obtained with these weighted statistics: depending on the wet troposphere correction choosen, SARAL/AltiKa's performance is equivalent or slightly better than the Jason-2 one.

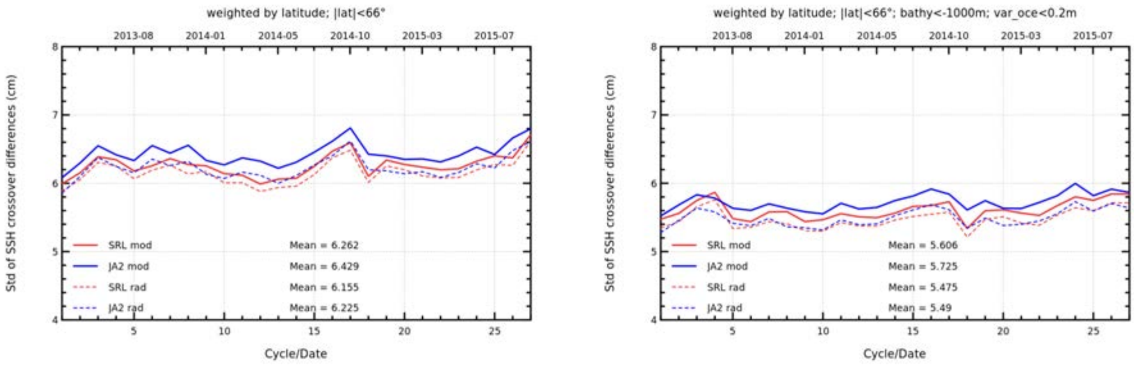

Figure 52: *monitoring of the standard deviaiton of SSH differences at crossovers for SARAL/AltiKa and Jason-2 for Saral cycles 1 to 28 using radiometer (dotted lines) or model (plain lines) wet troposphere correction*

5.5. Performances at crossover points of the different product types (Ogdr/Igdr/Gdr)

Saral/AltiKa data are also available as Ogdr and Igdr products, which are more rapidly available than Gdr products. The main differences between the different data products are listed in table 7.

Auxiliary Data	Impacted Parameter	Ogdr	Igdr	Gdr
Orbit	Satellite altitude, Doppler correction, ...	DORIS Navigator	Preliminary (Doris MOE)	Precise (Doris + Laser POE)
Meteo Fields	Dry/wet tropospheric corrections, U/V wind vector, Surface pressure, Inverted barometer correction,...	Predicted	Restituted	Restituted
Pole Location	Pole tide height	Predicted	Predicted	Restituted
Mog2D	HF ocean dealiasing correction	Not available	Preliminary	Precise
GIM	Ionosphere correction	Predicted	Restituted	Restituted

Table 7: *D*ifferences between the auxiliary data for the O/I/Gdr products (from [4])

Figure 53 displays the monitoring of the cycle per cycle mean and standard deviation of SSH differences at crossovers for the OGDR, IGDR and GDR products. Regarding the mean, all three products show a good stability, of course the temporal variablity is greater for OGDR and IGDR than for GDR data. As expected GDR products provide the best performance with a standard deviation of the differences at crossovers of 5.2 cm. But IGDR data also exhibit a very good performance, with an average standard deviation of the differences of 5.6 cm, very close to the GDR value despite degraded standards (GDR-T and GDR-T Patch1) at the beginning of the period. OGDR data show a higher standard deviation at ≈ 7 cm.

5.6. Estimation of pseudo time-tag bias

The pseudo time tag bias is found by computing at crossovers the regression between SSH differences and orbital altitude rate ($\dot{H}$), also called satellite radial speed :

$$\Delta SSH = \alpha \dot{H}$$

This method allows us to estimate the time tag bias but it absorbs also other errors correlated with $\dot{H}$ as for instance orbit errors. Therefore it is called "pseudo" time tag bias.

The Jason satellites had a pseudo time-tag bias close to -0.28 milliseconds with an approximately 60-days signal. The origin of this pseudo time tag bias of the Jason satellites was found by CNES in 2010 [5]. It has a mean of about -0.25 milliseconds and is dependent on the altitude of the satellite. For Jason-2 GDR-D data, the datation was directly modified in order to correct it

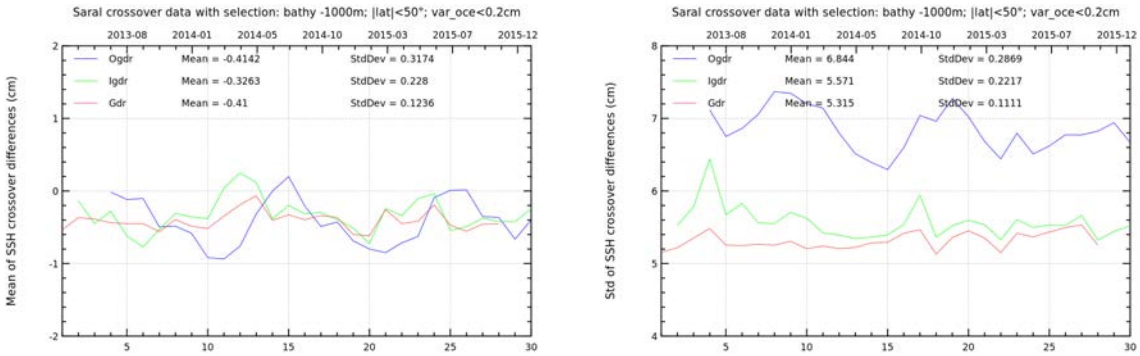

Figure 53: *Cycle per cycle monitoring of mean and standard deviation of SSH crossover differences for SARAL/AltiKa using radiometer wet troposphere correction and geographical selection (|latitude| < 50°, bathymetry < -1000 m and ocean variability < 20 cm rms).*

properly, whereas for Jason-1 GDR-C product it is taken into account thanks to a correction (pseudo_datation_bias_corr_ku). Therefore the average of the pseudo datation bias is now close to zero for the Jason satellites, nevertheless the periodic signal remains and is not yet explained.
Figure 54 shows the monitoring of the pseudo datation bias for SARAL/AltiKa and Jason-2 on a cyclic basis (respectively 35 and almost 10 days).
On average SARAL/AltiKa has a slightly larger pseudo time-tag bias than Jason-2, around -0.04 ms, but which appears to be more stable over time.

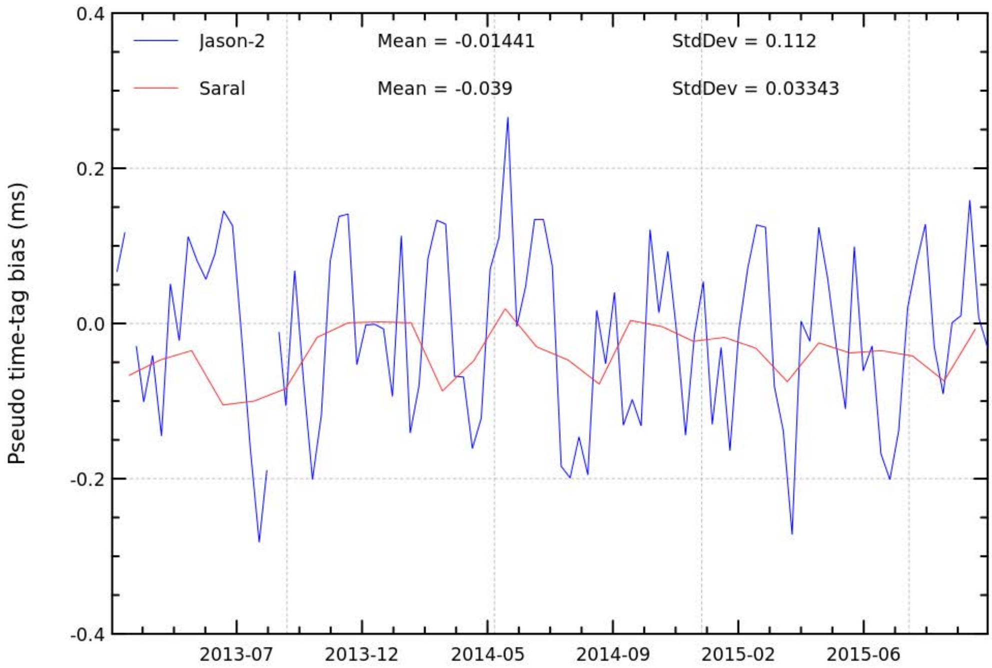

Figure 54: *Cyclic monitoring of pseudo time tag bias for SARAL/AltiKa and Jason-2*

6. Sea Level Anomalies (SLA) Along-track analysis

6.1. Overview

The Sea Level Anomalies (SLA) are computed along track from the SSH minus the mean sea surface with the SSH calculated as defined in previous section 5.1. :

$$SLA = SSH - MSS$$

where the mean sea surface is the CNES/CLS 11 model.
Figure 55 shows two maps of SLA from SARAL/AltiKa and Jason-2 over one cycle of SARAL/AltiKa (here cycle 27). The two maps show very similar patterns, with a very large dipole anomaly in the tropical Pacific Ocean linked with the positive phase of ENSO.

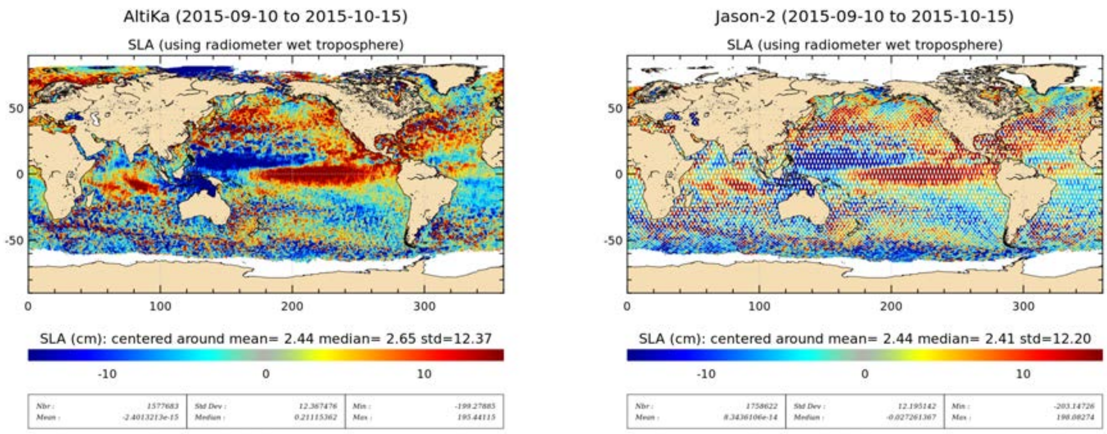

Figure 55: *Map of SLA for SARAL/AltiKa cycle 27 using the radiometer wet tropospheric correction, left is from SARAL/AltiKa data, right is from Jason-2 data over the same period.*

Computing differences between SARAL/AltiKa and Jason-2 as shown on figure 56 allows for a much better aprreciation of potential discrepancies between the two missions. Both maps show geographically correlated differences of the order of ≈ 2 cm. The patterns are very similar to the ones observed at SARAL/AltiKa/Jason-2 crossovers with a positive patch in the Atlantic Ocean and a negative one around Indonesia. There is a very good agreement between SARAL/AltiKa and Jason-2 over almost three years of SARAL/AltiKa data regarding SLA patterns.

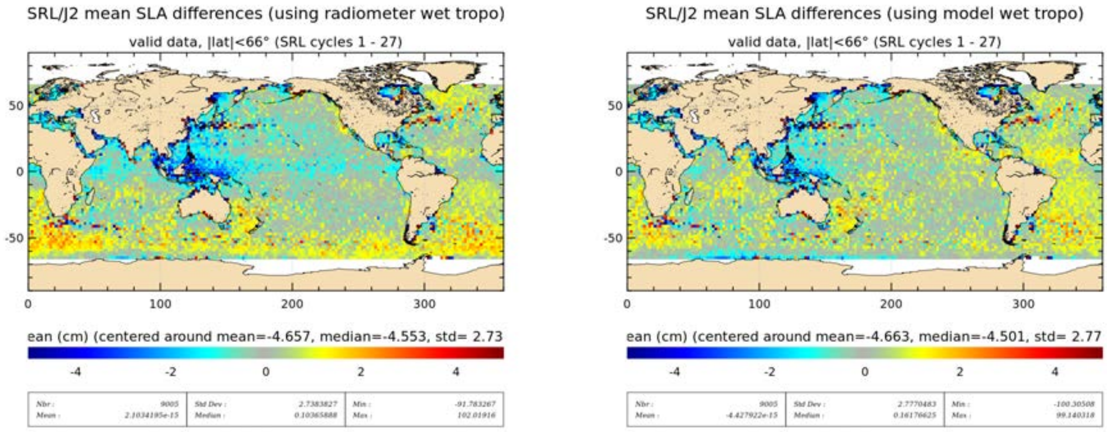

Figure 56: *Map of SLA differences between SARAL/AltiKa and Jason-2 using the radiometer (left) and modeled (right) wet troposphere correction for the 27 first cycles of SARAL/AltiKa.*

6.2. Along-track performances for Saral/AltiKa (GDR-T Patch1) and Jason-2

SLA analysis is a complementary indicator to estimate the altimetry system performances. It allows us to study the evolution of SLA mean (detection of jump, abnormal trend or geographical correlated biases), and also the evolution of the SLA variance highlighting the long-term stability of the altimetry system performances. Hereafter daily monitoring of mean (top left of figure 55) and standard deviation (top right of figure 55) of SARAL/AltiKa and Jason-2 SLA are shown.

Saral/AltiKa and Jason-2 daily mean of SLA show similar signals and evolution. There is an offset between SARAL/AltiKa and Jason-2 SLA of around -4.5 cm when using the radiometer wet troposphere correction, and -4.7 cm using the model wet troposphere correction. This bias between missions appears to be very stable over time, with no drift detected over the available period. The safe hold mode on SARAL/AltiKa might have had an impact on this bias, this question is adressed in section 7.3.. The daily standard deviations of SARAL/AltiKa and Jason-2 SLA are very similar (top right of figure 55), except for about one month before the SARAL/AltiKa's safe hold mode, when platform pointing accuracy was degraded.

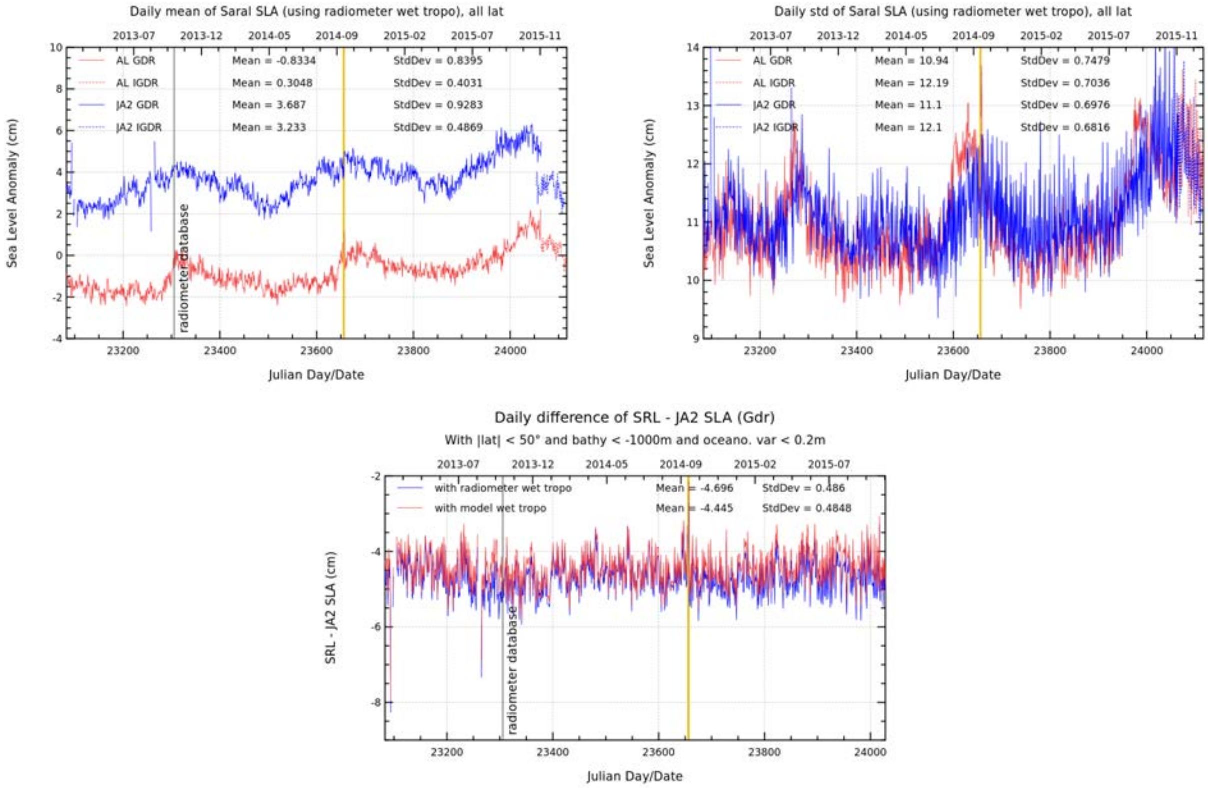

Figure 57: *Daily monitoring of mean (top left) and standard deviation (top right) of SLA (using radiometer wet troposphere correction) of GDR data (plain lines) and IGDR data (dotted lines). The statistics are done for valid data with all available latitudes. The gold band indicates the safe hold mode on Saral/AltiKa. Bottom: Difference of daily Saral/AltiKa minus Jason-2 SLA using either radiometer or model wet troposphere correction. The statistics are done for valid data with* $|latitudes| < 50^{\circ}$*, bathymetry* < -1000 *m and low ocean variability.*

6.3. Along-track performances of the different product types (Ogdr/Igdr/Gdr)

SARAL/AltiKa products are available for three data types (with different latency and precision): Ogdr, Igdr and Gdr. There are also some differences in the product content (see table 7). Hereafter the daily mean and standard deviation of SLA of the different data types is monitored (see figure 58). Note that only the Gdr data are an homogeneous data set (using Patch2 version for all cycles). For Ogdr and Igdr data Patch1 version was only used from July onwards (for precise dates see table 1). This explains the jumps visible in the Ogdr and Igdr SLA series. Another jump affects the IGdr and OGdr curves which occur when we switch from Cal/Val to DUACS database. These jumps correspond to the change in the MSS reference period: while Cal/Val uses a MSS referenced over a 7 years period (like in the products), DUACS uses a 20 years reference period. At the beginning of the period, Ogdr SLA exhibits furthermore some additional short-term (about 14 days period) variability. These were indentified in the 2013 SARAL annual report, after the application of Patch 2, the amplitude of these signals is greatly reduced, thanks to the new version of TRIODE software used to estimate the Ogdr orbit. The temporal evolution of the mean of Ogdr, Igdr and Gdr SLA are very close, observed biases come from the different MSS reference periods used. The standard deviation of SLA shows low values for all products(between 11 and 12 cm):

standard deviation of Gdr product is the lowest and the one of Ogdr products is the highest. But even the performance of Ogdr products is already very good (thanks to the good quality of the Doris/Diode navigator orbit).

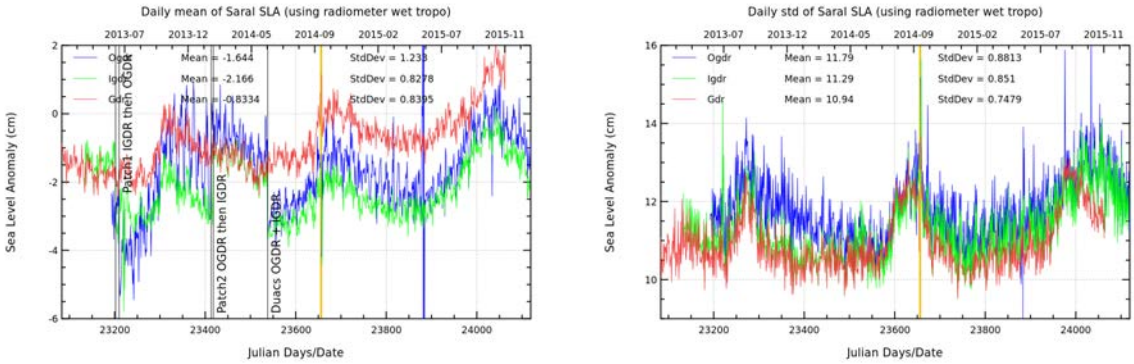

Figure 58: *Daily monitoring of mean and standard deviation of valid Saral/AltiKa SLA (with radiometer wet troposphere correction) for Ogdr, Igdr and Gdr products. No particular selection is used (latitude is not limited).*

6.4. SARAL/AltiKa as part of the GMSL record

SARAL/AltiKa data can easily be merged to the global Global Mean Sea Level (GMSL) record. The period is of course short to draw quantitative conclusions, but the results are shown here as an illustration of SARAL/AltiKa's very good performance level.

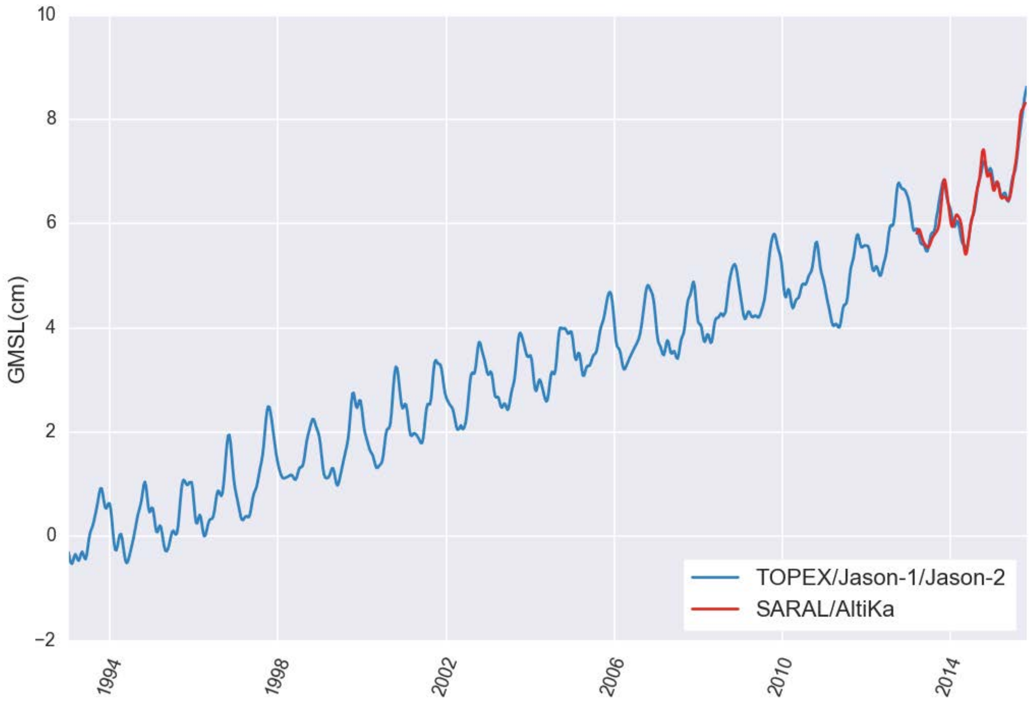

Figure 59: *SARAL/AltiKa global mean record compared to the reference global mean sea level from TOPEX/Poseidon, Jason-1 and Jason-2*

7. Particular Investigations

7.1. Mispointing

Since the beginninng of life of the mission, SARAL/AltiKa's pointing has experienced several events. A section of the 2014 yearly report was already dedicated to SARAL/AltiKa's mispointing. Over the course of 2015, other mispointing events occured. The present section is an update of last year's investigations on platform mispointing.

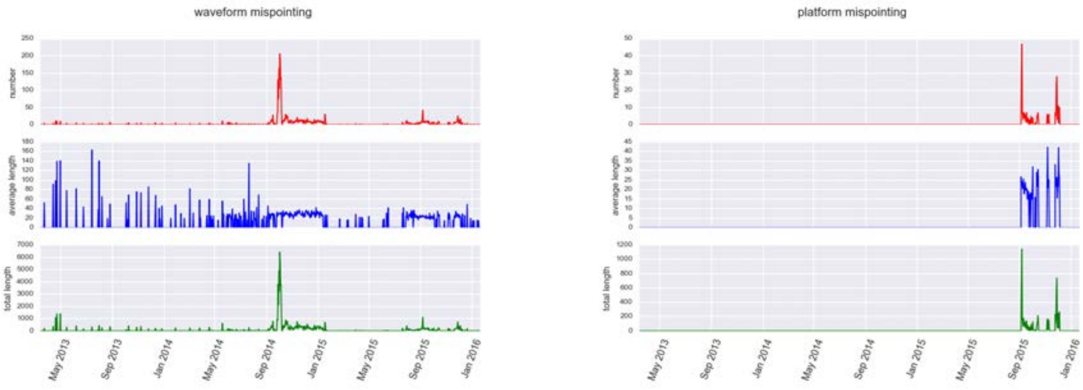

Figure 60: *number, average and total length of mispointed track sections from waveform estimation (left) and platform mispointing (right, only after September 1st, 2015)*

Figure 60 displays the monitoring of mispointed track sections on SARAL/AltiKa. These sections are defined as more than 15 consecutive measurements with mispointing values greater than 0.015 degrees squared. This definition is used in order to avoid detection of short mispointing events that might be related to rain events impacting the mispointing estimation from waveforms. Please note that the "high" mispointing events we monitor here remain below the specified pointing accuracy of $0.0225 deg^2$. We noticed no degradation of data quality due to these events, very high values are scarce and easily edited.

At the beginning of the mission, and after applying the biases detected by the first X-cal, SARAL/AltiKa's pointing was very accurate. Few mispointed track sections are detected, and are generally explained maneuvers. As a result of an increase in reaction wheel friction, the number of mispointing events rises from cycle 16 onward (September 2015). The reaction wheel eventually stopped, leading to the reconfiguration of the spacecraft to three wheel mode. Following this reconfiguration, ISRO performed a software upload, which failed (partial upload during the station overfly) leading to the spacecraft going into safe hold mode from cycle 17, pass 324 to pass 414 (from October 6th to 9th, 2014).

After the SHM, SARAL/AltiKa experienced a period during which mispointing events were associated to zero-crossings of the RW speed (friction at the crossing), resulting with a relatively constant number of events, all linked to command law of the spacecraft and with a characteristic geographical pattern (see figure 61, left panel). The command law was patched to avoid zero crossings of the RW wheel resulting in a pointing accuracy similar to the one obtained at the start of the mission.

During summer 2015, increased friction in the other reaction wheels lead to a new increase in the number of mispointing events. These events now occur randomly, as shown on the right panel of figure 61. There is no clear trend in the number of these events, and no steady rise can be found.

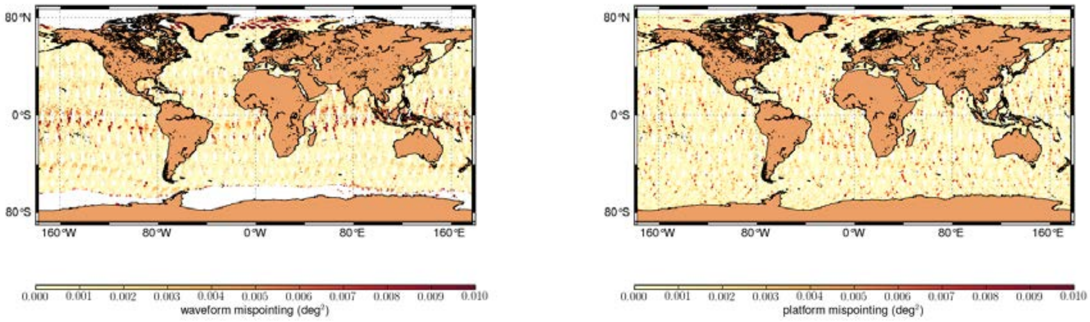

Figure 61: *map of waveform mispointing, associated with zero crossings of RW speed (left), and typical of the end of 2015 (right)*

7.2. Ground track shift

As a result of the issues on RW wheels, an unexpected thruster firing occured during a station keeping maneuver on March, 31st, 2015. As a result the thrust was larger than expected, and the ground track started to drfit westward. A second maneuver was performed on April 9th to correct this groud track shift. After an aborted maneuver on May, 1st due to RW stuck up, the ground track started to shift eastward. To avoid RW wheels stuck up, maneuvers from May, 26th onwards use the thrusters to perform attitude changes.
The above described sequence of maneuvers led to a large ground track drift (up to 15 km at the equator). Figure 62 displays the evolution of the cross-track distance to the nominal track at the equator. On this plot, positive values correspond to a westward shift. Maneuvers performed with thrusters are not always as accurate as maneuvers performed with RW, and the ground track of the spacecraft has not been maintained with the same accuracy after this event. In addition, this new way of performing maneuvers tends to lead to slightly more missing data on passes with maneuvers than before (about 15%).
With this ground track drift, areas of the ocean far from the mean profile are observed. It was shown ([19]) that deviation from the ground track was associated to en increase in the variance of the high frequencies of the SARAL/AltiKa SLA, in relation with increased errors of the mean sea surface in certain regions.

7.3. Impacts of the October 2014 SHM

SARAL/AltiKa experienced a three days SHM in October 2014. In last year's report ([16]) we stated that we were not able to find any significant impact of this SHM on SLA measurements by SARAL/AltiKa, partly because the post-SHM period was really short at that time. With one more year of data, we establish that the SHM has had an impact on the 37 GHz channel of the radiometer. Figure 63 displays the evolution of the brightness temperature differences between the two channels of the radiometer on the left, and the evolution of the wet troposphere correction differences on the right. On both figures, each year is overlaid over the previous so that the seasonnal varibility is visually removed. The difference between the two channels shows a 1K shift after the SHM, attributed to the 37 GHz channel. As a consequence of this brightness temperature shift, the wet tropospheric correction derived from the radiometer displays a 1 mm shift with respect to the model (although this is less clear due to the larger varibility of the wet tropo differences). This

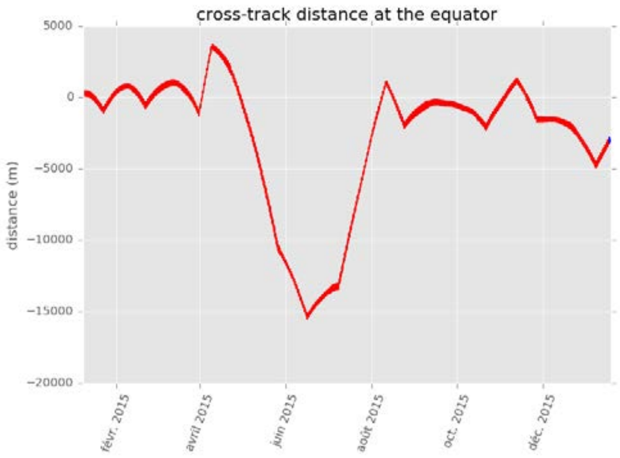

Figure 62: *SARAL/AltiKa cross-track deviation from the nominal track at the equator*

1 mm shift is directly applied on the SLA and GMSL measurements from SARAL/AltiKa, but this is barely noticed on the monitoring of SLA differences with Jason-2 (see figure 57)

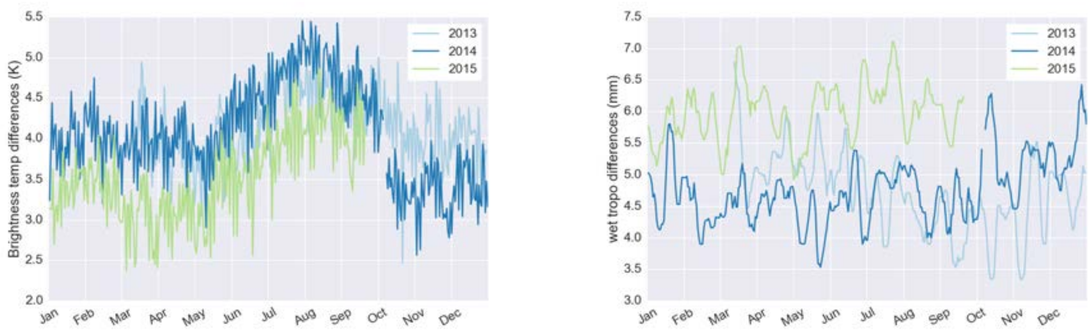

Figure 63: *(left) seasonnal cycle of the differences between the radiometer channels and (right) seasonnal cycle of the radiometer minus model wet tropo differences*

7.4. Radiometer drift assessment

As mentionned in last year's report ([16]) and previously in this report (see section 5.3.) there are two periods where SARAL/AltiKa and Jason-2 SLA differences increase. The first period is linked to the saturation of the radiometer hot calibration counts which translated into a SLA drift. The second period corresponds to the end of the mission (approximately from February 2015 onwards), when the mean differences at crossovers between SARAL/AltiKa and Jason-2 using the radiometer and the model appear to be drifting apart.
Comparing the radiometer minus model wet troposphere differences between SARAL/AltiKa and Jason-2 clearly show a different behaviour of the two missions over the course of 2015, with the Jason-2 curve going downwards and the SARAL/AltiKa one slighlty upwards (see left panel of figure 64). Please note that part of the apparent trend on SARAL/AltiKa is explaned by the 1 mm shift after the SHM (see section 7.3.). Using a wet tropo retrieval algorithm not using the 18.7 GHz channel on Jason-2 (light blue curve on the right panel of figure 64) reduces the discrepancies

between SARAL/AltiKa and Jason-2. This suggests that the origin of this drfit is the 18.7 GHz channel on Jason-2. Figure 65 compares radiometer minus model wet tropospheric differences over all Jason-2 years. Clearly year 2015 stands out as an anomaly over any Jason-2 previous year. The last part of these curves is from IGDR data (they were made for the OSTST meeting) and the downward trend behaviour of Jason-2 has been corrected by three radiometer calibrations at the end of 2015. A more detailed analysis of this event is available in the Jason-2 yearly report ([17]).

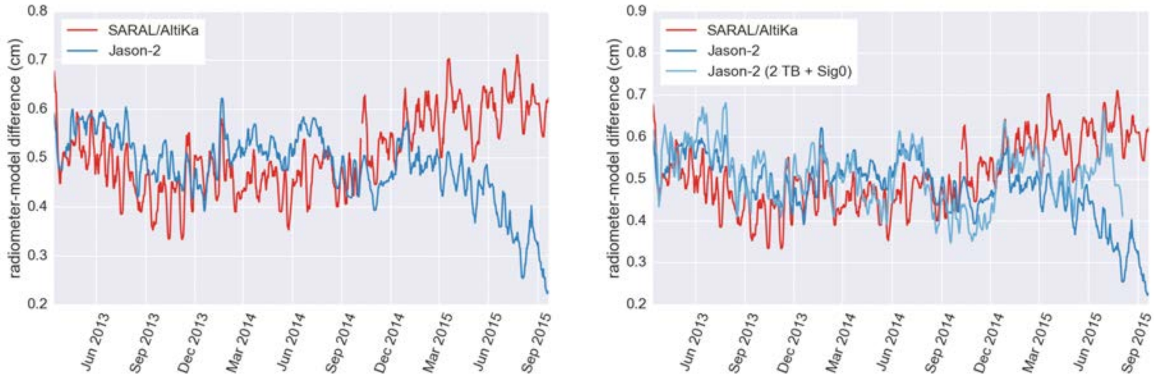

Figure 64: *(left) evolution of the wet tropospehric differences (radiometer minus model) for Jason-2 and SARAL/AltiKa, (right) similar with a 2 brightness temperatures and backscatter based retrieval algorithm for the Jason-2 wet troposphere (light blue curve)*

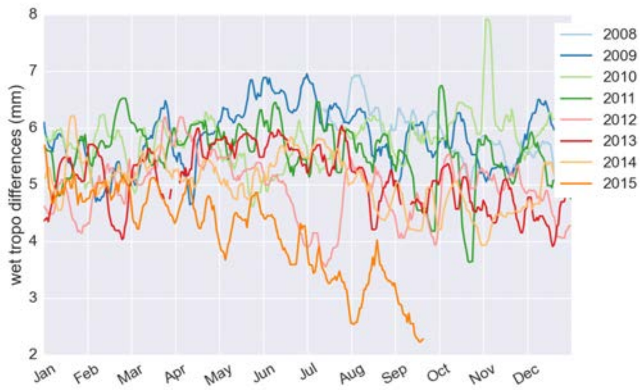

Figure 65: *Jason-2 radiometer minus model wet tropospheric differences for all mission years*

7.5. Investigating SARAL/AltiKa error budget

In 2015, part of the work on SARAL/AltiKa was devoted to the error characterization of the mission. In this section, we briefly present the results of the investigations performed on this topic. The approach was largely inspired by a similar work performed on Jason-2 in 2014 (see [18]), completed with investigations regarding spatial distribution and lower frequencies.

7.5.1. High frequency range errors

Here high frequency errors are understood as the noise level on different altimeter parameters. This noise level can be evaluated either from the spread of the 40 HR measurements used to make the 1 Hz measurement (or 20 for Jason-2), or from the the noise level from a spectrum estimation. Figure 66 displays the noise level, considering that high rate data are independent, estimated form the standard deviation of the range, for both SARAL/AltiKa and Jason-2. This is of course dependent on SWH and to two missions show a similar behaviour, with a lower noise level on SARAL/AltiKa than on Jason-2, a comparison confirmed by the spectrum. For a 2 m SWH, the noise level on SARAL/AltiKa is estimated to 0.8 cm, compared to 1,6 cm on Jason-2. This is in good agreement with the level of the plateau on the spectrum, once converted to noise level using the sampling frequency (0.87 cm on SARAL/AltiKa and 1.7 cm on Jason-2).

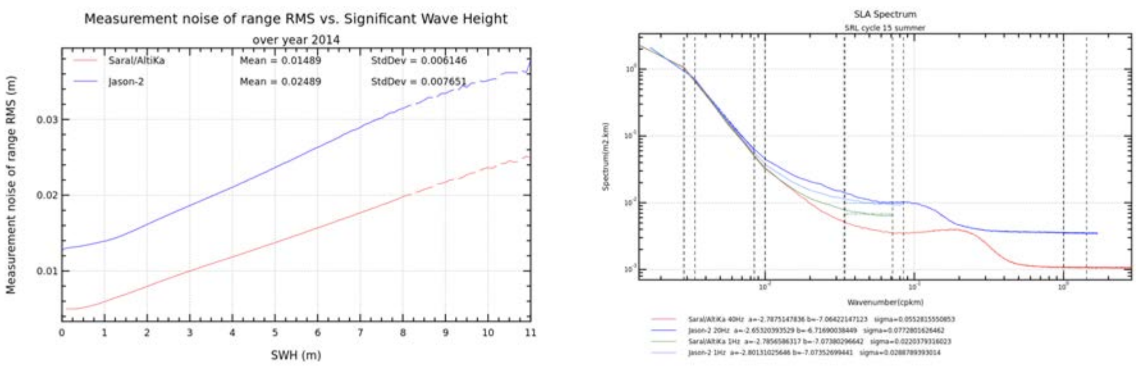

Figure 66: *(left) noise level from the standard deviation of the range and (right) SLA spectrum from SARAL/AltiKa and Jason-2 data*

This noise level is dependent on SWH and therefore presents an uneven spatial distribution. Figure 67 displays the map of the altimeter range noise level, compared to a similar map with the noise level deduced from the spectral plateau. These maps are estimated from one cycle of SARAL/AltiKa data in winter, and high sea state regions in northern mid-latitudes are observed on both estimates of the noise.

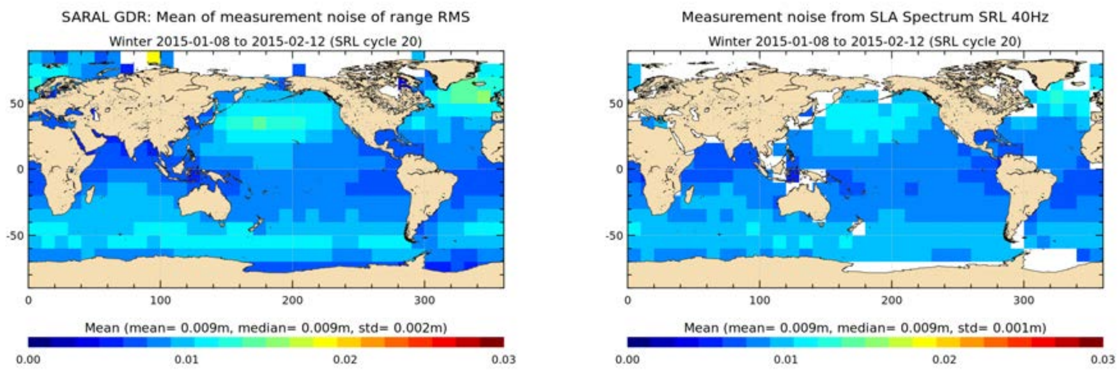

Figure 67: *(left) map of noise level from the standard deviation of the range and (right) map of the noise level from the SLA spectrum*

We also performed a small experiment to evaluate the impact of rain cells on the noise level of SARAL/AltiKa data. Starting from the noise level estimated from the standard deviation of the range measurements, we correct for the SWH dependecy using a linear fit on the curve of figure 66. This results in the left panel of figure 68, where positive values indicate noise levels larger than what is expected given the local wave height. The left panel diplays the rain rate estimated from colocations between SARAL/AltiKa and XX, with time differences lower than 3h. Clearly, some of the areas where the observed noise level is higher than expected can be related to high rain rates. This is not always the case, and we can only make hypothesis to explain such discrepancies: either the colocations are too wide and the rain level has changed between the two sensor times, or other events (like sigma blooms) could explain a higher noise level.

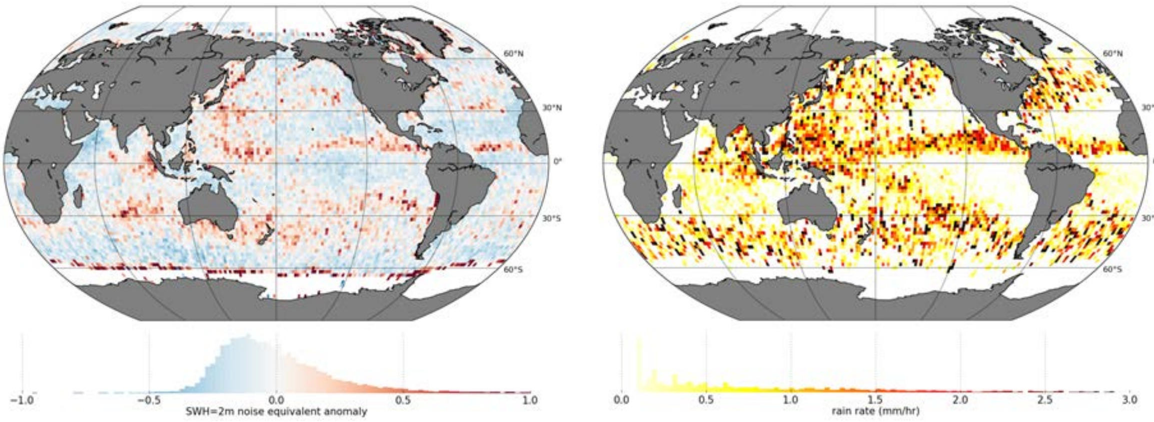

Figure 68: *(left) map of noise level anomaly with respect to SWH=2m (right) rain rate estimated from collocations with SARAL/AltiKa data*

7.5.2. High frequency errors on other parameters

8. Conclusion

SARAL/AltiKa was launched on February, 25th 2013, and is on its operational orbit Since March, 13th. Its the first altimeter satellite using the Ka-band frequency, instead of Ku-band. Despite this new frequency, the OGDR/IGDR products were delivered to users by the end of June/beginning of July 2013. The GDR products (GDR-T version Patch1) were available to the PIs from August,2nd 2013 onwards. Following the Saral/AltiKa NRT Verification workshop held end of August 2013 in Toulouse, the GDRs were released to all users from September 12th 2013.
About a year after launch (early february 2014), the GDR-T Patch 2 version of the products was released to users from cycle 10 for real-time products and from cycle 8 onwards for GDR products. The first 7 cycles of the GDR product were reprocessed in 2014 in order to provide a consistent delayed-time dataset. In 2015 (cycle 25), the orbit standard has changed to POE-E, but no reprocessing of the full period was performed.
In fall 2014, SARAL/AltiKa has experienced an increase in the friction of one reaction wheel, leading to an increase of the number of measurements impacted by high platform mispointing. This resulted in the wheel eventually stopping and the spacecraft going into safe-hold mode for three days from October 6th. After that, and over the full course of 2015, mispointing events are observed due to friction in the other reaction wheels. Update of the command law has provided a great improvement, yet friction remain present. The reaction wheel issue has led to abortion of station keeping maneuvers, resulting in a drift of the spacecraft from its nominal ground track, and a change in the maneuvering procedure: thrusters are now used rather than reaction wheels.
Despite the concerns on reaction wheels, we show in this report a variety of results, including comparisons with Jason-2 to demonstrate the the data quality of SARAL/AltiKa is still excellent.
The main points of this performance assessment are summarized below:

- SARAL/AltiKa provides an excellent coverage of the ocean, with more than 99% of measurements available over ocean,
- the data quality is excellent, with only 2.4% of edited measurements, a value lower than the Jason-2 one by about 1%,
- SLA statisitics show no long term drift with respect Jason-2, SARAL/AltiKa and Jason-2 observe very similar SLA features, both considering the temporal evolution of global averages and geographical patterns,
- the standard deviation of daily SLA averages differences between SARAL/AltiKa and Jason-2 is only 5 mm, despite the fact that the two missions are not flying over the same ground track,
- at crossovers SARAL/AltiKa shows a performance similar to the Jason-2 one with a standard deviation of 5.3 cm,
- a first assessment of the error budget demonstrates the excellent performance of the SARAL/AltiKa mission, with a range noise level lower than 1 cm.

With the recent launch of the Jason-3 mission, SARAL/AltiKa remains an important element of the satellite altimetry constellation, providing valuable data at high latitudes. Further data quality improvements are foreseen thanks to updated algorithms, for the radiometer retrieval for example.

9. Glossary

AMR Advanced Microwave Radiometer

CLS Collecte Localisation Satellites

CNES Centre National d'Etudes Spatiales

CNG Consigne Numerique de Gain (= Automatic Gain Control)

DEM Digital Elevation Model

DIODE Détermination Immédiate d'Orbite par Doris Embarqué

ECMWF European Centre for Medium-range Weather Forecasting

EDP Earliest Detection Part

GDR Geophysical Data Record

GDR-T Geophysical Data Record version T (test)

GIM Global Ionosphere Maps

GOT Global Ocean Tide

IGDR Interim Geophysical Data Record

JPL Jet Propulsion Laboratory (Nasa)

MLE Maximum Likelyhood Estimator

MOE Medium Orbit Ephemeris

MQE Mean Quadratic Error

MWR MicroWave Radiometer

MSS Mean Sea Surface

NSIDC National Snow and Ice Data Center

PF/RF PlatForm / RadioFrequency

PLTM PayLoad TeleMetry

POE Precise Orbit Ephemeris

OGDR Operational Geophysical Data Record

SALP Service d'Altimétrie et de Localisation Précise

SARAL Satellite with ARgos and ALtika

SSH Sea Surface Height

SLA Sea Level Anomaly

SLR Satellite Laser Ranging

SSB Sea State Bias

SWH Significant Wave Height

TEC Total Electron Content

TM TeleMetry

10. References

References

[1] Frery, M.-L. *et al.*, 2014, Correction du canal 37GHz du radiomètre AltiKa, CLS/DOS/NT-14-115

[2] Aouf, L. and J.-M. Lefèvre, 2013, The impact of Saral/Altika wave data on the wave forecasting system of Météo-France : update, Oral presentation at SARAL/AltiKa 1st Verification Workshop, Toulouse, France, available at http://www.aviso.oceanobs.com/fileadmin/documents/ScienceTeams/Saral2013/24_wave_lotfi.pdf

[3] Brown, G.S., 1977, The average impulse response of a rough surface and its application", *IEEE Transactions on Antenna and Propagation*, Vol. AP 25, N1, pp. 67-74

[4] SARAL/AltiKa Products handbook, 2013, *SALP-MU-M-OP-15984-CN* edition 2.3, available at: http://www.aviso.oceanobs.com/fileadmin/documents/data/tools/SARAL_Altika_products_handbook.pdf

[5] Boy, F. and J.-D. Desjonqueres, 2010, Note technique datation de l'instant de reflexion des échos altimètres pour POSEIDON2 et POSEIDON3, *TP3-JPOS3-NT-1616-CNES*

[6] Desjonquères, J. D. , G. Carayon , N. Steunou and J. Lambin, 2010, Poseidon-3 Radar Altimeter: New Modes and In-Flight Performances, *Marine Geodesy*, 33:1, 53–79, available at http://pdfserve.informaworld.com/542982__925503482.pdf

[7] Faugere, Y., A. Delepoulle, F.Briol, I. Pujol, N. Picot, E. Bronner; 2013, Altika in DUACS: Status after 2 months (and perspectives), oral presentation at SARAL/AltiKa 1st Verification Workshop, Toulouse, France, available at http://www.aviso.oceanobs.com/fileadmin/documents/ScienceTeams/Saral2013/34_Altika_in_Duacs_Faugere.pdf

[8] Griffin, D. and M. Cahill, 2013, Use of AltiKa NRT sea level anomaly in the Australian multi-mission analysis, Oral presentation at SARAL/AltiKa 1st Verification Workshop, Toulouse, France, available at http://www.aviso.oceanobs.com/fileadmin/documents/ScienceTeams/Saral2013/33_multi_mission_gridding_GRIFFIN.pdf

[9] Lillibridge, J., R. Scharroo, S. Abdalla, and D. Vandemark, 2013, One-and Two-Dimensional Wind Speed Models for Ka-band Altimetry, *Journal of Atmospheric and Oceanic Technology*, doi: http://dx.doi.org/10.1175/JTECH-D-13-00167.1

[10] Picot, N., A. Guillot, P. Sengenès, J. Noubel, N. Steunou, S. Philipps, P. Prandi, G. Valladeau, M. Ablain, S. Desai, B. Haines and S. Fleury, 2013, Data Quality Assessment Of The SARAL/AltiKa Ka-band Mission, Oral presentation at OSTST, Boulder, USA, available at http://www.aviso.oceanobs.com/fileadmin/documents/OSTST/2013/oral/Picot_SARAL_Data_Quality_Assessment.pdf

[11] Philipps, S. and V. Pignot, 2014, Saral/AltiKa reprocessing GDR-T Patch2, SALP-RP-MA-EA-22345-CLS/CLS.DOS/NT/14-031

[12] Scharroo, R., and J. L. Lillibridge, 2005, Non-parametric sea-state bias models and their relevance to sea level change studies, in *Proceedings of the 2004 Envisat & ERS Symposium*, Eur. Space Agency Spec. Publ., ESA SP-572, edited by H. Lacoste and L. Ouwehand

[13] Stenou, N., P. Sengenes, J. Noubel, N. Picot, J.D. Desjonquères, J.C. Poisson, P. Thibaut, F. Robert and N. Tavenea, 2013, AltiKa Instrument : In-Flight Stability And Performances, Oral presentation at OSTST, Boulder, USA, available at http://www.aviso.oceanobs.com/fileadmin/documents/OSTST/2013/oral/Steunou_OSTST2013_AltiKa_Instrument.pdf

[14] SARAL System Requirements, *SRL-SYS-SP-010-CNES*

[15] Thibaut, P., O.Z. Zanifé, J.P. Dumont, J. Dorandeu, N. Picot, and P. Vincent, 2002, Data editing: The MQE criterion, *Paper presented at the Jason-1 and TOPEX/Poseidon Science Working Team Meeting, New-Orleans (USA), 21-23 October*

[16] Prandi, P., V. Pignot and S. Philipps, 2015, Saral/ Altika validation and cross calibration activities (Annual report 2014), SALP-RP-MA-EA-22418-CLS available at http://www.aviso.altimetry.fr/en/data/calval.html

[17] Roinard, H., S. Philipps and O. Lauret, 2016, Jason-2 validation and cross calibration activities (Annual report 2015), SALP-RP-MA-EA-XXXXX-CLS available at http://www.aviso.altimetry.fr/en/data/calval.html

[18] Roinard, H., P. Matton and S. Philipps, 2015, Jason-2 validation and cross calibration activities (Annual report 2014), SALP-RP-MA-EA-22409-CLS available at http://www.aviso.altimetry.fr/en/data/calval.html

[19] Pujol, M.-I., Y. Faugere, G. Dibarboure, P. Schaeffer, A. Guillot and N. Picot, 2015, The recent drift of SARAL: an unexpected MSS experiment, oral presentation at the 2015 OSTST, Reston, VA

11. Annex

11.1. Content of Patch1

Hereafter the content of Patch1 is recalled. All GDR data were initially produced with this patch, however it was used to produce IGDR data only from cycle 4 pass 395 onwards.

Altimeter calibration file : The altimeter calibration stability has been analysed. Based on the actual data, we have implemented an averaging of the calibrations over a 7 days window for the low pass filter (identical to Jason-2) and 3 days for the internal path delay and total power (not used on Jason-2). This will slightly reduce the daily noise observed in the altimeter calibration data.

Altimeter characterization file : We have updated the altimeter characterization file using the flight calibration of the gain values (4 calibrations performed). The impact is very small (of the order of 0.01 dB).

Retracking look-up tables : We have updated the ocean retracking look-up tables using the flight calibration data (PTR). The impact is very small on the range and sigma0 values but of the order of 15 cms on SWH for low sea states.

MQE : We have analyzed the altimeter flight data and based on the observed MQE values over ocean a threshold of 2.3E-3 (Jason-2 value is 8E-3) is used for the 1Hz data computation.

Neural network : A first linear relation has been computed between the measured BT and the simulated one. This linear relation is applied on the 23.8 GHz only – the same analysis will be conducted on the 37 GHz and sigma0. This generates a bias on the radiometer wet tropospheric correction which is now much more consistent with the model one.

Atmospheric attenuation : The value outputted by the neural algorithm is now recorded in the level2 products (it was set to 0 at the beginning of the mission). Rad_water_vapor and rad_liquid_water: The values have been corrected to comply with the actual unit in the level2 products (kg/m^2). But the rad_liquid_water remains not reliable as an anomaly has been noticed in the neural network.

SSHA : The radiometer wet tropospheric correction is now used to compute this value (the model value was used at the beginning of the mission).

Controls parameters : The threshold values have been updated with the flight data. This is a first tuning – additional work is necessary.

11.2. Content of Patch2

Hereafter the content of Patch2 is recalled. It will probably be activated mid-January 2014. GDRs will be produced using Patch2 from cycle 8 onwards. Cycles 1 to 7 will be reprocessed with the Patch2.

Wind look-up table : The table provided by NOAA is used. This table is only based on the measured sigma0, taking into account the atmospheric attenuation (sigma0 at the surface). (Reference: Lillibridge et al. [9])

SSB look-up table : The table provided by R. Scharroo is used (same method as in [12]). We use only the significant wave height to compute the SSB.

Radiometer neural algorithm : Taking into account several months of AltiKa measurements, the neural network coefficients have been updated. Note that this modifies the radiometer related parameters (radiometer wet troposphere correction, atmospheric attenuation, radiometer liquid water content and radiometer water vapor content).

Ice-2 retracking algorithm : The algorithm has been updated taking into account the AltiKa Ka band specificities (ice2 algorithm was based on ENVISAT Ku band experience).

FES2012 tide model : This new tide model is included, improving the SSH accuracy in coastal zones. (Reference : http://www.aviso.oceanobs.com/en/data/products/auxiliary-products/global-tidefes2004-fes99/description-fes2012.html)

Matching pursuit algorithm : The algorithm based on J. Tournadre proposal has been tuned to comply to AltiKa Ka band specificities.

MQE parameter scale factor : The scale factor of the MQE has been modified.

Update of the altimeter characterization file : The altimeter characterization file has been modified in order to account for 63 values of altimeter gain control loop (AGC). This has impacts over sea ice and land hydrology, in some cases the AGC was set to default value in current P1 products.

Doris on ground processing (Triode) : The Doris navigator ground processing has been upgraded to reduce the periodic signal observed on the altitude differences with MOE/POE.